Nanyang Technological University

PREPARATIVE ENANTIOSEPARATION BY SUPERCRITICAL FLUID CHROMATOGRAPHY

PhD thesis
Submitted to the School of Chemical and Biomedical Engineering
of the Nanyang Technological University

by

CHEN WENDA

Advisor: Arvind Rajendran

04 Jan 2010

Abstract

Supercritical fluid chromatography (SFC), due to its high throughput and efficiency, environmental friendliness, small solvent consumption, has been recognized as a powerful technique for enantioseparations. Preparative SFC is being increasingly used as a reliable method for rapidly accessing enantiopure compounds. To develop optimum methods for the SFC enantioseparation processes, a systematic study on the effect of different controllable parameters on process performance has been performed. The optimization for preparative SFC has been formulated as a multi-objective optimization problem to simultaneously maximize the productivity and minimize the solvent consumption. It has been solved using a proper mathematical model integrated with suitable optimization algorithm under different operating conditions, product quality requirements and elution fashion. In particular, isocratic and solvent gradient methods have been explored in detail and an attempt has been made to experimentally implement the results of the optimization study. Although some deviations in the experimental results were observed, the thesis quantitatively confirms the key advantages, significant reduction in solvent consumption at high productivity. The rigorous optimization techniques developed have a general application and can be used to objectively compare different techniques and provide a basis for rational scale-up of SFC process.

Keywords: Enantioseparation, Supercritical fluid chromatography, Multi-objective optimization, Isocratic elution, Gradient elution

Acknowledgments

First of all, I would like to express my deepest gratitude to Prof. Arvind Rajendran, my supervisor, for his constant encourage and guidance. His punctilious attitude toward work and teaching impressed me and helped me to overcome the mistakes in the aspects of both experiments and theoretical study. Without his constructive suggestions and illuminating instruction, this thesis could not have reached its current form.

High tribute shall be paid to Prof. Mohammad Amanullah who has offered me valuable suggestions in simulation and optimization. He spent much time reading through the optimization parts of the thesis and provided me with inspiring advice.

I am also deeply indebted to Dr. Su Jincai and Reza Hangpannah who worked with me in lab. Without their cooperation and help, it would be difficult for me to finish all the experiments alone.

Thanks to Nanyang Technological University for the financial support.

Finally I would like to thank my beloved parents who have been assisting, supporting and caring for me for all my life.

Contents

List of Figures

List of Tables

Chapter 1

Introduction

1.1 General introduction

Chiral compounds are a class of chemical substances that have the same chemical formula and structures with different optical properties. Each form, a mirror image of the other, is called an enantiomer. Since in biological systems drug-receptor interaction can be stereo-selective, different enantiomers might have varied biological activities [2]. For example, one enantiomer may have the expected effect while the other can be either benign, or even toxic. Several active pharmaceutical ingredients (API) of blockbuster drugs are chiral in nature. Chirality has become an important issue in clinical trials and hence in the sale of the final product. It is worth noting that toxicological and pharmacodynamics properties of each enantiomer of a chiral drug must be tested before launch into the market [3]. It is worth noting that single enantiomer drugs constitute about 40% of the total drug sales [4]. However, in modern pharmaceutical industry, significant number of the compounds are usually synthesized through classical routes whose product is in racemic form containing equal amount of two enantiomers. Owing to these reasons, ways to resolve the mixture into pure enantiomers through efficient and economical means become an important topic of study for both academia and the industry.

Generally speaking, there are two approaches to produce the isolated enantiomer: (i) enantioselective synthesis of the desired product; or (ii) separation of the desired enantiomer from a racemate. The main disadvantage of enantioselective synthesis is the cumbersome multi-step process and high development cost. Moreover, the product of the chiral synthesis does not contain the desired enantiomer in a required pure state or the productivity is not sufficient enough to fulfil the requirements of the regulatory authorities. Thus, additional purification or an enrichment step must anyhow be added to the synthesis process. Compared to the chiral synthesis, enantioseparation is typically more economical and less time consuming in several instances. In the developmental stage of a drug, enantioseparation provides a big advantage that both enantiomers can be obtained in pure forms to carry out the individual tests in the shortest time [3].

There are many methods to implement enantiomeric separations, such as crystallization [5], chromatography [6], membranes [7, 8, 9] and extractions [10]. Chromatographic methods, particularly gas chromatography (GC) and high performance liquid chromatography (HPLC) have been considered as the first choice for the analytical separation of racemic mixtures [11]. Chiral chromatographic methods can not only be applied to analytical scale separations but are also suitable for preparative separations. In the recent years technical developments related with the equipment and chiral stationary phases (CSPs) with high selectivities have enhanced the efficiency of chromatographic enantioseparations and have raised the level of acceptance [12]. In spite of heavy investments on equipment and stationary phase, high value

addition to chirally pure substances can justify the high costs of liquid chromatography. Furthermore, the relatively short time required to develop a chromatographic method and the availability of robust chromatographic systems make it a better candidate compared to other separation methods.

Although HPLC can be used for semi-preparative separations of enantiomers for small scale applications such as drug discovery, it has certain shortcomings especially for large scale applications. One such shortcoming of HPLC is that of high pressure drops that are encountered at high throughputs. Large pressure drops cause stationary phase degradation and lead to unexpected results. Another drawback of large scale HPLC techniques is that the product must be recovered from a dilute solution usually by evaporation and the recycle or handling of the solvent increase the process cost and duration time. Moreover the complexities of chiral stationary phase selection and parameter optimization, also pose tremendous challenges for chiral method development. Compared to HPLC, supercritical fluid chromatography (SFC) can overcome these limitations due to its unique properties.

The overall goal of this research project is to develop an optimal preparative enantioseparation process using proper methodology based on a clear understanding of the process. To achieve this, a fundamental study of the enantioseparation process mechanisms under SFC conditions is performed first. Based on the experimental information, a design methodology with proper optimization algorithm was selected to obtain the optimum operating conditions with different elution modes. Finally, an attempt has been made to implement practically the results of the optimization.

1.2 Supercritical fluid chromatography

1.2.1 Supercritical fluids

The physical properties of a certain substance depends on the temperature and pressure. Fig. 1.1 shows the phase diagram of a chemical substance. The critical temperature (T_c) of a substance is the temperature at and above which its vapor cannot be liquefied while the critical pressure (P_c) is the pressure used to liquefy a gas under its critical temperature. A supercritical state, shown as the shaded area in Fig. 1.1 is defined as a state whose temperature and pressure is higher than critical temperature and critical pressure (T_c, P_c). When a certain substance reaches the critical point, its isothermal compressibility tends to infinity, thus the molar volume or density changes dramatically. Further a substance that is usually a gas at normal conditions will exhibit a much increased solvent capacity and a liquid-like density when it is in the supercritical region.

As seen from Table 1.1, the critical temperature, in general, increases as the molecular weight of the solvent increases or as the polarity or intramolecular hydrogen bonding of the solvent increases. This can be very useful information to choose a suitable solvent. For example, since the critical temperature of ethane, carbon dioxide and ethylene are near ambient temperature, they are attractive candidates for practical applications. In addition to its unique solubility characteristic other physicochemical properties make the supercritical fluid an attractive solvent. For example, over much of the range of industrial interests, supercritical fluids possess a liquid-like density, ex-

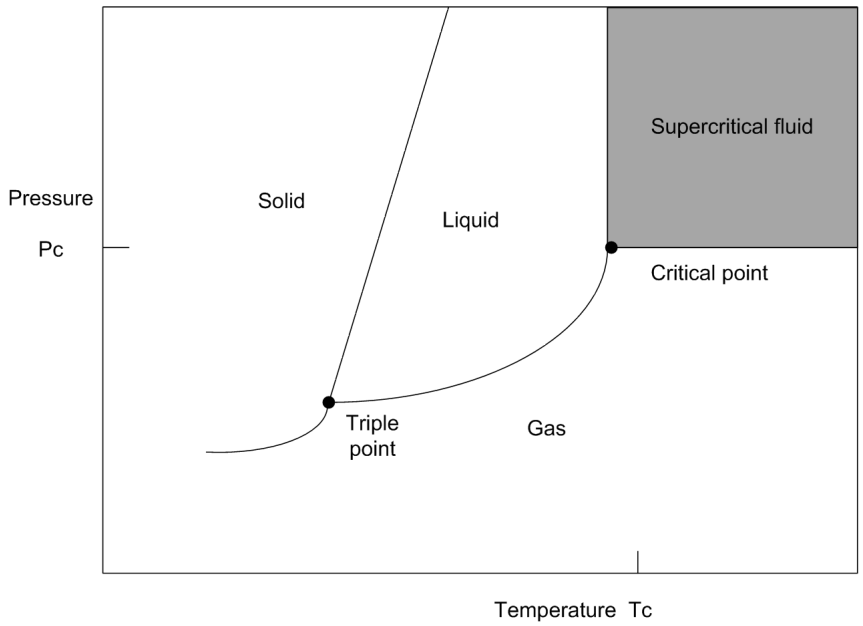

Figure 1.1: Phase diagram of a generic chemical species. The supercritical state is indicated by the shaded area.

hibit gas-like transport properties of viscosity and diffusivity [13]. These are advantages for being chosen as mobile phase in chromatographic processes. Among the different fluids, carbon dioxide has received particular attention for food and pharmaceutical applications owing to its mild critical properties, non-toxic nature and low cost. As shown in Table 1.1, the critical temperature of carbon dioxide is around 30°C which is close to room temperature and its critical pressure is around 70 bar which can be easily achieved by normal high pressure pumps. Carbon dioxide is non-flammable and easily evaporates upon depressurization making it an attractive alternative to traditional organic solvents. However, a major shortcoming of using CO_2, a non-polar material, is its poor solvent strength for polar solutes. To solve this problem, a certain amount of polar organic solvent is usually added into supercritical fluid carbon dioxide to increase the polarity while eluting polar

solute [14, 15]. Such solvent is called "modifier" whose addition is typically limited to less than 30% (by mass). In any case, the use of CO_2 leads to the reduction of organic solvents and hence these processes are termed as "green" processes.

Table 1.1: Physical parameters of selected supercritical fluids

Fluid	Critical Temperature T_c (°C)	Critical Pressure P_c (bar)
CHF_3	25.9	47.5
CO_2	31.3	73.9
NH_3	32.5	114.0
N_2O	36.5	73.4
SF_6	45.5	37.6
C_5H_{12}	196.6	33.7
H_2O	374.0	220.6

1.2.2 Supercritical fluid chromatography

Supercritical fluid chromatography (SFC) is a chromatographic method that uses a supercritical fluid as the mobile phase. Although the use of supercritical fluids as chromatographic mobile phases was reported more than 40 years ago, the benefits of employing SFC for enantioseparations have only been demonstrated recently [16, 17]. The viscosity of supercritical fluid is less than that of liquids and hence allows for the operation of preparative chromatographic columns at high flow rate with low pressure drop. This, in addition to the fact that the diffusion coefficients in supercritical fluids are larger compared to liquid, reduces the analysis time without compromising the column efficiency thereby leading to an increase in productivity [13]. Low pressure drop also facilitates the use of columns with longer length or

multiple columns connected in series without loss of efficiency [18]. Shorter re-equilibration time after changes in operating parameters also decreases the time for method development [19]. For preparative chromatographic separation methods such as HPLC, the collected fractions are mixtures of the desired solute and solvent. The final product (the solute) is obtained usually by an extra step such as evaporation which contributes to a portion of operation cost due to the power consumption and make the process time consuming. The use of carbon dioxide as mobile phase greatly reduces such costs because it can easily be separated by depressurizing leaving a much concentrated fraction. These features makes supercritical fluid chromatography an economical method compared to other chromatographic separation methods.

1.2.3 Mobile phase in SFC

Lovelock suggested that a supercritical fluid can be used as mobile phase for analytical chromatography in 1958 [15]. In 1962, Turner et al. also applied supercritical chlorofluoromethanes as mobile phase to separate porphyrin mixtures [20]. Although a number of compounds, whose critical points are achievable at a reasonable cost, have been tested as solvents used in SFC, most cannot be used. Much of the SFC studies in the early stage focused on either carbon dioxide or ammonia as the eluent, but compressed ammonia is combustible thus not proper for most users. Nowadays, most of the published SFC separations use carbon dioxide as the primary choice for the main component of eluent system.

Owing to the non-poplar nature of CO_2, SFC is generally classified as a normal phase chromatographic technique [21]. The solvent strength of supercritical fluids is strongly related to its density which can be tuned by changing pressure or temperature. Unlike liquids, the density of supercritical liquids changes dramatically with pressure, particularly near the supercritical state as shown in Fig. 1.2. This provides another degree of freedom for optimizing

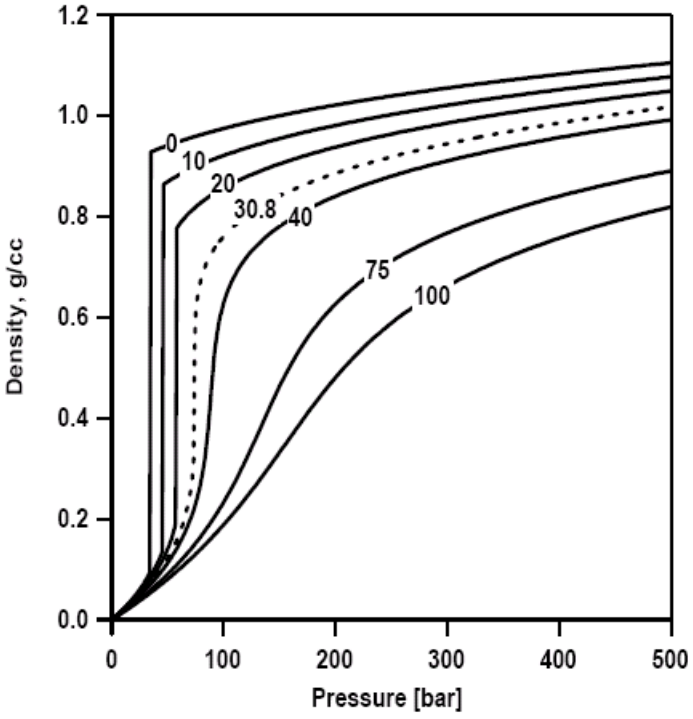

Figure 1.2: The dependence of CO_2 density on pressure for different temperatures (in °C). The dotted line indicates the density values at critical temperature.

chromatographic separations compared to other methods such as HPLC, for example by implementing pressure gradients that result in a better separation [22] and can also be used to tune retention. Temperature also affects the retention of solute in SFC condition. Generally, at a particular pres-

sure, the retention of solute increases with increasing temperature [23]. Such phenomenon is rare in the case of HPLC, but is often encountered in SFC because of the variation in mobile phase density [24]. It is because at a given pressure, a temperature increase reduces the density weakening the interactions between solute and the mobile phase [25]. At a high pressure and high modifier concentration, the effect of temperature is not obvious and the retention behavior is similar to HPLC. Moreover, in some cases, the change of temperature causes reverse of solute elution order which could dramatically change the separation results [23].

As described before, organic modifiers are added to CO_2 for the separation of polar solutes [15]. The elution of compounds with high polarity, such as basic or acid analytes can be achieved through the addition of polar modifiers to the mobile phase [26]. This behavior can be explained in two cases: at low concentration, the modifier masks the adsorption site on stationary phase surface while at a higher concentration the modifier increases the solubility and polarity of the bulk phase. The effect of modifier on retention and separation performances although also observed in other chromatographic methods such as HPLC, is more pronounced in SFC. The critical point of mobile phase also can be altered by adding different type and amount of modifier. The modified supercritical carbon dioxide has a higher critical temperature and pressure. The continuity of the fluid properties between the subcritical state and supercritical state has been reported which leads to little compromise in the separation performance and detectable chromatographic signal when moving from one state to the other [27, 28, 29, 30, 31]. Due

to the marginal difference between two domains, in the following part, the chromatography using mobile phase either at its supercritical or subcritical state is called supercritical fluid chromatography for simplification.

In some cases, other than modifier, a small amount of substance with high polarity is necessary to be added into the mobile phase. Such kind of substances are called additives. They can improve the separation where the a skewed peak shape are observed. These additives are generally acids which are typically used for acidic analytes or bases which are effective for compounds with anime functionality [32, 33]. Isopropylamine and trifluoroacetic acid are usually used additives. The function of additives can be included in several aspects, such as suppressing analytes ionization, competing for the available adsorption sites on the stationary phase, and modifying the polarity of the mobile phase.

1.2.4 Chiral SFC

Chiral separation is probably one of the most successful applications of SFC. The mobile phase of SFC can be either polar or non-polar which increases the flexibility of SFC allowing most of the HPLC separation to be successfully transferred into SFC applications. Due to the advances in stationary phases, detection and collection systems, SFC has become the technique of choice for both analytical and preparative scale separation. Although SFC cannot completely replace HPLC, in the field of chiral separations, during the last decade, SFC has shown its capability in solving enantio-separation problems from analysis of few milligram sample to purification of enantiomers in kg

scale.

The advantages of chiral SFC compared to HPLC include the low pressure drop, short analysis time, less use of organic solvent and convenient recovery of product as mentioned before. Due to the high mass transfer coefficient, the peak resolution is usually higher than HPLC. More controllable operation factors such as pressure, modifier composition, temperature etc. also helps to achieve better separation in SFC. Moreover, it has been reported that the column life in chiral SFC can be longer than in HPLC [34, 35]. This can be another important consideration in process design since the chiral stationary phase is normally expensive. Many relevant SFC applications in chiral separation have been demonstrated and part of them are listed in Table 1.2.

1.3 Preparative chromatography

Analytical chromatography aims at identifying and quantitizing various components in a mixture. The major goal of such separation is achieved as long as the desired components in a small amount of sample are separated with high resolution and the corresponding analysis chromatogram is obtained. In other words, no collection of the purified sample is required. Preparative chromatography differs from analytical chromatography mainly due to the different purpose of separation. Preparative chromatography aims at purifying a certain quantity of substance for further utilization. Usually a large sample is required to be separated in a relatively short time and the chromatographic system needs to modified in a corresponding manner. For

Table 1.2: Applications of enantioselective SFC

Compound	Mobile Phase	chiral stationary phase
Acetaminophen	CO_2/MeOH	Ionic column [36]
Aminoglutethimide	CO_2/MeOH	Cyclose β-6-OH, Cyclose β-6-OH-T [37]
Albendazole sulfoxide	CO_2/MeOH	Chiralpak AD,Chiralcel OD [38, 39]
Alprenolol	CO_2/MeOH	Vancomycin [40]
2-Amidotetralins	CO_2/MeOH	Whelk-O [41]
Chiral sulfoxides	CO_2/MeOH	Chirobiotic T,Chirobiotic TAG [42]
Coumachlor	CO_2/MeOH	Chirobiotic R [43]
trans-1,2-Cyclohexanediol	CO_2	Permethylated b-cyclodextrin [44]
Dichlorprop	CO_2/MeOH	Ristocetin A [43]
Dihydrofurocoumarin derivatives	CO_2/MeOH	Chirobiotic R,Chirobiotic T [45]
Diltiazem	CO_2/IPA	Chiralcel OF [46]
Dimethylaniline	CO_2/MeOH	Ethyl pyridine column [47]
Efavirenz	CO_2/MeOH	Chirobiotic R [48]
Fenoprofen	CO_2/MeOH	Ionic column [36]
Flurbiprofen	CO_2/MeOH	Chiralpak AD-H [49]
Furocoumarins	CO_2/EtOH	Discovery HS F5 [23]
Heterocyclic compounds	CO_2/MeOH	Chirobiotic T,Chirobiotic R [42]
Hexaconazole	CO_2/MeOH, EtOH, IPA	Chiralpak AD [50]
Ibuprofen	CO_2/IPA	Kromasil CHI-TBB [51]
Ketoprofen	CO_2/MeOH	Ristocetin A [43]
Mepivacaine and analogs	CO_2/MeOH	Vancomycin [40]
Methamphetamine	CO_2/EtOH	Chiralpak AD-H [52]
Metoprolol	CO_2/MeOH	Ionic column [36]
Mianserin	CO_2/MeOH	Chirobiotic V [53]
Naphthalene	CO_2/MeOH	Ionic column [36]
Nicardipine	CO_2/MeOH	Chirobiotic V [53]
Omeprazole	CO_2/MeOH EtOH, IPA	Chiralpak AD [54]
Paroxetine intermediate	CO_2/ IPA	Chiralpak AD [55]
α-Phenylethanol	CO_2/MeOH	Permethylated β-cyclodextrin [44]
Proline derivatives	CO_2/EtOH	Polysaccharide-type column[35]
Propranolol	CO_2/MeOH	Chiralpak AD-H [49]
N-protected amino acids	CO_2/MeOH	Chirobiotic T,Chirobiotic R [42]
Testosterone	CO_2/MeOH	Ionic column [36]
trans-Stilbene oxide	CO_2	Chiralpak AD, Chiralcel OD [56]
Thalidomide	CO_2/MeOH	Chirobiotic R [43]
Thioridazine	CO_2/MeOH	Chrialpak AD[57]
Triadimefon	CO_2/MeOH EtOH, IPA	Chiralpak AD [58]
Warfarin	CO_2/MeOH	Chirobiotic R [43]

example, the pump equipped in the system must be able to deliver high flow rates and the column size is usually larger compared to analytical columns. Moreover, unlike analytical separation, the separated compounds is the target in preparative separation thus a collection device is absolutely necessary.

The success and advances in analytical chromatography lead to a high hope for a preparative scale chromatography. The increasing need from industry and the advances in the equipment such as packing material, collection system promote the interest for a large scale chromatographic separation methods. Improved packing methods have increased the system efficiency resulting in shorter columns. Moreover, advanced control technology facilitates the chromatographic process and make it easy to arrange and automate thereby decreasing the operation cost. Due to the new drug discovery and rapid development of bioengineering, many new processes which require a large amount of pure enantiomers in a relatively short period of time are created. Preparative chromatography becomes one of the favored technologies for such process.

The basic mechanism for the separation of mixture by preparative chromatography is essentially the same as analytical chromatography. A pulse of the mixture is injected at the column inlet. Owing to the differences in the adsorption strength between the components and stationary phase, the velocities of each component differs along the column. The solute which is least strongly adsorbed to the stationary phase moves the fastest and elutes the column first. By suitably adjusting the operating conditions, provided the stationary phase can resolve the conditions, the purification of the desired

component can be achieved.

The entire system for a preparative chromatography consists of pumping system, injection system, separation system (column), collection system and in some cases, recycle system as shown in Fig. 1.3. The solute is dissolved in the solvent and filtered before entering the column to prevent contamination or column blockage. The total feed is then injected into the column in a sharp square pulse by the injection system. The column packing must be properly designed to ensure the entering fluid is evenly distributed across the cross section of column. The separation occurs as the components move along the column. Once the separated components elutes out of the column, they are sent to individual collectors using switching valves. This can be done automatically based on a pre-setting time or concentration measurements (UV, RI, conductivity, etc.). For a preparative system, stacked-injection is always the preferred fashion because it minimizes the cycle time and thus increases the productivity.

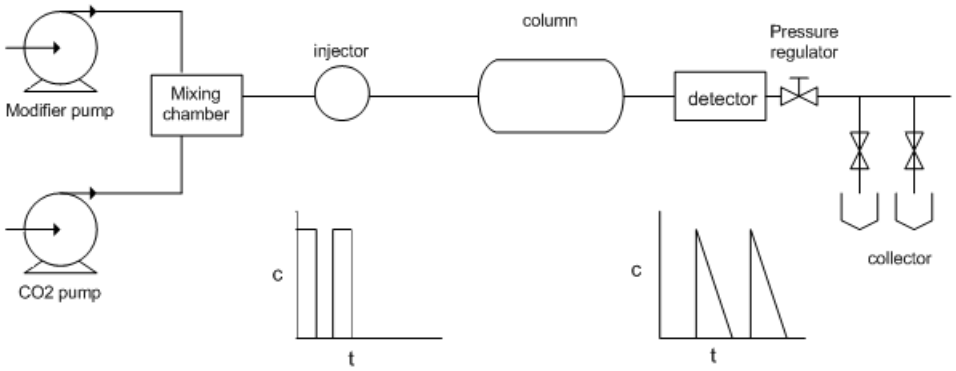

Figure 1.3: Schematic of a typical preparative chromatographic system

The product obtained in the collector is the purified desired component to-

gether with solvent. To obtain the final product, the component must be recovered from the remaining solvent or carrier gas. In gas chromatography (GC), this is usually done by condensers (cold traps). In liquid chromatography, evaporation, distillation, extraction or crystallization are normally available options. This brings an extra step and contributes to the total operation cost. In some cases, complete separation of solutes is not possible, to increase the recovery and productivity, the fraction containing both enantiomers is sent back to the column and recycled.

The total cost of a preparative chromatography system is controlled by many factors. Although the separations are done in the column, it is not always the controlling factor of total cost. With expensive packings such as affinity chromatography packings or bonded reverse-phase packings, the packing costs may be the major factor for the capital costs. With cheaper sorbents, the recovery of the solute from the collected fraction may control capital cost unless the stationary phase is replaced frequently. In cases where the gas or solvent is not recycled, the make-up expenses might be the highest operating cost. Since all the parts are important for the separation, to minimize the cost, the system must be optimized based on a systematic consideration of all parts. Generally, the higher the solute concentration leaving the column, the cheaper the separation and recovery costs.

Due to the development in theoretical studies in the past 20 years, several approaches have been proposed to model adsorption based processes. Different models such as ideal model, equilibrium-dispersive model and lumped kinetic model to describe the column dynamics have been developed [59].

The model together with the isotherm can be used to simulate the chromatogram at the column outlet. If the sample concentration is low, the equilibrium isotherm is at the linear range and analytical solution for the constituted equations is available. The process under such condition is easy to be simulated and the optimization for such system is straight-forward and relatively less time-consuming. However, since in most preparative scale chromatographic systems, the sample concentrations are kept high to obtain high productivity, the units are operated at conditions where the equilibrium isotherms are at non-linear range. There are several isotherm models to describe non-linear isotherm with different complexity. Unlike linear isotherm, analytical solution is available for non-linear isotherm only under limited and ideal conditions. The simulation for the column dynamics is performed by numerical methods which complicates the calculation and the necessary time for optimization increases compared to linear isotherm.

Although chromatographic separation methods typically are implemented as a batch process, simulated moving bed (SMB) has successfully converted it into a continuous enantioseparation technology [60, 61, 62]. The principle of SMB is to move the solid phase in a direction counter-current to that of the fluid phase by simultaneously switching the inlet and outlet ports. The schematic of a typical SMB process is shown in Fig. 1.4. The solutes and desorbent are fed into the system at the inlet of sections 3 and 1 respectively. The solid phase is recycled from section 1 to section 4 and the solvent elutes at section 4 is recycled to section 1. Desired components are collected at the extract and raffinate ports. In this fashion, the whole separation of

enantiomers turns into continuous mode since the feed and recycle are implemented continuously. The advantages of SMB include reduced solvent consumption and higher separating efficiency. Although compared to HPLC, SMB reduces the solvent consumption, it is still a solvent intensive process using about 200 L solvent for every kilogram of racemate resolved. Thus the need to replace the organic solvent with another environmental friendly fluid surges leading to the creation of SF-SMB. Besides the advantages mentioned above, the use of supercritical carbon dioxide as the mobile phase provides an easy separation of solute and mobile phase, low pressure drop and high column efficiency. Another attractive feature of using supercritical fluid is the larger number of the controllable factors to change the solvent strength in order to optimize the enantioseparation quality in SMB [22, 63]. The first enantioseparation by supercritical SMB was reported by Denet et al. and the separation of tetralol enantiomers was implemented [22]. The SF-SMB has been successfully designed and operated. Separations and its features are being explored [64, 65, 66].

1.3.1 General design consideration for preparative chromatography

Although preparative chromatographic methods are different with each other in many aspects such as stationary phase, mobile phase, etc.. There are some design requirements which are universal.

1. **Mobile and stationary phase requirement.** The ability of the stationary phase to separate the desired solutes is quantified by the

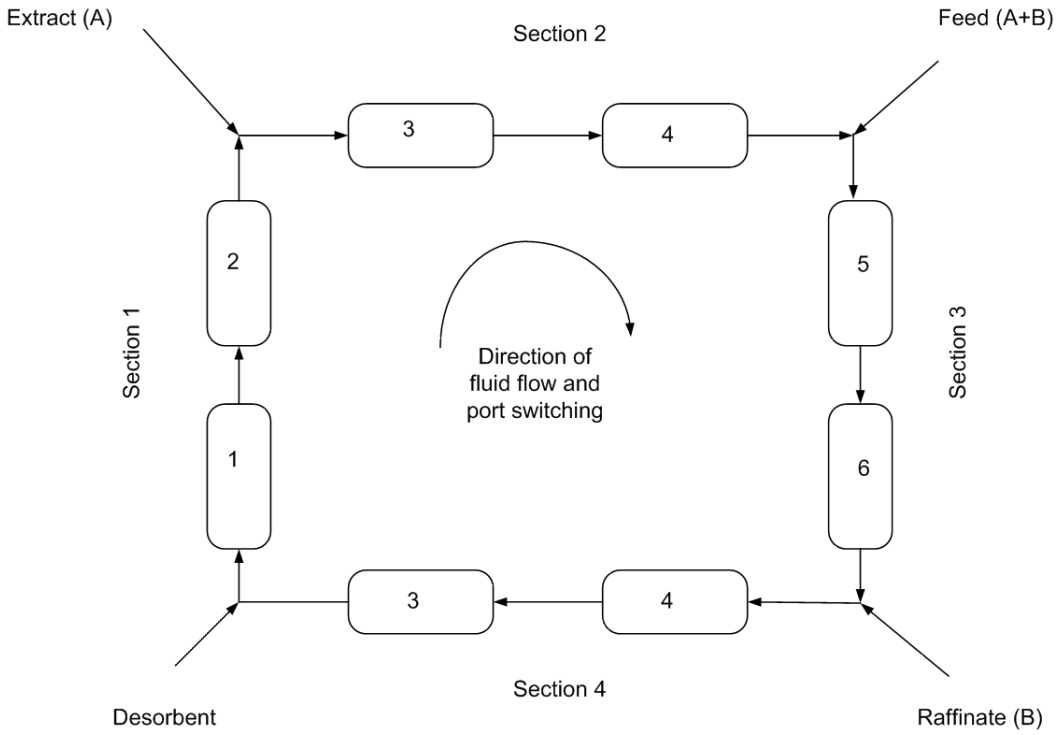

Figure 1.4: Schematic of a typical SMB system

selectivity which is the ratio of Henry constant (a measurement of adsorption strength) of two enantiomers. A selectivity close to 1 makes the separation impossible. As selectivity increase, the peak resolution improves which facilitate the separation allowing for injections of very large samples. If selectivity is higher than 1.5 or 2.0, the separation is considered easy to achieve. If selectivity is not high enough, for a preparative scale application, a study to increase the selectivity may be necessary. To obtain a satisfactory continuous separation results, the stationary phase must be rigid, chemically stable. Long life and high resistance to poisoning and fouling are highly desirable. This can be done by either changing or modifying the stationary phase or in liquid system adjusting the property of solvent. In addition to giving a high selectivity, the solvent in liquid systems must have good solubility of solute. For preparative scale separation, a large amount of solute is usually required to be separated. To increase the injection concentration and prevent precipitation inside the tubing and column, the solubility of solute must be high enough. The solvent or carrier gas must be easy to separate from the solutes and easy to purify and recycle. The solvent or carrier gas should have a low viscosity and high diffusivity, as these reduces pressure drop and height equivalent to a theoretical plate (HETP). A noncorrosive and nontoxic solvent or carrier gas which is inexpensive and readily available is desired.

2. **Column design requirements.** To ensure the solute move at the same velocity across the entire cross-section as narrow bands, an even

plug flow is desired. The axial mixing needs to be minimized both inside the packed section and in the distributors, valve, tubing, etc., since it destroys the separation. Dead volume of column must be minimized to prevent mixing. The distribution system at both ends should be designed to given even plug flow. Improperly designed distribution systems can drastically increase HETP. For some biological samples such as protein, the temperature must be controlled within a certain range to prevent degradation. In such case, a jacketed column is required. The solvent and sample must be pre-cooled/pre-heated before entering the column. As known, the HETP is related to particle diameter. The smaller particle size is, the smaller the HETP value is. To obtain high column efficiency, the manufacturer tends to produce long column with small particle size. However, this way for improving the separation efficiency is limited to some extent. The decrease in particle size brings a increase in pressure drop by order of 2. As mentioned before, a high pressure drop situation must be avoided. Thus a trade-off needs to be made between pressure drop and column efficiency.

1.4 Optimization of preparative chromatography

With the advances in equipment and stationary phase performance, preparative chromatography has been adopted as a major tool in many fields. A rational optimization for the purpose of avoiding costly, time and energy-consuming operation is an important objective in industry. Moreover, due to

the complexity of sample and mobile phase properties, process optimization requires a great deal of specialized knowledge. Preparative chromatography has many controllable instrumental and physicochemical parameters such as stationary phase characteristics, particle size, mobile phase composition, flow and temperature effect, all of these complicate the method development and optimization of the process. Although some of these parameters can be modeled theoretically, the attainment of an optimal preparative chromatography process still requires a lot of experimental work (parameter estimation and trial runs) and computational work (simulation and data handling) as well as the experience of the designer. A systematic approach to optimize a preparative scale chromatography process including the following steps:

1. **Screening of stationary phase and mobile phase**. A best combination of the mobile phase and stationary phase needs to be selected. The performance of sufficient number of commercially available stationary phase must be compared under various mobile phase compositions. A high selectivity and a relatively small retention factor are desired for an easy separation. The target components must have enough solubility in the mobile phase and the saturation capacity of the stationary phase must be large. These two points are normally not important for analytical scale separation but are of great importance for preparative separation since they play an important role for the economics of the process.

2. **Physico-chemical data collection.** Accurate measurements of chromatographic parameters are essential for a satisfactory estimation of

the optimal experimental conditions. These include the isotherm parameters with a suitable model to describe competitive behavior, the mass transfer parameters, viscosity and HETP values. There are many methods to obtain these parameters either by directly measurement or by inverse methods [67]. Both require significant time and effort. Caution should be exercised to those cases where the data obtained from analytical experiments is applied for the scale up of preparative separation. For example, the experimental data of isotherm is normally obtained from analytical scale injections at which the solute concentration in mobile phase is rather low compared with preparative scale separation. When applying the data for a scale-up, such variation has to be taken into account to prevent serious consequence.

3. **Computational work.** Once the physico-chemical data is available, a calculation program such as MATLAB or FORTRAN can be used to obtain the optimal operation conditions for any specific case. The formulation of the optimization problem is crucial. Different objective functions, product requirements and process limitations may lead to different optimization results. Selection of objective functions is based on reasonable estimation of the cost figure which is usually not straightforward and case-sensitive. After formulation of the problem, a proper optimization algorithm must be chosen to implement the calculation for the optimal solution.

4. **Experimental implementation** Finally, the optimal solutions given by the computer must be experimentally validated usually by a series of

experiments where the chromatogram and product quality are tested.

1.5 Objective and outline of the thesis

SFC has been recognized as an attractive auxiliary method for chiral separations. Although the applications of SFC in chiral separation, chemical analysis, natural product separation have been widely reported in last decade, there still exist certain scientific gaps in the field of SFC process study. Firstly, the fundamental mechanism of the separation process under SFC conditions is not clearly understood. Generally, the models which were used to describe the column dynamics in HPLC can be translated for the use of SFC. However, due to the unique properties of SFC, some phenomena encountered in SFC cannot be totally explained by these models. For example, the mobile phase in HPLC is considered to be a non-adsorbing component and the effect of it is negligible. In SFC, the supercritical CO_2 can actually adsorb to the stationary phase and must be taken into account for a satisfactory description of the adsorption in SFC [68]. Several papers regarding the effect of pressure, temperature and modifiers on the analytical separations have been published [69, 70]. However, a comprehensive study of the process is rare in literature. Thus a thorough understanding of SFC is necessary for the achievement of a efficient, economical and productive separation. Secondly, except several empirical optimization examples, few studies report regarding the SFC process optimization. Numerous operating factors in SFC bring both advantages and disadvantages. On one hand, such high number of factors provide opportunities to tune separation. On another

hand, all of these operating factors complicate the process and hinder the optimization study if a clearly understanding of the effect on separation is missing. Further a systematic study to understand the trade-off between productivity and solvent consumption for SFC separations is still missing in the literature.

Owing to the lack of studies in SFC, the motivation of this thesis is: to develop tools that will help the understanding of the fundamental mechanisms that dominate the SFC enantio-separation process and based on the theatrical modeling, to optimize the separation of enantiomers. The methodology for achieving this goal is shown in Fig. 1.5. It consists of four major steps: (i) complete screening, (ii) modeling, (iii) optimization and (iv) experimental implementation.

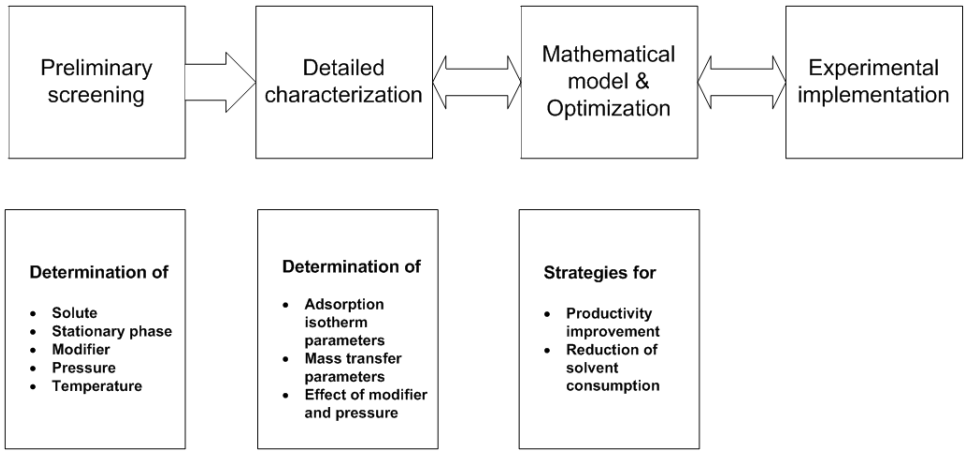

Figure 1.5: Schematic plan of the present study

i **Preliminary screening**. This involves the screening of different solutes and suitable stationary phase, pressure and temperature conditions. There exists no methodology for a priori determination of these

operation conditions. Performing screening experiments on an analytical scale is perhaps the best way to obtain this information quickly. This strategy was used in this study.

ii **Detailed characterization**. Once the chiral stationary phase, pressure, temperature, modifier type have been determined, the detailed characterization of the adsorption isotherm and mass transfer parameters shall be performed. These experiments shall be performed under column overload conditions, where the adsorption isotherm is in the non-linear range. At these conditions, it will be important to study the effect of various operating parameters on the separation. A particularly interesting issue to study will be the role of the modifiers. As discussed earlier, the modifier influences the separation through different mechanisms that are poorly understood. A systematic study of these effects through the use of experiments and mathematical models shall be used in order to elicit the effect of the modifiers and pressure in SFC.

iii **Mathematical model and optimization**. The development of a mathematical model is a key step. This model shall be used to determine the isotherm, mass transfer parameters under any given operating condition based on the collected data and for scale up of the separation. Moreover, the model shall be coupled with a suitable optimization algorithm to identify operating conditions that result in obtaining desired process performance. The optimization of different type of preparative chromatography process can be done by this model using a proper algorithm if enough experimental information is available. The search

for the optimal solutions based on given decision variables and satisfy constraints imposed by users is performed by the optimizer.

iv **Experimental implementation**. The last step of the study will involve the implementation of the given optimal scaled up separation condition and study of its performance characteristics. Particular attention shall be paid to the improvement of productivity and solvent consumption.

This thesis completed a total rational process design and optimization for a enantio-separation by SFC. The experimentally measured parameters were regressed in certain form and used to calculate the elution profiles under various operating conditions. The optimizations were carried out based on these parameters and optimum operating conditions under different requirements were obtained. Most important, these conditions were transferred onto real chiral separation operations and the final product was collected and examined.

Chapter 2 addresses the issue of measurement and regression of characterization parameters. It was implemented by injecting of sample with different concentration under various conditions and the parameters were obtained by inverse method. The effect of these parameters on the separation performance is also discussed.

Chapter 3 deals with the optimization of a isocratic SFC process. Suitable decision variables and objective functions were chosen based on the availability of experimental instrument and data. The optimization was carried

out under different requirements for two systems that differs in the flow rate setting. Optimum operating conditions were obtained and compared. The effect of decision variables on the separation performance is discussed.

Chapter 4 completes the optimization study for gradient elution by SFC. Solvent gradient was selected as the study target and due to the increased complexity in the operation, better separation performances were achieved. The optimum operating conditions under gradient elution were compared with the isocratic results. Finally, the effect of decision variables is studied.

Chapter 5 addresses the experimental implementation and collection of optimum operating conditions in Chapters 3 & 4. This is seldom reported in literature and efforts are necessary to ensure the successful transition from simulation to practical operation as it is not straightforward. Experimental elution profiles were compared with simulation and the desired products were collected. Various factors which affect the elution and collection are discussed.

Chapter 2

Preliminary screening and detailed characterization of the separation

The separation of the enantiomers of racemic flurbiprofen on an amylose-derived chiral stationary phase, Chiralpak AD-H, by supercritical fluid chromatography (SFC) under both linear and non-linear conditions is studied in this chapter. Pulse injections were implemented using supercritical CO_2 modified with methanol as a mobile phase at a temperature of 30°C. At linear conditions, the isotherm is determined directly from the chromatogram. Under overload conditions, the elution profiles were described by competitive Langmuir and bi-Langmuir isotherm. Isotherm parameters were estimated using the inverse method and the effects of operation variables such as pressure and modifier composition were studied. The value of selectivity is from 1.9 to 2.1 while the value of resolution is from 5.3 to 11.8. The number of theoretical plates is always greater than 5000 indicating high efficiency of SFC.

Keywords: Enantioseparation, Supercritical fluid chromatography, Competitive isotherm, Flurbiprofen, Model, Inverse method.

2.1 Introduction

The primary objective of this chapter is to elucidate adsorption isotherm in SFC; study the effect of modifier concentration and pressure on the isotherm in order to apply this knowledge to process optimization. In this study, flurbiprofen, a key non-steroidal anti-inflammatory drug, is used as the solute. Recent studies have shown that while both enantiomers can reduce the formation of a protein implicated in the formation of Alzheimer disease, the R-enantiomer shows much less action against the body's inflammatory response mechanism, thereby making it an ideal candidate for clinical studies [71, 72]. It is also worth mentioning that R-flurbiprofen is in a Phase II clinical trial for its potential role in treating prostrate cancer [73]. In this chapter, the linear and non-linear isotherms of flurbiprofen were measured using pulse injections. The adsorption isotherm parameters were elucidated by using the inverse method and influence of pressure and modifier composition on these parameters were studied.

2.2 Experimental

2.2.1 Materials

Racemic flurbiprofen (purity > 99%), pure enantiomers of flurbiprofen, S enantiomer with a purity of 98% and R enantiomer with a purity of 97%, were obtained from Sigma-Aldrich (Singapore). HPLC grade methanol was obtained from Aik Moh Paints and Chemicals, Singapore, and carbon dioxide with a purity of 99.8% was obtained from Singapore Oxygen Air Liquide, Sin-

gapore. A Chiralpak AD-H analytical column, 250×4.6 mm with an average particle size of 5 μm was obtained from Alpha Analytical, Singapore.

2.2.2 Setup and procedure

A Thar AMDS analytical SFC system (Thar Technologies, Pittsburgh, PA, USA) with minor modifications was used for the experiments. The CO_2 from the cylinder was cooled to 4°C and was pumped using a ISCO 260D syringe pump (Teledyne technologies company, Lincoln, NE, USA). Another ISCO 100DX syringe pump (Teledyne technologies company, Lincoln, NE, USA) was used to pump the modifier. The mobile phase consisting of CO_2 and the modifier flowed through an injection valve equipped with a 10 μL injection loop. The chromatographic column connected to the injection valve was housed in an air heated oven and the temperature was set to 30°C for all the experiments. A UV/Vis detector (151 Gilson, USA) fitted with a high pressure flow cell was used to measure the UV absorbance. A back pressure regulator located downstream of the UV detector controlled the system pressure.

Experiments were performed by pumping the desired flow rate of CO_2 and methanol using the syringe pumps and keeping the system back pressure at the desired level. For all the experiments, the CO_2 syringe pump was set to a constant flow rate of 1 mL/min with a pump head temperature of 4°C and the modifier syringe pump was set accordingly to provide the desired composition of methanol. After the system reached equilibrium, the sample was injected into the column. For the estimation of non-linear isotherm, the injections

were done in full loop mode which ensured that all the sample in the loop was positively injected. All the chromatographic responses were measured by the UV detector and recorded using a Process Suite software from Thar along with other experimental parameters, such as pressures, both upstream and downstream, and temperature. All injections were repeated at least three times to ensure reproducibility. The measured pressure drop across the column was less than 35 bar. The maximal and minimal density drop across the column were 15 g L^{-1} and 8 g L^{-1} respectively. This represented 1.63 % and 0.88 % drop in density respectively.

To calculate the density of the supercritical CO_2 and methanol mixture, the Peng-Robinson equation of state with a quadratic mixing rule is used [74]. It is worth noting that the Peng-Robinson equation of state may not yield accurate results especially for system near the critical conditions. Since the operating in the present study did not fall in this region. It was found that the calculated mixture densities were comparable to these in the literature [1], the deviations were always less than 5%. The average density along the column was used to obtain the volumetric flow rate inside the column and to characterize the Henry constants. Details of the Peng-Robinson equation of state are provided in Appendix A.

Prior to the isotherm estimation, the total porosity of column was measured. In this study, 1,3,5- tri -*tert*-butyl benzene (TTBB) which is usually considered as a non-adsorbing compound was used as the hold-up time marker [75]. Injections of TTBB were made to obtain the retention time of a non-adsorbing component t_0. Hence the total porosity, ϵ, can be calculated by

$\epsilon = t_0 Q/V$, where V is the column volume and Q is the volumetric flow rate. At a modifier composition of $c_{\mathrm{m}} = 13\%$, the measured voidage decreased from 0.863 to 0.785 as the pressure was increased from 120 bar to 210 bar. This behavior has been observed in other studies and can be attributed to the possibility that TTBB can indeed adsorb weakly at these operating conditions [69]. Hence, in this study, the lowest measured value, i.e. $\epsilon = 0.785$ was used for all calculations.

To investigate the influence of pressure and modifier concentration on the isotherm, pulse injections were performed at different pressure levels and modifier composition. For linear isotherm measurement, back pressure levels of $85, 100, 135, 170$ bar and modifier composition c_{m} of $13, 18, 23\%$ (w/w) were chosen as experimental conditions. The sample concentration was kept low to ensure that the isotherm is within linear range, which was confirmed by the symmetric chromatographic peaks. For non-linear isotherm measurement, pulse injections were made at back pressure levels of $100, 135, 170, 205$ bar and modifier composition c_{m}, of $13, 18, 20, 23\%$ (w/w). The choice of operating conditions ensured that no phase change of mobile phase occurred along the length of the column. The sample solution of racemic mixture and pure enantiomers of flurbiprofen were prepared by dissolving the solute in HPLC grade methanol. Three different concentrations namely, 75, 150, 300 g/L were chosen for the racemic injections while a 200 g/L sample was chosen for the two pure enantiomer injections.

2.3 Results and discussion

2.3.1 Linear isotherm

2.3.1.1 Screening of column and modifier

As described above, the Henry constant was obtained by performing pulse injections of dilute mixtures. Although the separation of flurbiprofen under analytical conditions in SFC has been reported in the literature [76, 77, 78], preliminary screening using different column and solvent combinations was performed. Two different kinds of chiral stationary phases namely, Chiralcel OD-H, Chiralpak AD-H and three modifiers, namely methanol, ethanol and 2-propanol, were tested for the enantioseparation of flurbiprofen. No separation was found on Chiralcel OD-H while complete separation of flurbiprofen enantiomers was achieved on Chiralpak AD-H. As shown in Fig. 2.1, all three modifiers yielded separations, with methanol offering the best selectivity and resolution. Hence, a Chiralpak AD-H column using methanol as modifier was used for the separation of flurbiprofen enantiomers.

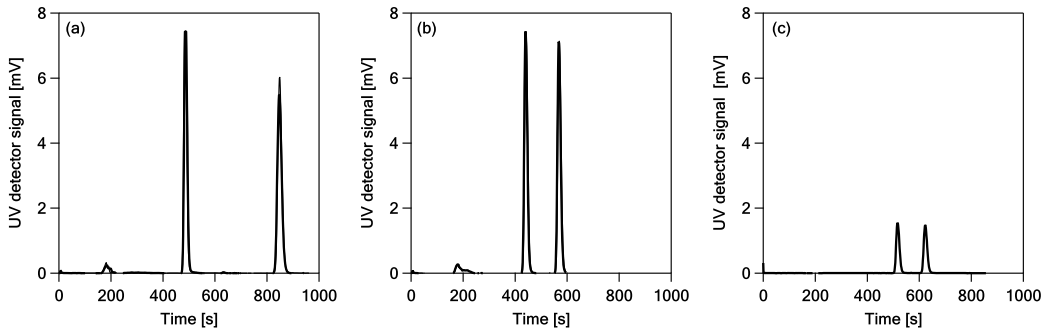

Figure 2.1: Effect of modifier type on the enantioseparation of flurbiprofen on Chiralpak AD-H (a) methanol, (b) ethanol, (c) 2-propanol. CO_2 flow rate: 1 cm^3 min^{-1}, modifier flow rate: 0.07 cm^3 min^{-1}, back pressure: 120 bar, column temperature: 30°C, UV wavelength: 220 nm.

2.3.1.2 Estimation of linear isotherm parameters

Under conditions where the isotherm is linear, the retention factor of component i, k_i, is calculated as:

$$k_i = \frac{t_i^R - t_0}{t_0} \tag{2.1}$$

where t_0 is the hold-up time, i.e. the retention time of a non-adsorbing component and t_i^R is the retention time of component i. The column hold-up time, t_0, was calculated using the void volume and the volumetric flow rate while the retention time, t_i, was obtained from the experimental chromatogram. If retention factor is known, the Henry constant, H_i can be calculated using the following relationship:

$$H_i = \left(\frac{\epsilon}{1-\epsilon}\right) k_i \tag{2.2}$$

The Henry constant of the two enantiomers of flurbiprofen as a function of fluid phase density under different modifier concentrations is shown in Fig. 2.2. It can be seen that for a given modifier concentration, the Henry constant decreases with an increase in pressure. This can be explained as mentioned previously by the fact that the density of a supercritical fluid is a strong function of pressure. At higher density the mobile phase has a stronger solvation power, hence resulting in a lower Henry constant. It can further be noticed that for a given density, the Henry constant decreases with increasing modifier composition. This is possibly due to the competitive effect of modifier as discussed before. These observations are consistent with earlier studies [22, 69]. Compared with the effect of pressure on retention time, the

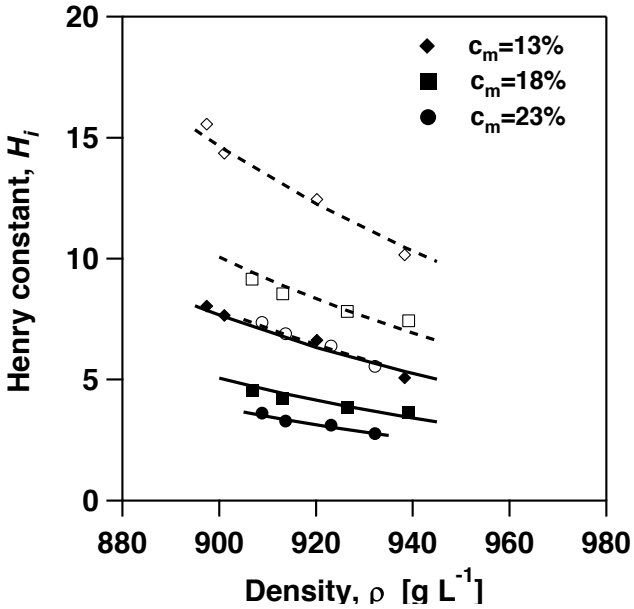

Figure 2.2: Dependence of Henry constant on mobile phase density at different modifier concentrations c_{m}, in %(w/w). The symbols are the experimental data, whereas the lines represent the correlation in Eq. 2.3. Closed symbols and solid lines correspond to the R enantiomer, while the open symbols and dotted lines correspond to the S enantiomer.

influence of modifier content was stronger. At a certain temperature, the Henry constant can be expressed as a semi-empirical function of mobile phase density and modifier concentration [69]:

$$H_i = \frac{1}{a_i c_m + d_i} \left(\frac{\rho^o}{\rho} \right)^{p_i c_m + r_i} \tag{2.3}$$

where c_{m} is the modifier concentration in %(w/w), ρ and ρ^o are the density at operating and reference conditions respectively, while parameters a_i, d_i, p_i and r_i are empirical constants. To obtain the best fit of the above equation to the experimental data, all the parameters were estimated simultaneously by reducing the sum of the residuals of the calculated and experimentally determined Henry constant. The resulting empirical parameters are reported in Table 2.1. The comparisons of experimentally determined Henry constant

Table 2.1: Empirical parameters, corresponding to Eq. 2.3, reference density $\rho^0 = 1000.0$ g L^{-1}

Component	a	d	p	r
R	0.0378	-0.165	0.0791	7.67
S	0.0172	-0.0636	0.104	6.72

and the predicted ones are plotted in Fig 2.2. As can be observed from the figure, the semi-empirical correlation is able to describe the influence of the fluid phase density and the modifier concentration on the Henry constant of the solute satisfactorily.

The selectivity, α, is defined as:

$$\alpha = H_2/H_1 \tag{2.4}$$

where the indices 1 and 2 correspond to the weakly and strongly adsorbed components respectively. In the present case, R & S enantiomers corresponded to the weakly and strongly adsorbed components respectively. The peak resolution of the enantiomers (R_s), in terms of the number of theoretical plates, N, retention factor of component 1, k_1, and selectivity, α, is given as:

$$R_s = \frac{\sqrt{N}}{2}\left(\frac{\alpha - 1}{\alpha + 1}\right)\frac{k_1}{1 + k_1} \tag{2.5}$$

where the number of theoretical plates, N, can be calculated from the experimental Gaussian peaks, by following expression:

$$N = 5.55\left(\frac{t_i^R}{w}\right)^2 \tag{2.6}$$

with w has the peak width at half peak height.

The dependence of selectivity and resolution on the mobile phase density and modifier composition is shown in Fig. 2.3. Within the range of parameters studied, the selectivity showed a modest dependence on the operating parameters. Further at a particular modifier composition, no clear trend for the dependence of selectivity on density was observed. Fig. 2.3(b) shows the dependence of resolution on the parameters. It can be seen that an increase in both density and modifier content leads to a decrease in the resolution. The values and trends are comparable to those reported in the literature [76, 77]. The effect of density on resolution was more profound at lower modifier compositions.

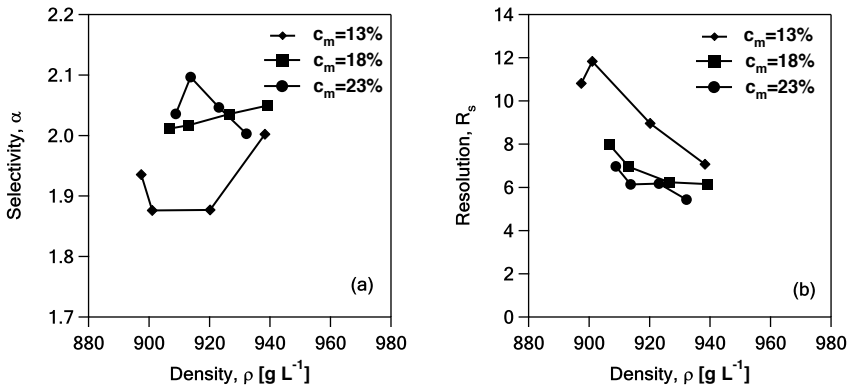

Figure 2.3: Dependence of (a) selectivity and (b) peak resolution of Chiralpak AD-H for the separation of the enantiomers of flurbiprofen on density at different modifier concentration (c_{m}, wt.%). Symbols correspond to experimental values, while lines are drawn to guide the eyes.

2.3.2 Non-linear isotherms

2.3.2.1 UV calibration

The linear isotherm parameters were estimated from the measurement of the peak retention time. For these measurements, no information about the

concentration along the elution profile is required. However, to calculate the non-linear adsorption isotherms using the inverse method, it is necessary to obtain the concentration of each point on the elution profile. Thus, it is essential to obtain a calibration curve that converts the UV signal to solute concentration [79].

Conventionally, the calibration curve under non-linear conditions is derived from the results obtained in frontal analysis or by injecting solutions of known concentration directly to the detector cell . These methods use large quantity of solute which especially for chiral compounds, can be expensive. In this study, an indirect method is employed to obtain the calibration curve [79, 80]. This procedure uses the same chromatogram for isotherm calculation which eliminates independent calibration of the detector and reduces the use of solutes. The following three parameter calibration curve was used to relate the fluid phase concentration c to the UV signal Sig:

$$c(Sig) = -b_1 ln\left(1 - \frac{Sig}{b_2}\right) + b_3 Sig \tag{2.7}$$

In the above expression, b_1, b_2, b_3 are positive constants which are fitted in order to minimize the sum of squared errors, J, between the estimated and the known injected amounts of solute which is defined as:

$$J = \sum_{k=1}^{N_{exp}} \left(\frac{c_k^{loop} V^{loop} - Q \int c_k(Sig) dt}{c_k^{loop} V^{loop}} \right)^2 \tag{2.8}$$

In Eq. 2.8, the first term in the numerator represents the amount of the solute injected, while the second term describes the amount eluting at the column outlet obtained by integrating the chromatographic peak. The difference of

the two terms is normalized to the mass injected thus giving equal weightage to all experiments. Since pressure and modifier concentrations can alter the UV absorbance characterizations, a different set of b_1, b_2 and b_3 was obtained corresponding to each operating condition.

2.3.2.2 Modeling

Several methods are available for the estimation of non-linear isotherms from experiments [67, 81]. The choice of the methods depend on several factors such as effort and accuracy required, availability of instrumentation, etc. Estimation of isotherms by injecting concentrated pulse is often performed as it reduces the amount of solute required for parameter estimation. However, a serious drawback of this method is that the concentration measured at the column outlet is lower than what is injected and hence the determined isotherm can be used with confidence only over a limited range of concentration. In this work the inverse method is used to estimate isotherm parameters [81]. In brief, the first step in this method is the measurement of experimental elution profiles. Then a proper isotherm model is chosen and numerical simulations are used to calculate the elution profile at conditions identical to the experiments. In the process, the isotherm and mass transfer parameter are evaluated by minimizing the difference between the experimental profile and the calculated one.

Let us consider a chromatographic column operating at constant temperature and negligible pressure drop. Under these operating conditions the material

balance of solute is given by:

$$\frac{\partial c_i}{\partial t} = D_{ax,i}\frac{\partial^2 c_i}{\partial z^2} - \frac{\partial (c_i v)}{\partial z} - \frac{1-\epsilon}{\epsilon}\frac{\partial n_i}{\partial t} \tag{2.9}$$

where c_i and n_i are the concentrations of i in the mobile phase and in the stationary phase respectively, v is chromatographic linear velocity, $D_{ax,i}$ is the axial dispersion coefficient and ϵ is the total porosity of column. The first term on the right hand side represents the axial dispersion; the second term the convection and the last term the accumulation in the solid phase. In current study, the pressure drop of the column and the change of velocity arising due to the adsorption of the solute are assumed to be negligible. These can be justified considering low flow rates and low concentration of the solute in the mobile phase. Under these conditions, Eq. 2.9 can be written as:

$$\frac{\partial c_i}{\partial t} = D_{ax,i}\frac{\partial^2 c_i}{\partial z^2} - v\frac{\partial c_i}{\partial z} - \frac{1-\varepsilon}{\varepsilon}\frac{\partial n_i}{\partial t} \tag{2.10}$$

The solid phase accumulation can be described at various levels of details depending on the governing resistance to mass transfer. However, a simple formalism, the linear driving force (LDF) model that lumps the different resistances into the mass transfer coefficient $k_{f,i}$ is used in the present study. The LDF model can be written as:

$$\frac{dn_i}{dt} = k_{f,i}(n_i^* - n_i) \tag{2.11}$$

where n_i^* is the concentration in the adsorbed phase in equilibrium with the concentration c_i in the mobile phase. The description of the solute material

balance is completed with the introduction of the adsorption isotherm:

$$n_i^* = f(c_i) \tag{2.12}$$

The set of partial differential equations can be solved once suitable initial and boundary conditions are obtained. In this case, the column is completely clean prior to the injection of pulse, and initial conditions are given by:

$$c_i(t=0,z): \; c_i^{init} = 0, \qquad i = 1...\ N \tag{2.13}$$

$$n_i(t=0,z): \; n_i^*(c_i^{init}) = 0, \;\; i = 1...\ N \tag{2.14}$$

The Danckwerts' boundary conditions, which take into account the effect of axial dispersion at the column inlet are used and can be expressed as:

$$At\ z = 0: \; c_i(t) = c_i^{inj}(t) + \frac{D_{ax,i}}{v}\frac{\partial c_i}{\partial z}\bigg|_{t,z=0}, \qquad i = 1...\ N \tag{2.15}$$

$$At\ z = L: \; \frac{\partial c_i}{\partial z}\bigg|_{t,z=L} = 0, \qquad i = 1...\ N \tag{2.16}$$

In SFC, owing to the mass transfer characteristics of the fluid and due to the small size of the stationary phase, mass transfer resistances are less significant compared to HPLC. Hence, in this study, all dispersion effects, caused either due to axial dispersion or mass transfer resistances, are lumped into the mass transfer coefficient, $k_{f,i}$, and a very low value for the axial dispersion coefficient for all the simulations $D_{ax,i} = 0.00001$ cm^2 s^{-1} was assumed. The PDEs were discretized in space using a finite difference scheme with 2000 grid points and the resulting ODEs were solved using the Gear's method as implemented in IMSL FORTRAN subroutines.

2.3.2.3 Isotherm models and parameters estimation

The isotherm model describes the mathematical formalism to determine the equilibrium between the fluid and solid phases. Several models have been proposed in the literature with varying levels of complexity. For systems that show a favorable behavior, the competitive isotherm is perhaps the simplest. In this study, we use the following form of the competitive Langmuir isotherm:

$$n_i^* = \frac{H_i c_i}{1 + \sum_{j=1}^{n} K_j c_j} = \frac{K_i \Gamma_i c_i}{1 + \sum_{j=1}^{n} K_j c_j}, \quad i = 1, ..., N \tag{2.17}$$

where Γ_i and K_i are the saturation capacity and equilibrium constant of the solute i. Here we allow the two species to have different saturation capacities. For a binary system, this represents an equation with four parameters: namely, Γ_R, Γ_S, K_R and K_S.

An alternative formalism that is often considered for chiral stationary phase which consist of selective and non-selective sites is the bi-Langmuir isotherm. Although there are several formalisms [82], we choose the following:

$$n_i^* = \frac{\Gamma_{ns} K_{ns} c_i}{1 + \sum_{j=1}^{n} K_{ns} c_j} + \frac{\Gamma_{sel} K_{sel,i} c_i}{1 + \sum_{j=1}^{n} K_{sel,j} c_j}, \quad i = 1, ..., N \tag{2.18}$$

In this formalism the saturation capacity of selective (Γ_{sel}) and non-selective sites (Γ_s) are assumed to be equal for two enantiomers. Hence, this isotherm expression results in five parameters namely, Γ_{ns}, Γ_{sel}, K_{ns}, $K_{s,R}$, $K_{s,S}$.

From the equations described above, it is clear that for a particular operating condition, the mass transfer coefficient, $k_{f,i}$ and isotherm parameters, K_i, Γ_i for the Langmuir isotherm and K_{ns}, $K_{sel,i}$, Γ_{ns}, Γ_{sel} for the bi-Langmuir isotherm have to be estimated. In the frame of the inverse method these

parameters are obtained comparing the calculated profiles to those measured experimentally. The best fit parameters are obtained by minimizing the objective function Ψ which is given as:

$$\Psi = \frac{1}{c_k^{loop}} \int_0^{\infty} |c_i^{sim} - c_i^{exp}| \, dt \quad (i = R, S) \tag{2.19}$$

For all the cases these parameters were estimated from the elution profiles of the pure enantiomers. To obtain the parameters, a Simplex method was used. Since the observed experimental elution profiles showed a minor effect of band broadening, high values of mass transfer coefficient were used as initial guesses. For the isotherm parameters, good initial guesses were obtained from the retention time method [83] and the Henry constant measured at linear conditions. Using the values estimated, the elution profile of the racemic injections were calculated.

2.3.2.4 Experimental results for non-linear isotherm estimation

A representative set of experimental elution profiles for different injected concentrations is shown in Fig. 2.4 and 2.5. It can be seen that both pure enantiomers and racemic injections show elution profiles that are typical of systems that have a favorable isotherm. Sharp fronts indicate that the mass transfer resistances are negligible. This can be caused due to two contributing factors, namely the use of small particles (5 μm) together with the use of a mobile phase that results in reduced resistance to mass transfer and broadening. Similar observations were found for other experimental conditions which are shown in appendix B.

The competitive Langmuir isotherm parameters obtained from inverse

method are also used to calculate elution profiles using the equilibrium theory of chromatography where axial dispersion and mass transfer resistances are not considered. The comparison are shown in Fig. 2.6. The nice match confirms both the validity of the isotherm parameters and the fact that mass transfer resistances are indeed negligible.

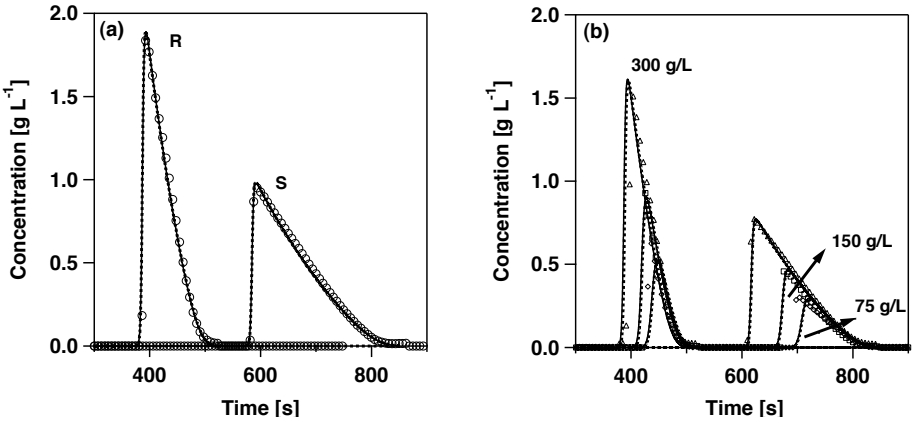

Figure 2.4: Experimental (symbols) and simulated (lines) pulse response of the enantiomers of flurbiprofen on Chiralpak AD-H. (a) pure component injections, (b) racemic injections. Pressure: 100 bar, modifier concentration: 13 % (w/w). Solid lines indicate simulated results using a competitive Langmuir model while the dotted lines represent the simulation using a bi-Langmuir model.

2.3.3 Estimation of mass transfer coefficient

The values of the mass transfer coefficient $k_{f,i}$ under different operating conditions are listed in Table 2.2 and Table 2.3. It can be seen that the mass transfer coefficients are rather high compared to the corresponding HPLC cases. This is confirmed visually by the sharp peaks observed in the elution profiles shown in Fig. 2.4. No clear trend of mass transfer coefficient with respect to pressure or modifier concentration was observed. The estimated mass transfer coefficients are rather high and do not influence the profiles,

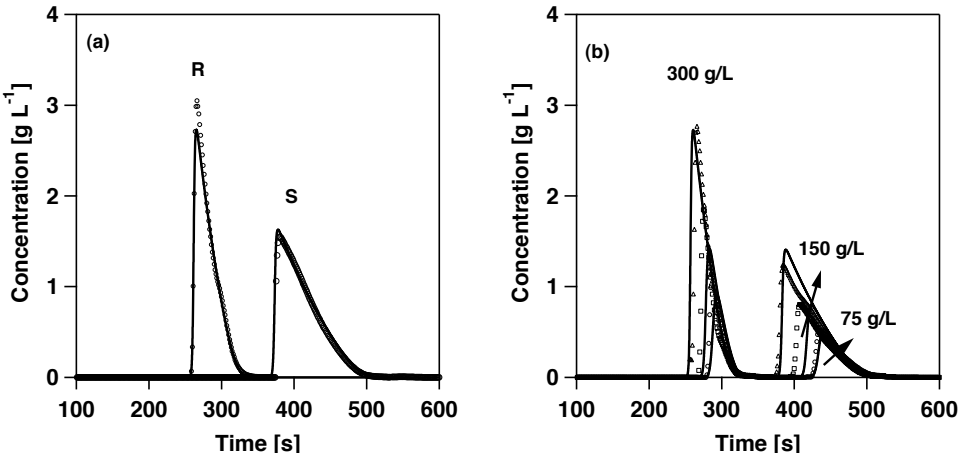

Figure 2.5: Experimental (symbols) and simulated (lines) pulse response of the enantiomers of flurbiprofen on Chiralpak AD-H. (a) pure component injections, (b) racemic injections. Pressure: 100 bar, modifier concentration: 20 % (w/w). Solid lines indicate simulated results using a competitive Langmuir model.

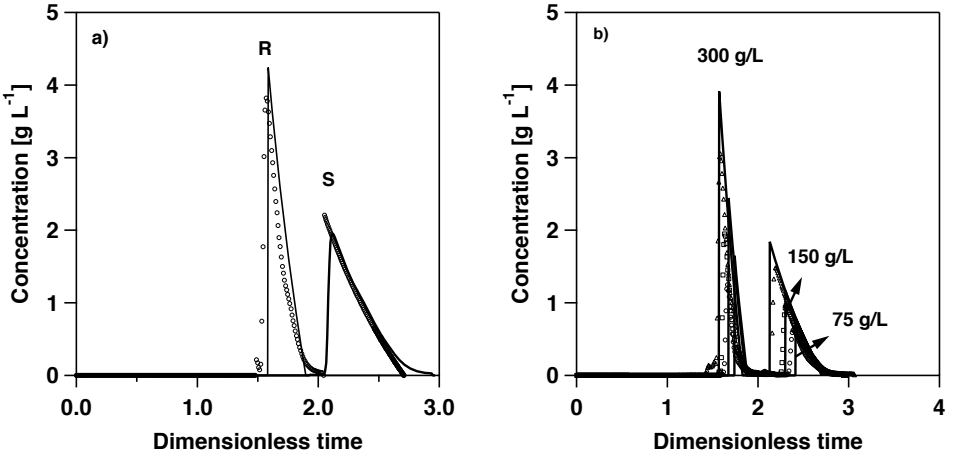

Figure 2.6: Experimental (symbols) and simulated (lines) pulse response of the enantiomers of flurbiprofen on Chiralpak AD-H. (a) pure component injections, (b) racemic injections. Pressure: 135 bar, modifier concentration: 23 % (w/w). Solid lines indicate simulated results using a competitive Langmuir model and equilibrium theory.

even if they are varied. This can be attributed to a low resistance to mass transfer which is an attractive feature of SFC. It is also worth recollecting that in this work the effects of both axial dispersion and mass transfer are lumped into the mass transfer coefficient.

Table 2.2: Estimated adsorption isotherm parameters for the competitive Langmuir model.

c_m (% w/w)	Pressure (bar)	K_R (L g^{-1})	Γ_R (g L^{-1})	$k_{f,R}$ (s^{-1})	K_S (L g^{-1})	Γ_S (g L^{-1})	$k_{f,S}$ (s^{-1})
13	100	0.0910	81.2	8.83	0.219	66.9	10.6
	135	0.0630	97.6	7.11	0.204	61.7	4.48
	170	0.0642	84.6	10.9	0.171	62.6	6.13
	205	0.0560	85.4	27.8	0.157	61.3	22.7
18	100	0.0884	54.7	19.3	0.237	40.8	20.0
	135	0.0562	71.9	17.7	0.154	54.7	11.0
	170	0.0507	73.6	21.4	0.153	51.2	14.5
	205	0.0673	54.5	20.9	0.162	45.2	8.91
20	100	0.0715	53.0	25.5	0.128	64.9	21.3
	135	0.0364	85.8	23.3	0.125	55.3	16.8
	170	0.0308	90.2	7.66	0.107	58.8	14.7
	205	0.0326	83.3	24.8	0.0958	61.0	16.5
23	100	0.0516	61.6	52.3	0.117	57.1	26.9
	135	0.0563	58.0	3.80	0.125	49.8	3.25
	170	0.0309	83.2	45.0	0.0849	63.8	17.2
	205	0.0563	45.2	15.4	0.117	45.8	21.0

2.3.4 Estimation of isotherm parameters

For the determination of the competitive Langmuir isotherm, all the four parameters were fitted using the method describe above. The isotherm parameters were estimated using the pure component injections alone. The estimated parameters are listed in Table 2.2 and the corresponding isotherms are plotted in Fig. 2.7. From the figure, it can be seen that at particular modifier concentration, lower pressure leads to a higher non-linearity of the isotherm.

Table 2.3: Estimated adsorption isotherm parameters for the bi-Langmuir model.

c_m (% w/w)	Pressure (bar)	Γ_{ns} (g L^{-1})	K_{ns} (L g^{-1})	Γ_s (g L^{-1})	K_R (L g^{-1})	$k_{f,R}$ (s^{-1})	K_S (g L^{-1})	$k_{f,S}$ (s^{-1})
13	100	34.674	0.066	48.504	0.106	10.469	0.257	12.500
	135	82.481	0.038	30.391	0.102	10.313	0.330	11.250
	170	50.026	0.046	37.395	0.085	10.938	0.228	10.313
	205	52.760	0.029	43.190	0.077	12.500	0.187	10.000
18	100	35.609	0.083	20.034	0.093	6.000	0.340	4.500
	135	54.495	0.062	21.586	0.029	7.813	0.234	3.500
	170	58.824	0.058	16.856	0.019	7.820	0.259	2.875
	205	45.556	0.074	14.232	0.021	6.500	0.286	3.250
20	100	20.165	0.024	57.280	0.061	4.813	0.137	3.125
	135	68.992	0.019	36.128	0.050	4.390	0.154	2.875
	170	70.500	0.026	28.783	0.034	9.500	0.158	3.750
	205	47.350	0.020	42.534	0.041	8.531	0.115	4.250
23	100	34.738	0.042	38.226	0.041	3.844	0.132	2.625
	135	24.901	0.007	46.568	0.060	4.688	0.130	2.675
	170	43.826	0.025	43.960	0.032	5.117	0.092	2.367
	205	23.333	0.031	33.033	0.050	2.438	0.141	2.250

In addition, at a particular pressure, increasing the modifier concentration reduces the non-linearity. The comparison of experimental elution profile and the calculated one is shown in Fig. 2.4. It can be seen that the comparison is rather excellent. The values of the saturation capacity are plotted against modifier concentration and density in Fig 2.8. Theoretically, the value of Γ_i is expected to decrease with increasing modifier concentration since more of the available sites are occupied by the modifier. However, no clear trend was found for the relationship between Γ_i density and modifier concentration in this study as compared to previous studies [79]. It is worth emphasizing that these experiments were at moderate loading compared to saturation capacities and hence a physical interpretation of the parameter should be performed with caution, and these should rather be treated as model parameters. Although we recognized this shortcoming, which are typical of injections of

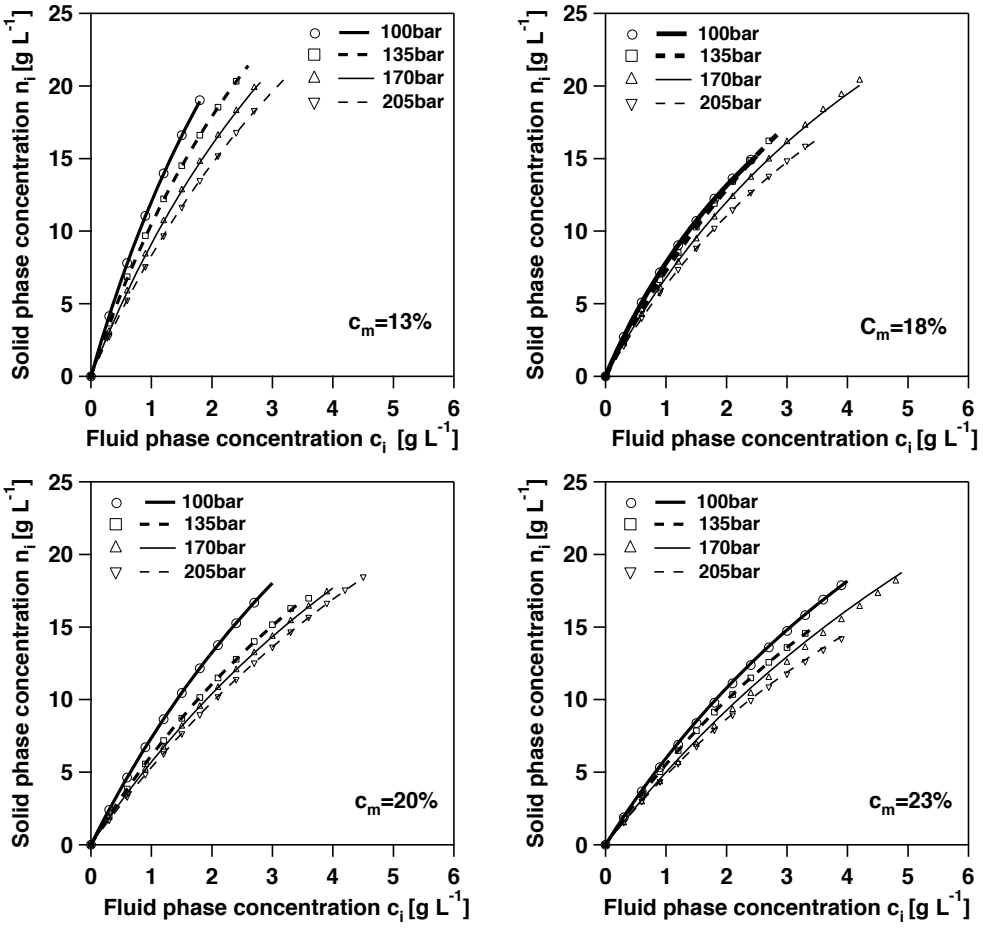

Figure 2.7: Measured non-linear isotherms for the S enantiomer of flurbiprofen at different operating conditions. The lines and symbols correspond to isotherm described by the competitive Langmuir and bi-Langmuir models respectively.

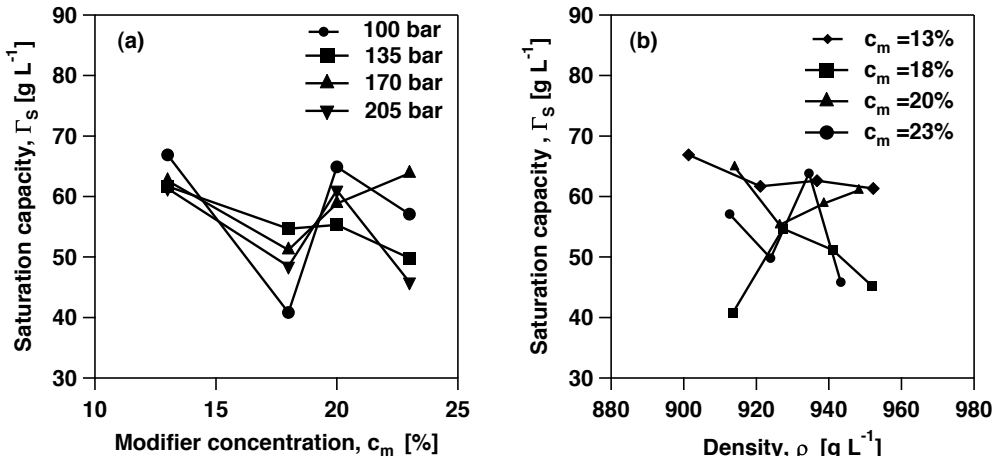

Figure 2.8: Dependence of saturation capacity of S enantiomer on (a) modifier concentration and (b) density. The symbols indicate the values fitted to the competitive Langmuir model while the lines are drawn to guide the eye.

short pulses, the parameters obtained can still be used for process design with confidence. This has been demonstrated earlier where isotherm parameters estimated from analytical conditions, using the inverse method, was successfully used for the design of supercritical SMB [65]. The parameters of the bi-Langmuir isotherm were obtained in the same manner as above. The estimated parameters are listed in Table 2.3 and the corresponding isotherm are plotted in Fig. 2.7. It can be seen from Fig. 2.7 the isotherms calculated by the Langmuir and bi-Langmuir equations are comparable. Similar to the case of the competitive Langmuir isotherm, the saturation capacities did not show a clear trend with respect to neither the density nor with the modifier composition. The comparison of the experimental elution profiles and the calculated one is shown in Fig. 2.4a. A remarkable match can be observed.

It is worth noting that the Henry constants obtained from the overloaded injections were comparable to those obtained from dilute injections. The

average deviation of Henry's constant between linear and non-linear cases is less than 7.5%. This reassures the confidence in the parameters over the range of concentrations that have been experimentally covered.

2.3.5 Racemic injections

After the parameters were estimated, they were used to calculate the elution profiles of racemic injections. For these calculations, the numerical technique described in section 2.3.2.2 was used. Fig. 2.4b shows the comparison of the experimental and calculated elution profiles. Although minor derivations are seen in the predictions of the front at low injection concentrations, the comparison is rather good at large injected composition. The ability of the two isotherm models to predict the elution profiles of the racemic injections was compared using the average value of the errors which is defined as:

$$\overline{\Psi} = \frac{1}{N_{\text{exp}}} \sum_{k=1}^{N_{\text{exp}}} \frac{|c_k^{sim}(t) - c_k^{exp}(t)|}{c_k^{loop}} \tag{2.20}$$

where N_{exp} is the number of racemic injections. For each modifier concentration $N_{\text{exp}} = 12$. The calculated values of the $\overline{\Psi}$ is given in Table 2.4. It can be seen that the bi-Langmuir model yields marginally better results compared to the competitive Langmuir model. However, it could be argued that the simplicity of the Langmuir model is perhaps suitable enough to model the competitive behavior for the range of concentrations studied. This has been demonstrated in our recent studies, where the Langmuir isotherm resulted in good predictions of experimental profiles even under gradient operations as discussed in the Chapter 4.

Table 2.4: Errors between experimental and calculated profiles by Langmuir and bi-Langmuir models

c_{m} (% w/w)	$\overline{\Psi}_{\mathrm{Langmuir}}$ (-)	$\overline{\Psi}_{\mathrm{bi-Langmuir}}$ (-)
13	0.469	0.301
18	0.509	0.384
20	0.414	0.391
23	0.530	0.360

2.4 Conclusions

The SFC enantioseparation of flurbiprofen, a key non-steroidal anti-inflammatory drug, on Chiralpak AD-H was studied. Experiments were performed at both dilute and overloaded conditions. The linear isotherms showed characteristics typical to SFC systems, i.e, the Henry constants decreased with increasing density and modifier conditions. Non-linear isotherm were measured using the inverse method by matching experimental elution profiles of pure enantiomer with calculated ones based on competitive Langmuir and bi-Langmuir isotherm. The isotherm parameters were obtained from single component injections. It was found that mass transfer coefficients were rather high and this was reflected by the sharp elution profiles. The saturation capacities did not show regular trends with neither the density nor the modifier concentration. The isotherm parameters from single component injection were used to calculate the profiles of racemic injections. Although minor deviations were found at low injected concentrations, the elution profiles were well predicted especially for high injected concentrations. The effectiveness of these parameters have been verified for

process optimization studies, details of which was presented in Chapter 3 and 4.

Chapter 3

Optimization of isocratic supercritical fluid chromatography process for enantioseparation

This chapter presents multi-objective optimization analysis of a single column isocratic supercritical fluid chromatography process for the enantioseparation of flurbiprofen. The single column process is simulated using a detailed model with equilibrium description by competitive Langmuir isotherm. The HETP and pressure drop under different modifier composition were measured and have been taken into account in the optimization. The optimization problem has been formulated as a multi-objective optimization. The objectives are maximization of productivity and minimization of solvent consumption under different purity and recovery constraints with different operating parameters: namely, injection concentration, injection volume, flow rate and modifier composition. The results indicate significant performance improvement in terms of increased productivity and reduced solvent consumption compared with performance reported in the literature. Moreover, the effect of each decision variable on the objective functions is discussed.

Keywords: Enantioseparation, Supercritical fluid chromatography, Multi-objective optimization, Isocratic elution, Generic algorithm

3.1 Introduction

Supercritical fluid chromatography (SFC) is one of the most promising chromatographic methods in achieving fast enantioseparations with high productivity [84]. However, optimal operation of the SFC process that maximizes the productivity and further decreases the solvent consumption is yet scarce in practice. This is primarily due to the large number of controllable instrumental and physicochemical parameters in SFC process, In this chapter, optimization of the isocratic SFC process has been undertaken using a detailed mathematical model. Genetic algorithm has been used for the search of optimal operating conditions. Since both productivity and solvent consumption influence the economy of the SFC process, the optimization problem has been formulated as a multi-objective optimization problem, instead of a single objective optimization problem. The enantioseparation of flurbiprofen is considered as a model system. The optimization studies have been done with actual experimental data under different purity and recovery constraints.

Any optimization problem begins with the selection of objective functions and decision variables. The objective functions translate the performance and characteristics of separation into quantitative parameters. An ideal objective function must be able to compare and differentiate between good and poor separation quality and effectively describe the quantitative scaling of separation performance. Also, the objective functions must be suitable for the purpose of the chromatography and should be affected by operating parameters or controllable factors whose values are to be chosen. Moreover, the objective functions must be correlated with controllable parameters in such

a way that it can be interpreted rationally. The objective functions should not have any internal mathematical limitations or inconsistencies.

For the case of preparative chromatography, the best objective function is clearly the product cost. However, due to the complexity of the whole cost composition, reasonable estimation is usually not available. Mostly used objective function in academic studies is the productivity. Maximization of productivity is only realistic in cases where the capital costs consist the major portion for the total costs. In practice, the operation cost especially the energy consumption for product recovery and cost spent on solvent recycle and handling consist a big portion of the total cost. Thus to optimize a single objective function is not enough to represent the real economics of the process and the optimization problems are normally formulated as multi-objective optimization. Additional objective functions are usually solvent consumption, yield etc.

After the objective functions are chosen, the next step for the problem formulation is to choose decision variables and constraints. The decision variables are the controllable factors used to affect the separation. Different combination of decision variables lead to different separation results. Each set of them serves as one solution to the problem. The given results need to satisfy certain requirements called constraints. The constraints can either be the product quality, equipment limitation or all of them. The final optimal results are sets of decision variables which give the optimum value of objective functions and satisfy all the constraints set by end user.

Single objective optimization and multi-objective optimization are conceptu-

ally different. For single objective optimization, there only exists one single solution to either maximize or minimize the objective function. For multi-objective optimization, if the objectives are competing, a compromise must be made between the objective functions. Further, it is usually not possible that the possible optimum values of all the objective functions can be achieved by the same values of decision variables. In such cases, the resulting optimal operating conditions are a series of optimal conditions called Pareto curve. Among the Pareto curve, all the points are optimal solutions because moving from one point to another, one objective function improves while the other deteriorates. To solve multi-objective optimization problems, many approaches have been used, for example, minmax formulation [85] where no preferences are provided and directly optimizes the overall maximum value or weighted sum method [86] in which the preference information is given by the designer. Most of the traditional optimization algorithm tends to approach the optimum value step by step, which means the solution updates in each iteration. These methods have the possibility falling into a local minimum. To avoid such situation, evolutionary algorithms such as genetic algorithm can be applied [87]. Genetic algorithm solves multi-objective optimization problems based on the mechanism of natural selection and natural genetic. The algorithm uses a population of chromosomes which are composed of a particular set of decision variables. The algorithm begins with a generation of randomly chosen or given set of chromosomes. The fitness (related with objective functions) of each chromosomes is evaluated and sorted with those having better fitness. The higher the fitness is, the more possible it can survive. Next generation of chromosomes are created based on the previous

generation but undergo reproduction, crossover and mutation. Crossover is to exchange parts of a set of randomly chosen parent chromosomes and create the offspring chromosomes. Mutation is performed to randomly change the parts of next generation generated from the crossover. Such step is to prevent the solution trapping into local optimum. The procedure repeats to create the next new generation of chromosomes. Generally, the fitness of each generation is better than the previous one. The optimization terminates at a given number of generations or until a satisfactory improvement of the objective functions is achieved. In this chapter, a few key experimental parameters necessary for the optimization are first measured. Then the optimization problem is formulated and solved. The results are analyzed and the effect of decision variables on process performance are discussed.

3.2 System characterization

3.2.1 Material and experimental set-up

The materials and experimental set-up used for experiments are identical to those described in chapter 2. Further a detailed study that explores the effect of pressure and modifier composition on the adsorption equilibrium and mass transfer characteristic has also been described in chapter 2. These values have been used in this study as well. Besides, data to account for the effect of flow rate on pressure drop and efficiency was needed to carry out the optimization studies. These experiments are discussed below.

3.2.2 Pressure drop characterization

The pressure drop measurements at different flow rates and modifier concentrations were performed at a fixed back pressure of 135 bar. The measured pressure drops are plotted in Fig. 3.1. As expected, the pressure drop increased with increasing flow rate and modifier concentrations [70]. The pressure drop across the column in SFC can be described by the Darcy's law [88]:

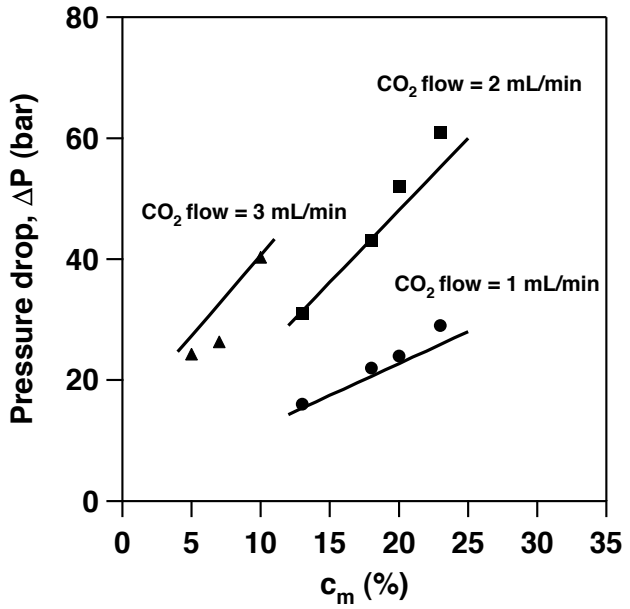

Figure 3.1: Experimental (symbols) and calculated pressure drop by Eq. 3.1(lines) under different CO_2 flow rates and modifier concentrations. Back pressure: 135 bar.

$$\frac{\Delta P}{L} = -\beta \frac{(\rho v)\mu}{\rho} \tag{3.1}$$

where ρ and μ are the fluid phase density and viscosity respectively. The parameters: v is the interstitial velocity and β is a system dependent parameter, that is typically fitted to experimental results, In the present work,

although pressure drop up to 60 bar were measured, owing to the rather high modifier composition the property change with respect to change in pressure were marginal. Hence, average values of density and viscosity corresponding to the average pressure (arithmetic mean of inlet and outlet pressures) were used to regress the value of β. The fluid density was calculated using the Peng-Robinson equation of state along with a 2 parameter mixing rule. The fluid viscosity was calculated as weighted mole fraction average of the CO_2 and methanol viscosity [89]. The value of β=5.785×10^{-13} m mL^{-1} was regressed by minimizing the error between the experimental and calculated pressure drop. The calculated values of pressure drop are plotted in Fig. 3.1 and show an acceptable description of the experimental trends.

3.2.3 HETP characterization

The height equivalent to a theoretical plate (HETP) is a commonly used parameter to estimate column efficiency. Large values of HETP represent peak broadening that deteriorate separation. Operating conditions such as flow rate, mobile phase composition affect HETP. Previous studies have shown that pressure drops contribute to loss of efficiency in SFC when the mobile phase was compressible [70, 88]. Hence, it was important to determine the effect of flow rate and modifier composition on the HETP. In order to investigate these effects under SFC conditions, the HETP values were measured under different flow rates and modifier concentrations by injecting dilute sample of racemic flurbiprofen, the results of which are shown in Fig. 3.2. As observed from the figure, both flow rate and modifier composition had a minor effect on HETP over the range of operating conditions investigated

in this work. Further, the value of HETP is rather small (around 10 μm) showing a high efficiency of the column. Such high column efficiency may be attributed to the high diffusivity of supercritical fluids and small particle size (5 μm) of stationary phase. Hence, in the entire study, the minor variation of HETP was not accounted for and assumed to be adequately described by the fitted mass transfer coefficients reported earlier [90].

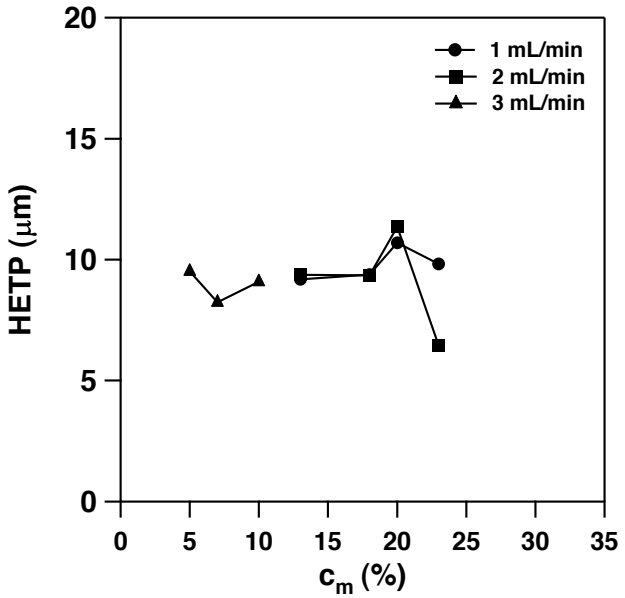

Figure 3.2: Experimentally measured HETP values under different operating conditions.

3.3 Modeling of column dynamics

The same equation in Chapter 2 was used to describe the column dynamics here:

$$\frac{\partial c_i}{\partial t} = D_{ax,i}\frac{\partial^2 c_i}{\partial z^2} - \frac{\partial (c_i v)}{\partial z} - \frac{1-\epsilon}{\epsilon}\frac{\partial n_i}{\partial t} \tag{3.2}$$

where c_i and n_i are the concentrations of the solute i in the mobile phase and in the stationary phase respectively, v is the interstitial velocity, $D_{ax,i}$ is the axial dispersion coefficient and ϵ is the total porosity of the column. Note that Eq. 3.2 is the more general form of Eq. 2.10 as the velocity is considered to be a function of column length.

In this chapter, the density change brought by pressure drop is less than 3% and therefore, the change of velocity arising due to the adsorption of the solute can be neglected. Under this assumption, Eq. 3.2 can be written as:

$$\frac{\partial c_i}{\partial t} = D_{ax,i}\frac{\partial^2 c_i}{\partial z^2} - v\frac{\partial c_i}{\partial z} - \frac{1-\varepsilon}{\varepsilon}\frac{\partial n_i}{\partial t} \tag{3.3}$$

which is identical to Eq. 2.10 A linear driving force (LDF) model and a competitive Langmuir isotherm were used in this chapter to describe the adsorption situation. The formulations of the models are same as Chapter 2.

In this chapter, to simplify the optimization, the back pressure was fixed at 135 bar. Under these conditions, a simple linear relationship as given below was experimentally obtained which adequately represented the dependence of Γ_i on c_m:

$$\Gamma_R = -3.87c_m + 148.82 \tag{3.4}$$

$$\Gamma_S = -1.12c_m + 76.13 \tag{3.5}$$

The maximum deviation of the experimentally determined values of Γ_i with respect to the linear relation was 17%. The description for Henry constant is the same as Eq. 2.3 in Chapter 2 and the same values for the empirical

constants were used in this chapter. Eq. 2.3, 3.4 and 3.5 provide the complete description of the isotherms for the region of interest.

The set of partial differential equations with suitable initial and boundary conditions were discretized in space using a finite difference scheme with 40 grid points per 1 cm of column length. The resulting set of ODEs were solved using the Gear's method as implemented in IMSL FORTRAN subroutines.

3.4 Validation of simulation for isocratic elution

The modeling for the column dynamics is based on a disperse-equilibrium model with experimentally measured isotherm parameters at 4 particular modifier compositors. It is necessary to examine the simulation code experimentally. The simplest method is to compare the retention time obtained from a dilute injection. Under this condition, symmetric Gaussian peaks occur in the chromatogram and the retention time is determined by the Henry constant. Two dilute injections (c_{inj}=10 g/L, v_{inj}=10 μL) under isocratic elution with modifier concentration of c_{m1} (14.2%) and c_{m2} (22.7 %) was implemented. The CO_2 flow rate was fixed to 1 mL/min during all the experiments. Modifier flow rate was changed accordingly to provide desired modifier composition. Comparison of retention time by experiments and simulation is shown in Table 3.1. As observed, satisfactory prediction of the retention time (deviation less than 4%) under linear isotherm was achieved.

Table 3.1: Comparison of retention time under isocratic elution

	t_r^{exp} (min)	t_r^{sim} (min)	deviation (%)
isocratic (c_{m1}) 1st peak	4.14	4.27	3.1
isocratic (c_{m1}) 2nd peak	6.27	6.04	3.7
isocratic (c_{m2}) 1st peak	6.27	6.34	3.7
isocratic (c_{m2}) 2nd peak	10.56	10.43	1.2

3.5 Process Optimization

3.5.1 Definition of parameters

Purity, recovery, productivity and solvent consumption are important parameters to evaluate the separation efficiency and quality. In this work, recovery (Y) and purity (P) are defined with respect to the individual fractions as:

$$\begin{aligned} Y_i &= \frac{\text{Amount of solute i collected in a fraction}}{\text{Amount of solute i injected}} \\ &= \frac{Q \int_{t_i^{start}}^{t_i^{end}} c_i \, dt}{V_{inj,i} c_{inj,i}} \quad i = R, S \end{aligned} \tag{3.6}$$

$$\begin{aligned} P_i &= \frac{\text{Amount of solute i collected in a fraction}}{\text{Total amount of two enantiomers collected in the same fraction}} \\ &= \frac{\int_{t_i^{start}}^{t_i^{end}} c_i \, dt}{\int_{t_i^{start}}^{t_i^{end}} c_R \, dt + \int_{t_i^{start}}^{t_i^{end}} c_S \, dt} \quad i = R, S \end{aligned} \tag{3.7}$$

The symbols t_i^{start} and t_i^{end} denote the start and end time of collection for the fraction that is predominantly i. Note that in the simulations, the efficiency

of fraction collection is considered to be 100%. In other words, all the solute that is to be collected between t_i^{start} and t_i^{end} are collected without any loss in the cyclone. The productivity is defined as the kg of product collected per kg of chiral stationary phase per day as shown in Eq. 3.8:

$$\begin{aligned} PR &= \frac{\text{Total amount of both enantiomers in respective fractions}}{\text{(Amount of stationary phase)(cycle time)}} \\ &= \frac{V_{inj}}{w_{csp} t_c}[c_{inj,R} Y_R + c_{inj,S} Y_S] \end{aligned} \tag{3.8}$$

where V_{inj} is the injection volume, $c_{inj,i}$ is the injection concentration of component i, w_{csp} and t_c are the weight of stationary phase and cycle time respectively. The cycle time is defined as the minimum time interval between two continuous injections and is equal to $t_S^{end} - t_R^{start}$.

In chromatographic separation, product recovery and solvent handling both contribute to the cost of separation. In SFC where a modified mobile phase is used, it is important to carefully define the solvent consumption. While the chromatographic separation itself is carried out at high pressure, the product is collected at low pressure. Under these conditions, the CO_2 is evaporated while the solute, along with the modifier precipitates and is collected. In the next step, the solute is separated from the modifier typically through evaporation. Compared to the pumping of the mobile phase, evaporation is more energy intensive and only the amount of modifier in the product contributes to the cost. Hence in this work, the solvent consumption is defined as the volume of modifier required per kg of the product produced:

$$S = \frac{\text{Total amount of modifier used in one cycle}}{\text{Total amount of both enantiomers collected in one cycle}} = \frac{Q_{mod} t_c}{V_{inj}[c_{inj,R} Y_R + c_{inj,S} Y_S]} \tag{3.9}$$

where Q_{mod} is the volumetric flow rate of modifier.

3.5.2 Choice of cut time

In preparative chromatography, the choice of collection intervals is crucial to maintain product quality and performance of the process. In general, when the mixture to be separated consists of two components in comparable quantities, a strategy has to be developed for choice of collection times. Current work is limited to a binary separation and it is assumed that peaks from consecutive injections are at least baseline separated. In other words, only the peaks of the two components in a particular injection are allowed to overlap.

With the mathematical model, an elution profile can be obtained for a given set of operating conditions. A simulated chromatogram is shown in Fig. 3.3 in order to explain the fraction collection scheme and cut time. In order to illustrate the general methodologies, a simulation where the peaks of the two component overlap is shown. The illustration assumes that the R enantiomer is the light component. The selection of t_R^{start}, the time at which the fraction contains R starts and t_S^{end}, the time at which the fraction contains S ends are rather straightforward. If the expected purities are equal to 100% then this can be achieved by selecting $t_R^{end} = t_s$ and $t_S^{start} = t_r$ as shown in Fig. 3.3. t_s corresponds to the time at which S starts eluting and t_r corresponds to the

time of which R has fully eluted. It is worth noting that although this results in 100% purities, the recovery is compromised as the fraction between t_r and t_s is not collected.

For cases, where purity requirement is less than 100%, the following strategy is used: it can be seen that shifting the cut time from t_s to t_r results in decreasing the purity of first component but increasing the purity of the second component. Therefore, there exist a point (t_p) where purities of two components are equal (P_R=P_S=P_p). Under these circumstances, three possible scenarios can be concluded:

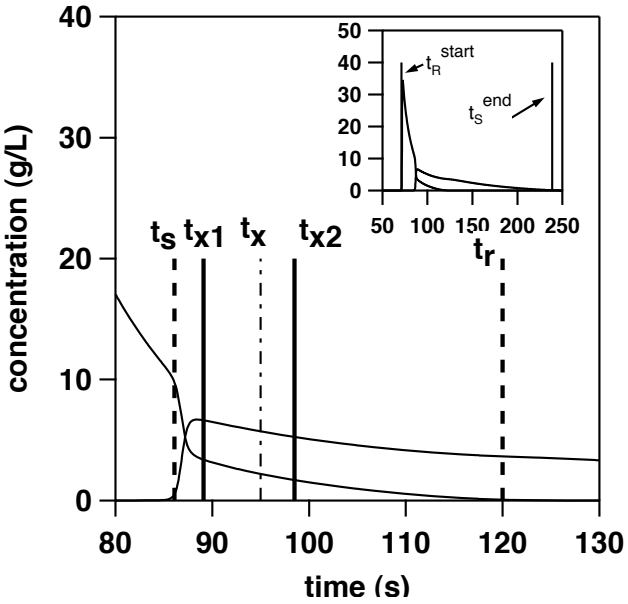

Figure 3.3: Illustration of strategy to decide cut time. The cycle time is t_S^{end}-t_R^{start}. R enantiomer is collected from t_R^{start} to t_{x1} (t_R^{end}) and S enantiomer is collected from t_{x2}(t_R^{start})to t_R^{end} to ensure the constraints are satisfied. Insert shows the complete chromatography.

1. If $P_p > P_{min}$, to keep high recovery, only one cut (at t = t_x) should be made. The productivity (solvent consumption is not affected by the

decision of cut time) is calculated at different position between t_r and t_s and t_x is chosen at the position where the productivity is maximum and the minimum purity requirement is satisfied.

2. If $P_p = P_{min}$, t_x is set to the position of t_p.

3. If $P_p < P_{min}$, only one cut can not fulfill purity constraint and two cuts (t_{x1}, t_{x2})are necessary. t_{x1} moves from t_s to right hand side until the purity constraint is satisfied. Similarly, t_{x2} moves from t_r to the left hand side until purity requirement is fulfilled. The recovery of two components will then be calculated based on the cut points. This scenario will result in three fractions. The middle fraction is not recycled.

3.5.3 Optimization problem formulation

Optimization problems can be sorted into two kinds with respect to the number of objective functions, single objective optimization and multi-objective optimization. These two kinds of optimization problems are conceptually different. Single objective problems seek to maximize or minimize one objective function and result in an unique set of decision variables. In the case of multi-objective optimization there may not be one optimum (i.e., a single point) with respect to all the objectives. Instead, there would be an entire set of optimal solutions (i.e., a curve) known as Pareto curve when the objectives conflict with each other. For example, in chromatographic separations, it is desired to maximize productivity but minimize solvent consumption. Every point on the Pareto curve is an optimal solution since moving from one point to another at least one objective function improves and the other worsens.

The final choice of an optimal Pareto point depends on relative cost of the two objectives.

For SFC process, a large number of operating parameters make the optimization problems challenging. Actually, the additional degrees of freedom in the SFC process (e.g. modifier concentration) compared with HPLC process renders the optimization problem more demanding. As a matter of fact,although multi-objective optimization for single column and multi-column chromatography and hybrid processes are available [87, 91, 92], an optimization study of the SFC process is rare in the literature. It is well known that appropriate formulation of the optimization problem is the most crucial part in an optimization study. Since the economics of the SFC process has opposite interests in terms of solvent consumption and productivity, the optimization for SFC can properly be set as a two objective optimization problem with the aim of minimization of the solvent consumption and maximization of the productivity.

Objective functions are functions of decision variables which are selected as the operating parameters, i.e., separation conditions that significantly influence the process performance. In this study, injection volume (V_{inj}), injection concentration of the solutes to be separated (c_{inj}), modifier concentration (c_m) and mass flow rate of CO_2 (m_{CO_2}) have been chosen as the decision variables. The summary of objective functions is shown in Tables 3.2. The solution to an optimization problem must satisfy one or several constraints defined in the space of objectives or decision variables. The constraints can be either from the limitation of the equipment or from the production require-

Table 3.2: Objective functions and constraints for the optimization study.

Case I	Objective functions	1. Max: PR(v_{inj}, c_{inj}, c_m)
		2. Min: S(v_{inj}, c_{inj}, c_m)
	Constraints	1. P=x± 0.002, x=95%, 97%, 99%
		2. Y=y±0.002, y=95%
Case II	Objective functions	1. Max: PR(v_{inj}, c_{inj}, c_m, m_{CO_2})
		2. Min: S(v_{inj}, c_{inj}, c_m, m_{CO_2})
	Constraints	1. P=x± 0.002, x=95%, 97%, 99%
		2. Y=y±0.002, y=95%
		3. ΔP $\leq$50 bar

ment. Two kinds of constraints were used in this study. One is the physical limitation (maximum pressure drop which the stationary phase can withstand) and the other is the quality of the product (recovery and purity). The physical limitation is a "hard" constraint since the equipment cannot be operated above such condition. Recovery and purity are "soft" constraints. Since the optimization is carried out over a range of recovery and purity values. The ranges of the decision variables are decided considering the equipment limitation such as maximum sample loop volume available in lab and the isotherm data which can be obtained from literature and they are compiled in Table 3.3.It is worth noting that, although we present results for a specific system (flurbiprofen), the analysis bears general applicability.

There are several methods to solve multi-objective optimization problem. In this work, non-dominated sorting generic algorithm (NSGA), a modified version of simple GA is used [93]. Non-domination refers to a better solution than another in at least one objective. The mutation and crossover operators are the same as simple GA. A random or given seed was used as the first

Table 3.3: Range of decision variable values.

Decision variable	Range
c_{inj} (g/L)	100 - 300
V_{inj} (mL)	0.05 - 0.5
c_m (w/w)	13.0 - 23.0 %
m_{CO_2} (g/s)	0.01 - 0.1

generation. Under mutation and crossover, next generation was calculated and sorted according to the fitness of the solution. Such step repeats for a pre-set number of generations to obtain the optimal solution. Compared to a single objective optimization algorithm such as Simplex, NSGA guarantees escape from converging into a local optimum. The parameters used by NSGA for all the optimization runs are list in Table 3.4.

Table 3.4: Parameters of NSGA used in multi-objective optimization study.

Parameters	Value
Number of generations	60
Population size	60
String length	24
Crossover probability	0.20
Mutation probability	0.05

3.6 Results and discussion

3.6.1 Case I Multi-objective optimization for a fixed flow SFC system

The first case study considers the multi-objective optimization of an SFC separation where the CO_2 flow rate is fixed at 1 mL/min. Pareto optimal set for three different purities: 95, 97 and 99 % are found for a fixed flow rate of CO_2 of 1 mL/min. The decision variables are feed concentration, injection volume and modifier concentration as given in Table 3.3. The results are shown in Fig. 3.4 where the axes correspond to the two objective functions, namely productivity and solvent consumption. As a general trend, with decreasing product purity requirement, it is observed that the Pareto curves move down and right indicating less solvent consumption and more productivity.

As observed, under all three purity constraints, steep Pareto profiles were obtained which means increase in the productivity will cause a rapid increase in the solvent consumption. This is because addition of modifier in the mobile phase results in earlier elution of the component to be separated, thus reducing cycle time which in turn increases productivity. Figure 3.4 also indicates maximum achievable productivity (under the constraints) for different purity values. Figure 3.4 enables us to calculate required solvent amount for a fixed productivity value. For example, for a productivity at 4 kg/kg/day, 50 L/kg rac of solvent will be necessary for both purity and recovery of 95%. The final decision on which Pareto point should one operate depends on the cost of the solvent and product. It is worth emphasizing that

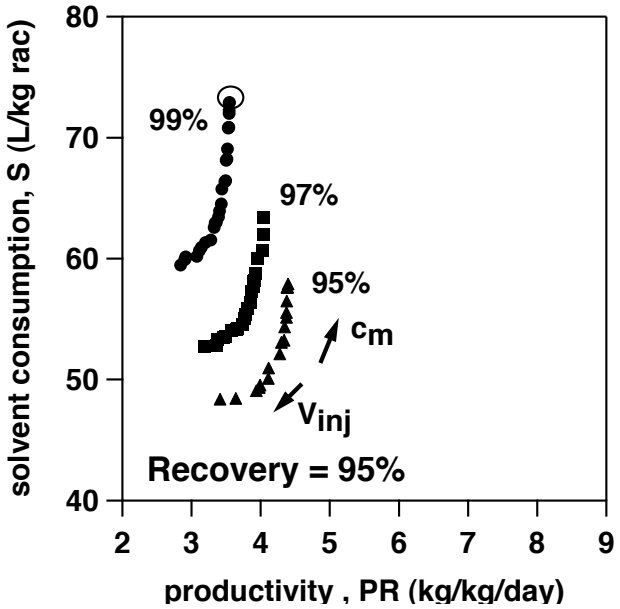

Figure 3.4: Pareto curves showing the trade-off between the two objective functions namely, productivity and solvent consumption for Case I under different values of purity. Recovery is fixed at 95%.

liquid phase SMB separations which typically have comparable productivities result in much higher solvent consumption [94]. These results provide strong motivation for practitioners to consider SFC as a powerful alternative.

Figure 3.4 is very useful to select an optimum point for the operation of the process with appropriate trade-off between productivity and solvent consumption for different purity requirements. In case that the solvent and its handling is inexpensive, one can operate the process at the top-right part of the Pareto curve to obtain maximum productivity. On the other hand, the right side of the flat part of the Pareto set is the favorable region to work with when the solvent or solvent handling is expensive, since increase in productivity does not require too much increase in solvent consumption.

3.6.2 Case II Multi-objective optimization for SFC system: CO_2 flow rate as decision variable

In Case I, the CO_2 flow rate was fixed at 1 mL/min. However, for practical applications, the flow rate is also used as a decision variable in order to obtain high productivity. Therefore, in Case II, CO_2 flow rate has been used as a decision variable and the modifier flow rate was accordingly adjusted to obtain the desired modifier concentration for three different purity values. Objective functions and constraints are the same as in Case I. The range of decision variables of Case II is listed in Table 3.3. The resulting Pareto optimal results are shown in Fig. 3.5. It is observed from Fig. 3.5 that the maximum obtainable productivity indicated by circled point is 8 kg/kg/day. This is 100% higher than the maximum obtainable productivity in Case I which is 4 kg/kg/day. This increase due to the reduction in the cycle time caused by high flow rate. The variable flow rate also gives another degree of freedom. This feature makes the slope of Pareto curve is smaller compared with Case I which provides more favorable operating conditions. It is worth noting that, for the maximum productivity points on all the three Pareto sets in Case II, the pressure drop is close to the maximum allowable value which was not observed in Case I. The general trend of Pareto under different purity requirement conforms to the same trend as in Case I, i.e., decrease in purity constraint leads to productivity increase and a decrease in solvent consumption.

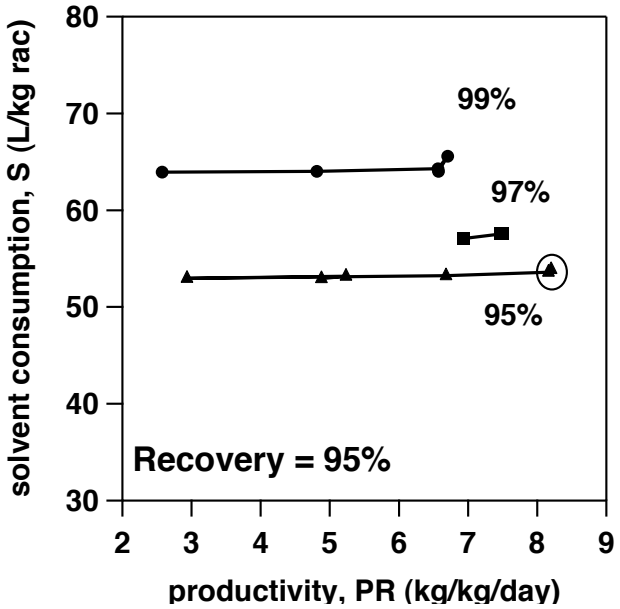

Figure 3.5: Pareto curves showing the trade-off between the two objective functions namely, productivity and solvent consumption for Case II under different values of purity. Recovery is fixed at 95%. Lines are shown as a guide to the eyes.

3.7 Effect of decision variables on the SFC performance

An optimal solution is a set of a combination of best decision variables searched by the optimization algorithm. An understanding of how each decision variable affects the separation performance will yield deep understanding of the process. A detailed discussion of the effect of the decision variables on isocratic SFC separation process is presented below:

3.7.1 Effect of modifier concentration

To elute a polar solute, a highly polar organic solvent such as methanol or ethanol is usually added to the mobile phase. With modifier, the solute nor-

mally elutes earlier compared to the use of pure CO_2 as an eluent since the modifier can either increase the polarity or directly compete for the adsorption sites with solute. The effect of modifier concentration on productivity and solvent consumption in this study is shown in Fig. 3.6. It is clear from Fig. 3.6 that increasing modifier concentration leads to increasing productivity and solvent consumption. This is because addition of modifier reduces the elution time of enantiomers thus decreasing the cycle time. The effect of modifier addition on productivity is more pronounced at lower modifier composition, while the effect on the solvent consumption shows the opposite trend.

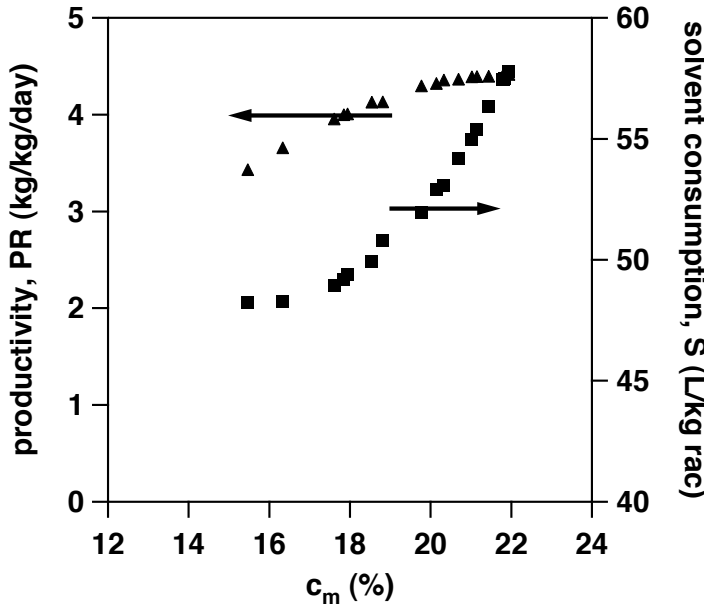

Figure 3.6: The effect of modifier concentration on productivity and solvent consumption for Case I. Purity: 95%, Recovery: 95 %.

3.7.2 Effect of throughput parameters

Throughput parameters include injection volume and injection concentration. High injection amount of solute can be achieved either by high concentration with small injection volume or by injecting large volume with low concentration of solute. In this study, both injection volume and concentration have been used as decision variables to investigate the optimal injection conditions. The effect of both injection concentration and volume is shown in Fig. 3.7 a) and b) indicating no clear trend for these individual throughput parameters on productivity and solvent consumption. However, when the total injected amount ($c_{inj}V_{inj}$) is plotted against the objective functions, as shown in Fig. 3.7 c), a clear trend is observed along the Pareto curve: higher productivities are obtained when smaller amount of the solute is injected under the purity and recovery constraints.

3.7.3 Effect of flow rate

Flow rate is a key decision variable and it is easy to implement. In the current study, the mass flow rate of CO_2 was selected as decision variable and the modifier was added accordingly to provide desired modifier composition. The effect of flow rate on productivity and solvent consumption is shown in Fig. 3.8. It is clear from the figure that high flow rate increases the productivity since the cycle time decreases . However, increasing flow rate also increases the pressure drop [95] therefore, there is a upper limit for increasing the flow rate. The maximum flow rate resulted in both maximal productivity and maximum pressure drop (50 bar). For solvent consumption,

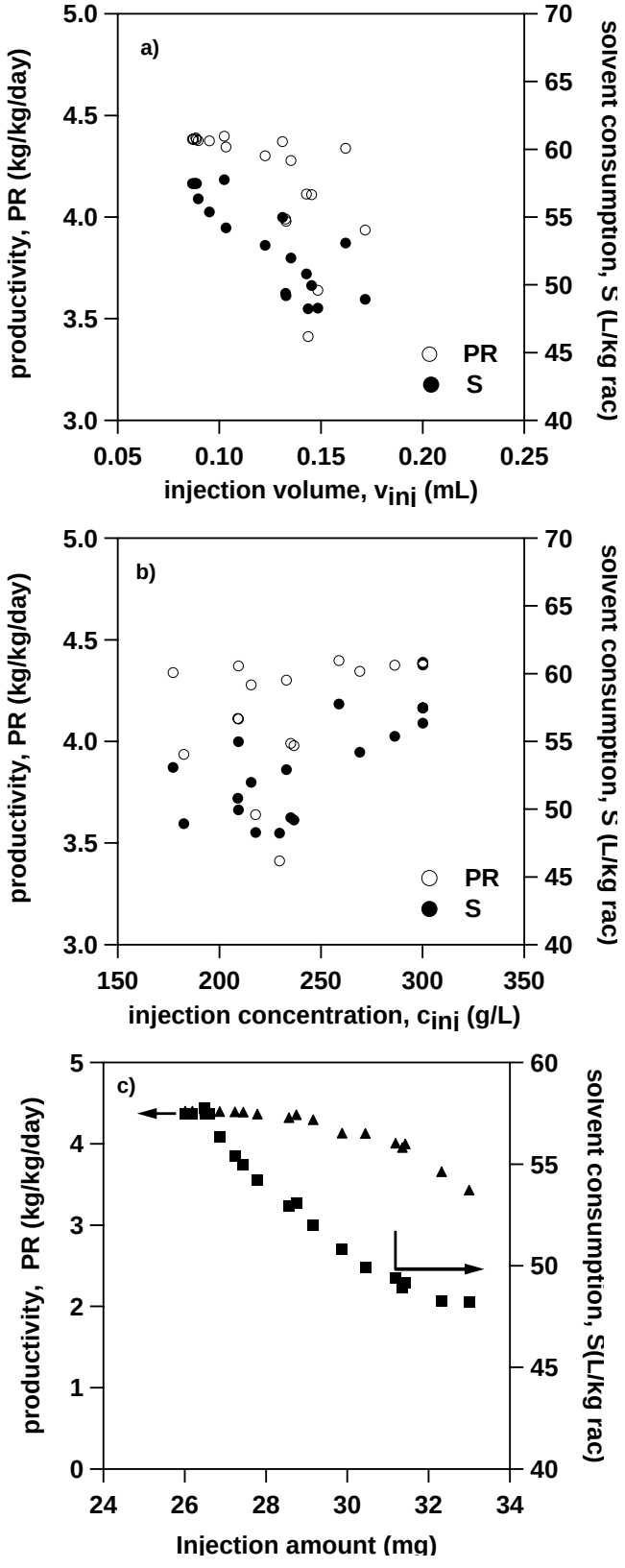

Figure 3.7: The effect of a) injection concentration, b) injection volume and c) injected amount on productivity and solvent consumption for Case I. Purity: 95%, Recovery: 95 %.

the flow rate did not show much effect. The solvent consumption remained almost constant for different volumetric flow rate of mobile phase. In SFC, at least under the experimental conditions studied, the effect of flow rate on HETP has been minimal. Hence, pressure drop and not column efficiency seems to dictate the maximum flow rates that can be used in SFC.

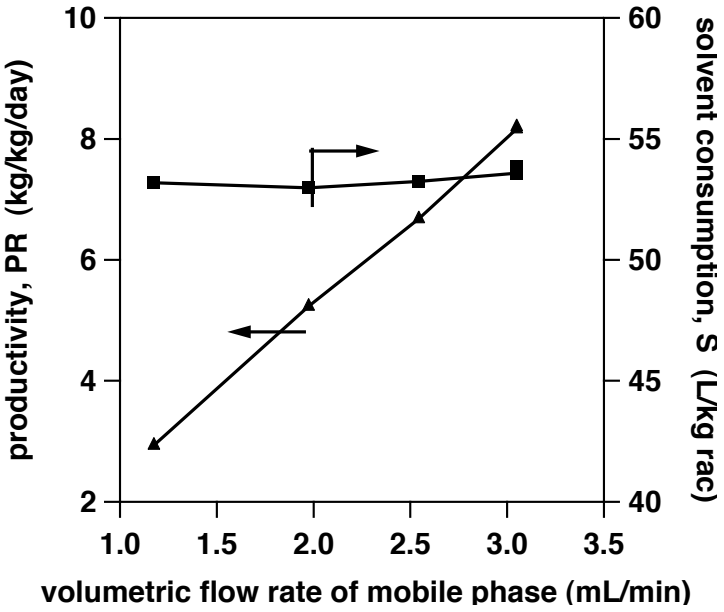

Figure 3.8: The effect of mobile phase flow rate on productivity and solvent consumption for Case II. Purity: 95%, Recovery: 95 %. Lines are shown as a guide to the eyes.

3.8 Conclusions

In this chapter, multi-objective optimization analysis of a single column isocratic SFC process was presented. The enantioseparation process was simulated with a detailed model using competitive Langmuir isotherm. The optimization was carried out to maximize the productivity and minimize the solvent consumption under different purity and recovery constraints. In-

jection concentration, injection volume, flow rate and modifier composition were chosen as the decision variables. The results indicate significant performance improvement in terms of increased productivity and reduced solvent consumption compared with those reported in the literature.

The advantages of SFC: low solvent consumption, high throughput have been demonstrated. Comparing to conventional HPLC and SMB technology, significant reduction in solvent consumption is achieved. This can be clearly observed that for all the optimal points, the solvent consumption is less than 80 L/kg which in the case of HPLC this number is usually more than 200 L/kg for much lower value of productivity [96, 97]. Less solvent consumption not only reduces the cost but also result in an environmental friendly process. These investigations confirm the potential of SFC process for practical applications and also demonstrate the advantage of using rigorous design methods with mathematical models and optimization algorithms.

Chapter 4

Optimization of gradient supercritical fluid chromatography process for enantioseparation

This chapter presents multi-objective optimization analysis of a single column gradient supercritical fluid chromatography process for the enantioseparation of flurbiprofen. The enantioseparation process is simulated using a detailed model with equilibrium description and a competitive Langmuir isotherm. To simply the optimization and compare the performance under isocratic and gradient elution, modifier concentration is selected as the operating parameter for gradient in this chapter. Two simple types of gradient, namely, step and linear gradient are studied. The problem has been formulated as a multi-objective optimization to simultaneously maximize productivity and minimize solvent consumption. Injection concentration, injection volume, flow rate and modifier gradient shape are optimized to obtain the optimum operating conditions. Product purity, recovery and column pressure drop are chosen as the constraints. The resulting Pareto curves under different constraints are shown and compared with those obtained in isocratic case.

Keywords: Supercritical fluid chromatography, Multi-objective optimization, Gradient elution

4.1 Introduction

Unlike analytical chromatography, total baseline separation is not required at preparative scale. For many cases, to maximize the productivity, high feed concentration with large mobile phase flow rate are often encountered in preparative chromatography leading to peak overlap. Proper operating conditions must be selected to adjust such overlap so that the final product is obtained with desired quality in a relatively short time. Generally, there are two different approaches which can be used to decrease the cycle time while maintain necessary peak resolution. One is to design and use more efficient columns by increasing their lengths or decreasing the particle sizes which increases the capital cost. Another is to operate the same system but under gradient elution rather than isocratic conditions. Obviously, the latter one is easier and more practical to implement.

Isocratic operation refers to a process whose operating conditions are kept constant from injection until collection. The isocratic elution is simple to operate and the cost is inexpensive since no extra design or operation adjustment are necessary. However, in isocratic elution mode, several problems can often be encountered. Firstly, the strong component may elute with a long tail or large peak width which might lead to the dilution of the product if high recovery is expected. Secondly, since the operating conditions do not vary during the separation, a long operating time may be necessary for completing the separation. This increases the cycle time and thus reduces the productivity. Finally, if there are strongly retained compounds in the feed, eluting them can lead to unusually long cycle time. Many of these problems

can be solved if a gradient elution is used.

Under a gradient elution, at least one operating variable is changed in a certain fashion during the time between sample injection and product collection which makes the separation programmable. The elution times of different components can be adjusted by changing solvation strength of mobile phase in a gradient mode. For example, with a binary mobile phase, a weaker solvation power can be used as the initial condition for a binary separation which has components that have significantly different adsorption strength. After majority of first compound elutes, an intensive parameters, e.g., solvent composition, temperature, is changed according to a pre-defined operating strategy in order to elute the second component faster. This leads to a reduced separation time while maintaining of the peak resolution. There are many choices of the pattern of gradient profiles, e.g., step, linear, convex or concave profiles and in some cases, more complex elution such as double linear gradients are used to achieve satisfactory separation results [98].

Many operating variables are chosen to implement gradient. In HPLC or GC, gradients using temperature, mobile phase composition or flow rate have been widely used to enhance the separation. Compared with HPLC, SFC has more degrees of freedom for operation which provides potential to improve separation. This is typically accompanied with an increase in the process complexities and hence a suitable design strategy is necessary. As known, the solvation power is related to the density of the mobile phase which is strongly affected by pressure near the critical point. Thus the pressure gradient of SFC system can be used to tune the separation. Another normally

used parameter for gradients in SFC is the modifier concentration which affects the polarity of mobile phase. It is worth noting that gradient using different parameters (density, modifier, etc.) were implemented in SFC before [23, 99] although under conditions where the isotherm is linear. For preparative separation, the feed concentration is so large that the isotherm is usually at non-linear range. To our knowledge there has been no study that has reported gradient preparative SFC separation processes based on a clear understanding of the non-linear isotherm. A rational process design based on proper column dynamics and isotherm models for overloaded injections under SFC conditions is also rare in literature. This provides the motivation, to design a SFC gradient process based on a clear understanding of separation process.

As mentioned, the choices of operating parameter for gradient in SFC are many. However, pressure and modifier composition may be considered as the most obvious ones to implement. No matter which of the two variables chosen as the intensive variable, the primary limitation is to ensure condition such that the solubility of solute in the mobile phase is high enough. It is well known that high modifier concentrations are indeed important to ensure that the solubility constraints are met. Once this is established the next step is to choose the intensive variable that will affect the maximum flexibility to alter retention situations. It has been shown in Chapter 2 that the effect of modifier on the retention is much more pronounced compared to pressure and hence we limit our study to designing modifier gradient. During the process, the temperature and back pressure are kept constant. The modifier

gradient can be carried out by adjusting the flow rate of two syringe pumps that pump CO_2 and methanol respectively.

The selection of decision variables and objective functions is crucial to an optimization study which has been stressed in the previous chapter. Obviously the gradient pattern is the first choice of decision variable which the designer should consider. In this chapter, both step and linear gradient were chosen and the corresponding initial and final modifier concentration, gradient slope and time are decision variables to improve separation. Other than gradient elution profile, injection concentration, injection volume and mobile phase flow rate which are related with the throughput were also selected. To evaluate the separation performance, productivity and solvent consumption were chosen as objective function. Modifier gradient using both step and linear gradient profiles were optimized for the purpose of maximizing productivity and minimizing solvent consumption simultaneously. The resulting multi-objective optimization problems were solved by a genetic algorithm under different purity and recovery constraints. The optimization results which are in the form of Pareto profiles were also compared with isocratic case and the effects of decision variables have been discussed.

4.2 Modeling

4.2.1 Modeling of column dynamics

Chromatographic model that accounts for convection and axial dispersion was used to describe the column mass balance under gradient elution:

$$\frac{\partial c_i}{\partial t} = D_{ax,i}\frac{\partial^2 c_i}{\partial z^2} - \frac{\partial (c_i v)}{\partial z} - \frac{1-\epsilon}{\epsilon}\frac{\partial n_i}{\partial t} \tag{4.1}$$

where c_i and n_i are the concentrations of i in the mobile phase and in the stationary phase respectively, v is chromatographic linear velocity, $D_{ax,i}$ is the axial dispersion coefficient and ϵ is the total porosity of column. For an isocratic elution, the composition of the mobile phase is constant throughout the run and hence it is sufficient to solve Eq. 4.1. However, for gradient elution, the composition fronts of the CO_2 and the modifiers also travel through the column and hence Eq. 4.1 should also be solved for the mobile phase components as well. In contrast to the solutes it can be assumed that the CO_2 and modifier, do not adsorb. Several studies have shown that both CO_2 and the modifier do adsorb onto the stationary phase, although weakly. Hence, their adsorption is not explicitly accounted for in the present study. The local density of mobile phase mixture is calculated based on inlet pressure and the local mobile phase composition. In our implementation, the mass flow rate of CO_2 is kept constant while that of the modifier in mass units changes to obtain desired modifier composition. Thus the total feed flow rate is not constant during the gradient process. However, the back pressure regulator at the downstream automatically adjusts the outlet to prevent pressure build-up and thus no mass gradient occurs along the column. Based on this, the total

mass flow rate at column inlet was used to calculate the linear velocity at different position of the column. It is also worth mentioning that due to the connection between modifier pump and mixing chamber, it takes sometime for the gradient modifier fronts to travel through this volume. This dead volume causes a delay at gradient profile between pump and column inlet. This dead volume was measured by comparing the elution time of modifier and the simulated one in a step gradient. The calculated value is 0.6 mL based on the difference in eluting time and flow rate. This value was used in the simulation code for all the gradient elution in this section.

The mass balance equation 4.1 together with mass transfer equation same as Eq. 2.11 and isotherm equations same as Eq. 2.17, 2.3, 3.4 and 3.5 complete the description for the column dynamics. The group of PDEs was solved to obtain the elution profile at column exit. The set of partial differential equations with suitable initial condition and boundary conditions were discretized in space using a finite difference scheme with 40 grid points per 1 cm of column length. The resulting set of ODEs were solved using the Gear's method as implemented in IMSL FORTRAN subroutines.

4.2.2 Advantage of gradient operation

In order to highlight the unique advantages of gradient operation, we consider a case where 95% purity of both components are expected. Two isocratic cases representing the two levels of the modifier gradient are considered and the simulation results along with the gradient elution is shown in Fig. 4.1. In all the three cases, the same amounts of solute at identical concentrations

are injected. The gradient elution starts with a lower modifier concentration of c_{m1}. At a certain time it is increased to a higher concentration of c_{m2} for a period of time and then returns to c_{m1}. Comparing Fig. 4.1 a) with b), the peak width reduces due to the increasing modifier composition, however, the overlap of two enantiomer peaks is enhanced thereby decreasing the purity and recovery. The use of gradient operation eliminates this problem. Comparing Fig. 4.1 a) and c), the mixing part in the middle is reduced while the peak width is maintained. Thus, the final product can be obtained in a short time with better quality. Such effect can be explained by the modifier gradient showed in Fig. 4.1 c). The gradient first runs at low composition to avoid much mixing between two components. After the major part of first component elutes out, the modifier composition increases to help second component come out faster decreasing the cycle time.

4.3 Validation of simulation for gradient elution

To verify all the assumptions and simplifications in the column mass balance and isotherm model under gradient SFC condition, a dilute injection was made under a step gradient. As mentioned in chapter 3, at low concentration, the isotherm is at linear range where the Henry constant dominates the isotherm and determines the retention time of chromatographic peaks. By comparing the experimental and simulated retention time, the validity of modeling can be examined.

The same experimental set-up described in Chapter 2 was used. The step

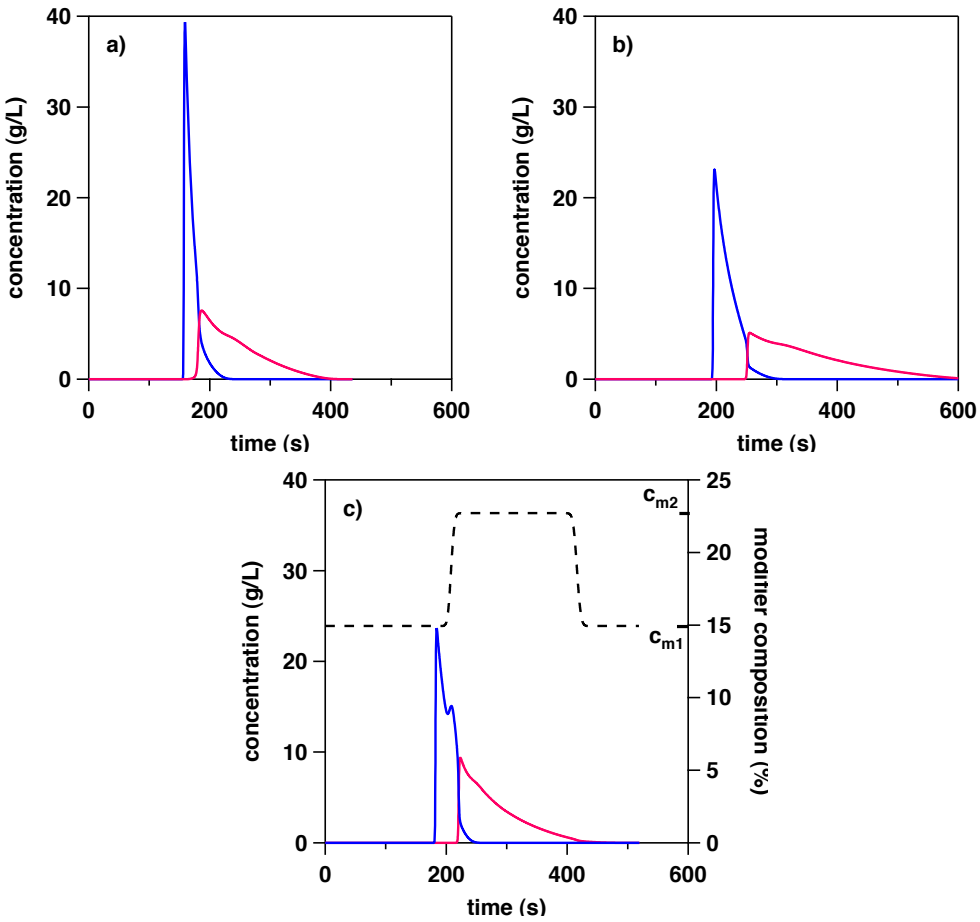

Figure 4.1: Comparison of elution profiles under isocratic and step gradients. a) isocratic elution with $c_m = 14.2\%$, b) isocratic elution with $c_m = 22.7\%$ and c) step gradient with $c_{m1} = 14.2\%$ and $c_{m2} = 22.7\%$. Blue lines represent the R enantiomer, red lines represent the S enantiomer, dotted line represents the modifier composition at column exit.

gradient was implemented by changing the flow rate of modifier pump at desired time. The modifier concentrations of $c_{m1} = 14.2\%$ and $c_{m2} = 22.7\%$ for the modifier composition for the step were used in the experiment. Considering the dead volume, the gradient times at the column inlet for these two compositions are 1.48 min and 3.13 min respectively. The schematic of the gradient implementation is shown in Fig. 4.1. In order to compare the experimental results , we perform a simple analysis using the method of characteristics. Here the propagation velocities of the solute i is given by

$$\left.\frac{dz}{dt}\right|_i = \frac{v}{1 + \frac{1-\epsilon}{\epsilon} H_i} \tag{4.2}$$

where v is the interstitial velocity and H_i is the Henry constant. During gradient elution, the velocity of the mobile phase changes according to the operating condition. The Henry constant of the solute is a function of the mobile phase composition. Hence it is important to properly account for the change in velocity. In this analysis, it is assumed that the velocity along the column is constant and is based on the inlet conditions. Hence, for $0 <$ t $<$ 1.48 min the interstitial velocity in the column, v_1 corresponds to the conditions corresponding to c_m=c_{m1}=14.2%. For the time 1.48 min <t $<$ 4.61 min, the interstitial velocity is v_2 which corresponds to c_m=c_{m2}=22.7%. Finally for t $>$ 4.61 min, the velocity in the column equals to v_1. Now, let us consider the characteristics corresponding to the modifier composition. In the current situation, the modifier is assumed to be non-adsorbing. Hence, the velocity leading edge of the front is given by

$$\frac{dz}{dt} = v_1 \tag{4.3}$$

and that of the traveling edge is given by

$$\frac{dz}{dt} = v_2 \tag{4.4}$$

Once the velociies and the propagation of the modifier band is indentified, the propagation velocities of the solute can be calculated using Eq. 4.2. The propagation of the two solutes are shown in Fig. 4.2 a). The conditions in the rest ranges can be deduced by analogy. The analysis estimates that the elution times of lighter and heavier components to be 5.2 min and 7.7 min respectively. These compare well with experiments that show elution times of 5.3 min and 7.9 min which is within 3% of the predicted values. These demonstrate that the assumptions made by the model are reasonable and can be used to study gradient SFC.

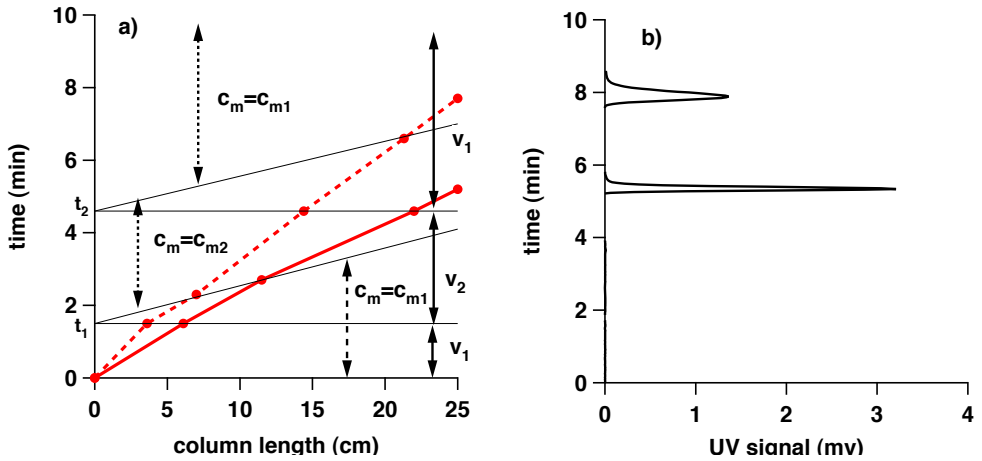

Figure 4.2: Comparison of retention time of R (solid line in a) and S (dashed line in a) enantiomer under step gradient elution. a) the physical plane along with the characteristic. b) experiemntal results.

4.4 Process optimization

4.4.1 Optimization problem formulation

Formulation of the optimization problem is the most important part in the optimization study. The decision variables, objective functions and constraints must be clearly defined before the optimization calculation. Compared to HPLC, SFC has more operation variable such as pressure, temperature and modifier concentration which can be used to alter the separation results. To simplify the problem and to demonstrate the ability of gradient elution, only the modifier concentration is selected to implement gradient. In this section, two simple gradient profiles: step gradient and linear gradient were considered. The schematic of these two gradient is shown in Fig. 4.3. As shown, c_{m1} is the initial modifier composition and c_{m2} is the modifier con-

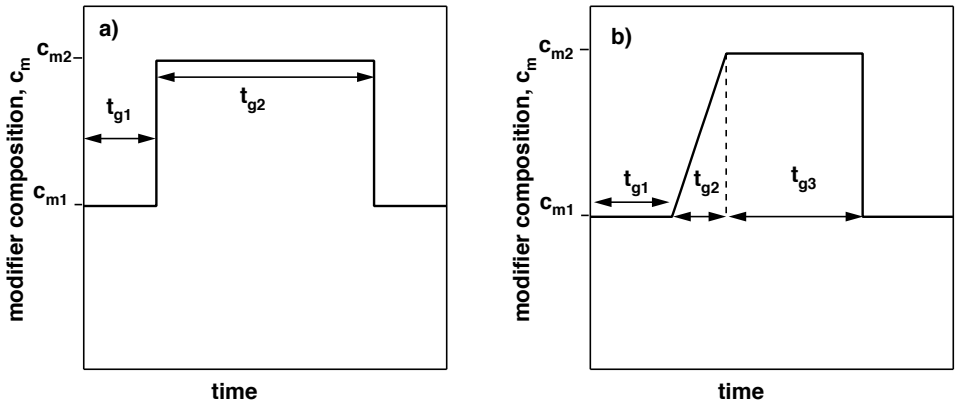

Figure 4.3: Schematic of modifier profiles at column inlet. a) step gradient. b) linear gradient

centration for next step. t_{g1}, t_{g2} and t_{g3} are the gradient time for individual modifier composition. As can be seen, step gradient is a special case of the

linear gradient. It is worth noting that there is no constraint imposed on the relative magnitudes of c_{m1} and c_{m2}. In other words, situations where $c_{m1} > c_{m2}$ or $c_{m1} < c_{m2}$ are allowed.

Similar to the previous chapter, two cases were studied. In the first case, the CO_2 flow rate was fixed at 1 mL/min while in the second case, it was treated as a decision variable. For both cases, the injection concentration (c_{inj})and injection volume (v_{inj}), the gradient parameters, c_{m1}, c_{m2}, t_{g1}, t_{g2}, t_{g3} (for linear gradient) were treated as decision variables. The range of decision variables has been listed in Table. 4.1.

Table 4.1: Range of decision variable values

Decision variable	Range
c_{inj} (g/L)	100 to 300
V_{inj} (mL)	0.05 to 0.5
c_{m1} (%)	13.0 to 23.0
c_{m2} (%)	13.0 to 23.0
t_{g1} (s)	5.0 to 300.0
t_{g2} (s)	5.0 to 300.0
t_{g3} (s)	5.0 to 300.0
m_{CO_2} (g/s)	0.01 to 0.1

Another important aspect of optimization is the definition of objective functions. Optimization problems can be sorted to either single objective optimization or multi-objective optimization based on the number of objective functions. These two kinds of optimization problems are conceptually different. Similar to isocratic optimization study considered in the Chapter 3, productivity and solvent consumption have been selected as the objective

functions since both of them contribute to the cost of process. The definitions of productivity and solvent consumption are same as in Chapter 3. Thus the optimization for SFC in this section is formulated as a multi-objective optimization problem with the aim to maximize the productivity and minimize the solvent consumption simultaneously.

Other than decision variables and objective functions, constraints are an important part to complete the problem formulation. The same constraints as isocratic optimization have been used in this chapter, namely, purity, recovery and pressure drop. Purity and recovery constraints are related with product quality while pressure drop is a constraint related with equipment limitation. The calculation of purity and recovery is based on same method as in chapter 3. During the gradient elution operation, the modifier concentration keeps changing with time leading to a change in pressure drop. To ensure the equipment is operated under safe condition, the maximum pressure drop during the process was calculated using the values of decision variables that determine pressure drop, namely flow rate and mobile phase composition. If the constraints are not satisfied, the optimizer terminates current simulation and proceeds to consider next set of decision variables. The total description of the optimization study for step and linear gradient is shown in Table 4.2 The resulting optimization problems were solved by non-dominated sorting generic algorithm (NSGA) which is a modified version of simple GA [87]. The parameter values for NSGA algorithm was same as Chapter 3 and is not repeated here.

Table 4.2: Objective functions and constraints for the optimization study.

Case I	Objective functions	1. Max: PR (v_{inj}, c_{inj}, c_{m1}, c_{m2}, t_{g1}, t_{g2}, t_{g3})
		2. Min: S(v_{inj}, c_{inj}, c_m)
	Constraints	1. P=x± 0.002, x=95%, 97%, 99%
		2. Y=y±0.002, y=95%
Case II	Objective functions	1. Max: PR(v_{inj}, c_{inj}, c_m, m_{CO_2})
		2. Min: S(v_{inj}, c_{inj}, c_m, m_{CO_2})
	Constraints	1. P=x± 0.002, x=95%, 97%, 99%
		2. Y=y±0.002, y=95%
		3. ΔP $\leq$50 bar

4.4.2 Choice of cycle time

Before proceeding to the optimization study, there are several issues, particularly related to the definition of cycle time that must be described first. Based on the chromatographic model and isotherm parameters, elution profiles for enantiomers can be obtained at any given operating conditions and injection amount. However, to obtain the final product separation, a proper cutting scheme must be defined for the objective function calculation. The same fraction cutting method as Chapter 3 has been used here. For a particular chromatogram, this method guarantees a maximum productivity and a well satisfaction of purity and recovery constraints.

Other than the fraction cut times, another issue faced in gradient elution is the decision of cycle time. The cycle time refers to the time interval between two continuous injections. For preparative scale separation, to increase the productivity, the length of cycle time must be reduced to a minimum. In the isocratic case, the decision of cycle time is quite straightforward and

is equal to the peak width of target enantiomers measured at the baseline. A continuous, back-to-back chromatograms will be observed if consecutive samples are injected at this interval. However, in gradient elution, since the operation conditions change between injection and collection, the cycle time must be appropriately designed to minimize the operation time length and to ensure the gradient elution implemented consecutively. Fig. 4.4 is used to illustrate the choice of cycle time. As shown in the figure, $t_{chrom} = t_S^{end}$-t_R^{start} is

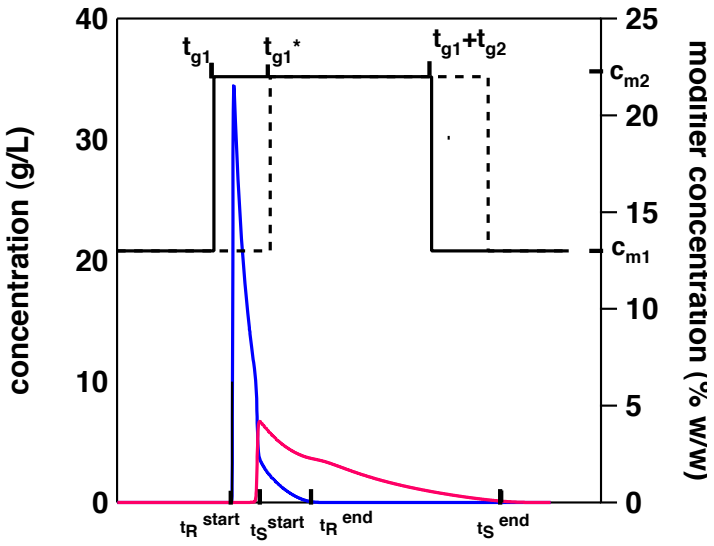

Figure 4.4: Illustration of strategy to decide cycle time. Chromatogram of R (blue line) and S (red line) enantiomers with modifier profile at column inlet (black line) and column outlet (dotted line).

the peak width of two enantiomers. Without considering the gradient effect, t_{chrom} is the minimum interval between two injections. Thus the cycle time is firstly set to t_{chrom} and then based on the gradient effect, it will be decided whether t_{chrom} is appropriate. The total gradient time, t_g, in the case of step gradient, t_g= t_{g1}+t_{g2} and in the case of linear gradient, t_g= t_{g1}+t_{g2}+t_{g3}. To

maximize the productivity, the cycle time needs to be as short as possible and the gradient of next injection must not affect the current one. In other words, the leading edge of modifier front with a concentration of c_{m2} must not interfere with the racemate of the next injection. To account for this, t_m is used to represent the traveling time of modifier flow c_{m2} through the column which is equal to t^*_{g1}- t_{g1}. Comparing t_g and t_{chrom} the following possible scenarios can be expected:

1. t_{chrom} is larger than t_g. As mentioned, cycle time is firstly set to t_{chrom}. Since t_g is less than t_{chrom}, the gradient can be completed within one cycle. Next, situations at column outlet are taken into account. It takes t_{g1}+t_m for modifier front of next injection to travel from the column inlet to outlet. To avoid interference from modifier front and inject next sample at t_{chrom}, t_S^{end} must be larger than (t_{chrom}+t_{g1}+t_m). In this case, cycle time is equal to t_{chrom}. If t_S^{end} is less than (t_{chrom}+t_{g1}+t_m), the cycle time is equal to (t_S^{end}-t_m-t_{g1}) to ensure that the modifier front does not affect the solute elution and the cycle time is minimum.

2. t_{chrom} is less than t_g. In this case, t_{chrom} cannot be chosen as the cycle time since the gradient will not complete. Thus the cycle time is set to t_g firstly. Next the conditions at column outlet is considered. If (t_g+t_{g1}+t_m) is larger than t_S^{end}, the cycle time is equal to t_g since the modifier front will not interfere the solute. If (t_g+t_{g1}+t_m) is less than t_S^{end}, to avoid the effect of modifier front, (t_S^{end}-t_m-t_{g1}) is selected as cycle time. Same as first case, this choice of cycle time ensures no mixing of modifier front and the solute and the time is minimum.

4.5 Results and discussion

4.5.1 Case I Multi-objective optimization for a fixed flow SFC system

To study the effect of flow rate and to simplify the optimization problem, the study was firstly carried out under a system where the volumetric flow rate of CO_2 is fixed to 1 mL/min. Three different purities 95, 97 and 99% all with a recovery of 95% were selected as the constraints. To compare gradient and isocratic elution, the resulting Pareto curves under 3 modes, namely, isocratic, step and linear gradients are shown in Fig. 4.5. Under all 3 elution modes, the ranges of common decision variables are the same for a fair comparison. As a general trend, with decreasing product purity requirement, the Pareto curves move down and right for all 3 elution modes indicating increased productivity and decreased solvent consumption. Lower purity requirement allows more overlapping between peaks to be collected thus result in an increased productivity. The step gradient can be treated as a special form of linear gradient ($t_{g2} = 0$) and isocratic is a special case of gradient ($c_{m1} = c_{m2}$). Thus in principle the optimization results of linear gradient should be at least same if not better than step gradient and isocratic elution. The trend observed from the optimal Pareto curves confirms this expectation. Under the purity of 99% and 97%, the Pareto of linear gradient shows larger productivity and less solvent consumption. This difference between two gradient mode becomes minor under the purity of 95% because of the lower purity constraints but the gap between gradient and isocratic is still considerable. Further, it is observed that using a gradient it is

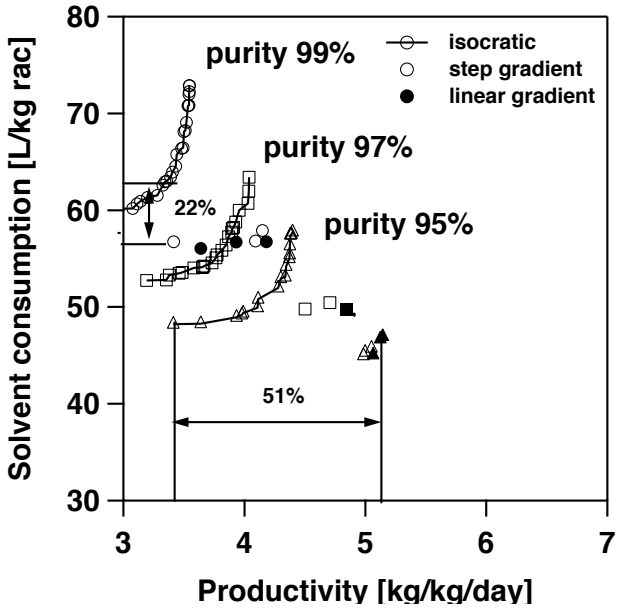

Figure 4.5: Comparison of Pareto curves using isocratic, step and linear gradient operation for Case I under different value of purity constraint. Recovery is fixed at 95%.

possible to achieve productivities that are not possible with isocratic elution. For comparable values of solvent consumption, a 51% (indicated by arrow on x axis in Fig. 4.5) increase in productivity can be achieved, and a 22% (indicated by arrow on y axis in Fig. 4.5) reduction in solvent consumption compared to isocratic elution can be achieved for comparable productivities. These results clearly indicate that operation under gradient conditions can lead to significant improvement in process performance measured in terms of productivity and solvent consumption.

The simulated elution profiles for the maximum obtainable productivity point using linear gradient and isocratic under the purity constraint of 95% are shown in Fig. 4.6. The injection amount in isocratic is 26.5 mg and the value in case of linear gradient is 32.1 mg. It is shown in the figure that by gradient,

the modifier concentration increases after most of 1st component elutes. It helps to decrease the elution time of 2nd component reducing the cycle time while maintain the product quality when the more solute is injected. It is worth noting that although the cycle time are comparable, it is possible to inject more solute for the case of gradient elution.

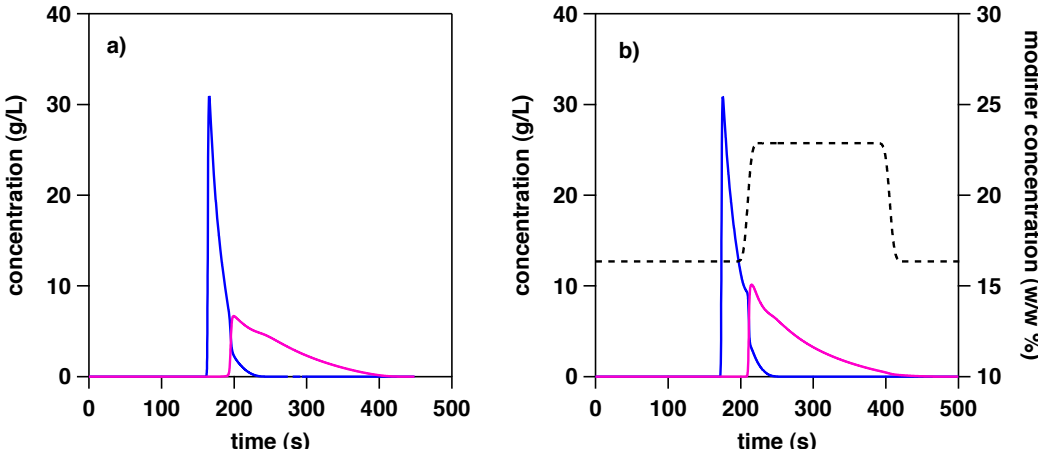

Figure 4.6: Simulated elution profile of R (blue lines) and S (red lines) enantiomers with modifier gradient profile at column exit (dotted line) for Case I by a) isocratic elution and b) linear gradient. The injection conditions for a): c_{inj} = 260 g/L, v_{inj} = 102 μL, c_m = 22% and for b): c_{inj} = 283 g/L, v_{inj} = 113 μL, c_{m1} = 16.3%, c_{m2} = 22.9%, t_{g1} = 39 s, t_{g2} = 5 s, t_{g2} = 181 s. Purity: 95%, Recovery: 95%.

4.5.2 Case II Multi-objective optimization for variable CO_2 flow gradient SFC system

To study the effect of flow rate on the objective functions, in this section, the CO_2 flow rate was also chosen as a decision variable for the optimization of gradient elution. To compare all 3 elution modes in this system, the resulting Pareto curves are shown in Fig. 4.7. It is observed from Fig. 4.7 that the maximum obtainable productivity is about 8 kg/kg/day. This is 60% higher than the maximum obtainable productivity when the CO_2 flow rate is fixed.

This shows the effect of mobile phase flow rate on the productivity. High flow rate decrease the cycle time thus increasing the productivity. A further increase in flow rate is not possible as it will lead to the violation of the pressure drop constraint. Same trends as in section 4.5.1 for all 3 modes was observed in this system. Decreasing product purity requirement causes an increase in productivity and a reduction in solvent consumption. Compared with fixed flow rate system, the slope of Pareto curves is much smaller. It indicates that in this system, improvement in producibility does not lead to a considerable increase in solvent consumption which is favorable.

Comparing three different operation modes under same purity constraint, the difference in separation performance is small. Although this observation is different with the Case I, the same principle is still applicable. Increasing the number of decision variable, the results are expected to be at least same if not better. Since no deterioration in the separation performance occurs while the complexity of elution mode increase, the optimization results are consistent with the expectation. Under the 95% purity, the linear gradient elution tends to spend slightly less solvent while producing the same quantity of product compared with step gradient and isocratic elution. However, as we will show in the next section the resulting gradient profiles are indeed close to isocratic conditions. It indicates that when pressure drop is the limiting constraint, the difference in process performance between various modifier elution modes becomes minor. Thus to obtain high productivity and decrease the process cost by avoiding complicated operation, isocratic separation may be indeed preferable. It is worth noting that although this

conclusion is only applicable for system studied in this chapter, the trends may be similar for other separations.

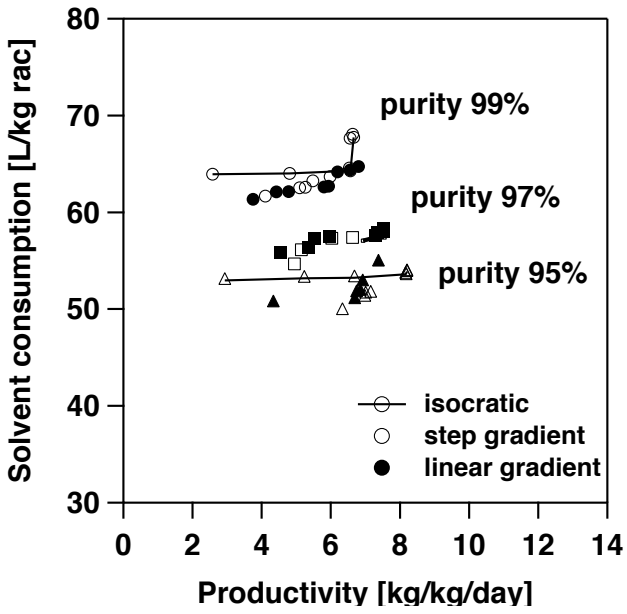

Figure 4.7: Comparison of Pareto curves using isocratic, step and linear gradient operation for Case II under different value of purity constraint. Recovery is fixed at 95%.

To compare the gradient and isocratic elution in this system, the simulated elution profiles of maximum obtainable points by linear gradient and isocratic under purity constraint of 97% are shown in Fig. 4.8. The injection amounts for two operations are similar. As observed, the difference between two modifier concentration in gradient is marginal which makes the gradient similar to isocratic. This explains the overlap of Pareto curves obtained for isocratic and gradient.

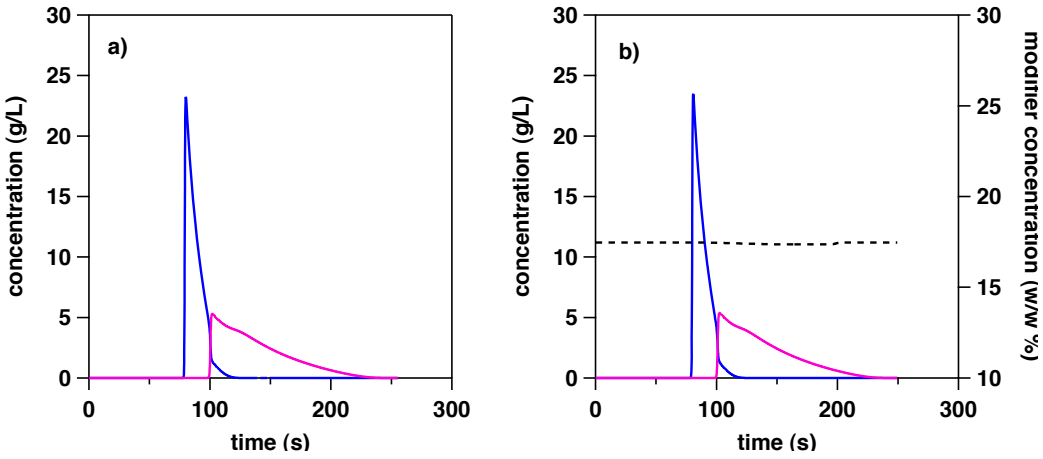

Figure 4.8: Simulated elution profile of R (blue lines) and S (red lines) enantiomers with modifier gradient profile at column outlet (dotted line) for Case II by a) isocratic and b) linear gradient. The injection conditions for a): c_{inj} = 173 g/L, v_{inj} = 160 μL, c_m = 16.7%, m_{CO_2} = 0.039 g/s and for b): c_{inj} = 213 g/L, v_{inj} = 126 μL, c_{m1} = 17.4%, c_{m2} = 17.5%, t_{g1} = 48 s, t_{g2} = 49 s, t_{g2} = 213 s, m_{CO_2} = 0.038 g/s. Purity: 97%, Recovery: 95%.

4.6 Effect of decision variables on the SFC performance under gradient elution

Each decision variable has its own effect on the separation performance. The analysis of these effects helps to understand the process and select proper operating parameters. A detailed discussion of the effect of the decision variables on gradient SFC separation process is presented below.

4.6.1 Effect of gradient profile

Unlike isocratic elution, the modifier concentration changes with time in gradient elution. The modifier concentration alone is not enough to illustrate the effect on the separation performance and a complete gradient profile is necessary to be studied. The investigation is firstly implemented in a fixed

flow system. The modifier gradient profiles at the column inlet for two points with maximum productivity (circled) from the Pareto curves of step and linear gradient in Fig. 4.5 is shown in Fig. 4.9. As observed from the figure,

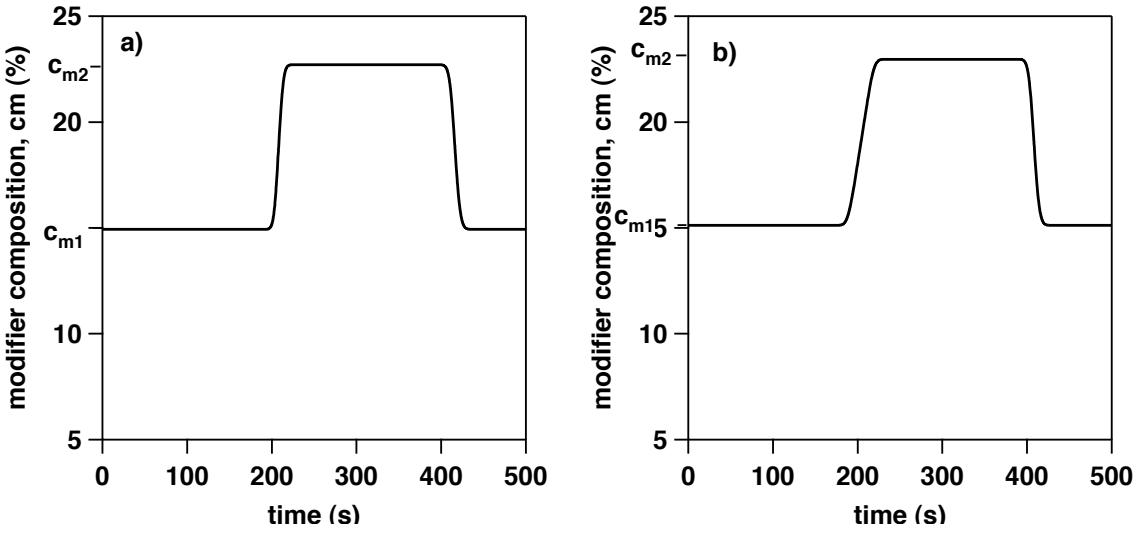

Figure 4.9: The modifier gradient profile at column outlet for optimum conditions in a) step gradient and b) linear gradient for Case I. Purity constraint: 97%.

positive gradient appears in optimum conditions for both two gradient modes. The values for c_{m1} and c_{m2} are generally same in step and linear gradient, i.e., for c_{m1}, it is about 15% and for c_{m2}, it is about 23%. In other words, they are close to the bounds. hence the best performance can be expected when the difference (c_{m2}-c_{m1}) is large. The reason for this can be explained by noting that injecting at lower composition allows the introduction of the high amount of the solute while the gradient helps in improving the resolution and reducing the elution time of tail of the second component. In linear gradient, a gradual increase from c_{m1} to c_{m2} enhances such effect and thus increase the productivity.

The gradient profiles for points with maximum obtainable productivity with

purity constraint of 97% from Fig. 4.7 are plotted in Fig. 4.10. These two points correspond to runs that show maximum productivity. It clearly explains why the the difference between Pareto curves of isocratic and gradient elution is so small. As observed, the gradient elution at the optimum conditions is actually isocratic due to the modest changes in modifier concentration. It is worth noting that at 95% purity constraint, there exist such optimal points with lower productivity whose elution profiles show that the gradient is more pronounced which proves that the optimizer has searched the gradient range. However, to obtain high productivity, it is recommended that the process is carried out at isocratic elution due to its simplicity in operation.

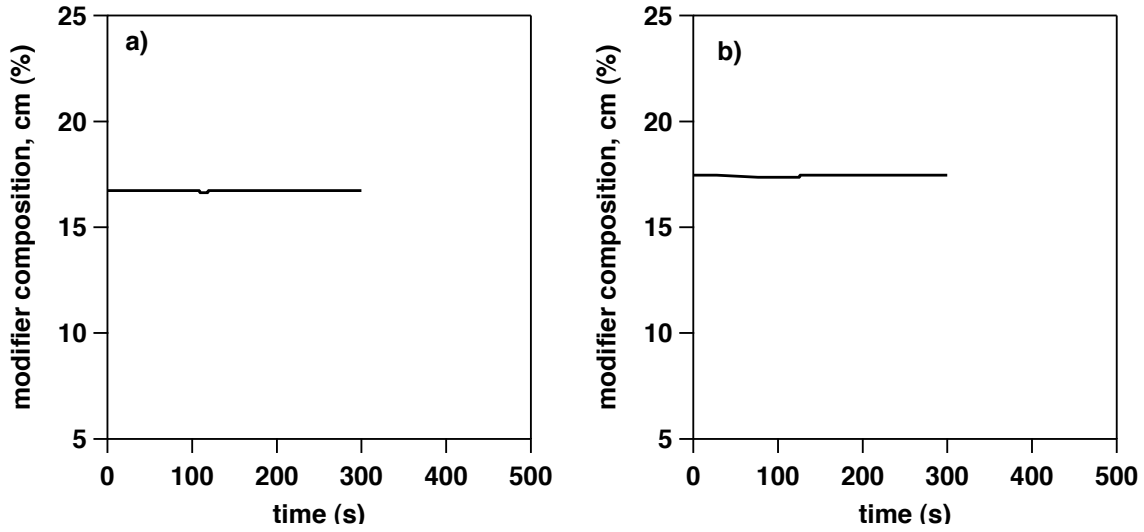

Figure 4.10: The modifier gradient profile at column inlet for optimum conditions in a) step gradient and b) linear gradient for Case II. Recovery constraint: 95%, Purity constraint: 97%.

4.6.2 Effect of throughput parameters

Throughput parameters are related with the loading ability. In the optimization, both the injection concentration and volume are decision variables. The dependence of productivity and solvent consumption on the injection concentration, volume and total injection amount is shown in Fig. 4.11. As observed from Fig. 4.11 a), generally an increase in injection concentration leads to increase in productivity. An opposite effect of injection volume on productivity is shown in Fig. 4.11 b). The effect of injection volume and concentration on solvent consumption is minor. No clear trend for injection amount on on either productivity or solvent consumption was observed.

4.6.3 Effect of flow rate

It has been demonstrated in isocratic optimization that flow rate is a key decision variable which can be used to improve the productivity. The effect of flow rate is also examined in the case of gradient. Since the linear velocity changes with respect to time in gradient operation, the CO_2 (majority of mobile phase) mass flow rate was selected as the decision variable. The dependence of productivity and solvent consumption on CO_2 mass flow rate is shown in Fig. 4.12. It clearly shows a positive effect of flow rate on the productivity from the figure. Increasing flow rate reduces the cycle time thus increases the productivity. Due to the pressure drop constraint, the optimum condition tends to remain at the range where the pressure drop is close to the specified limit. The flow rate has a minor effect on solvent consumption.

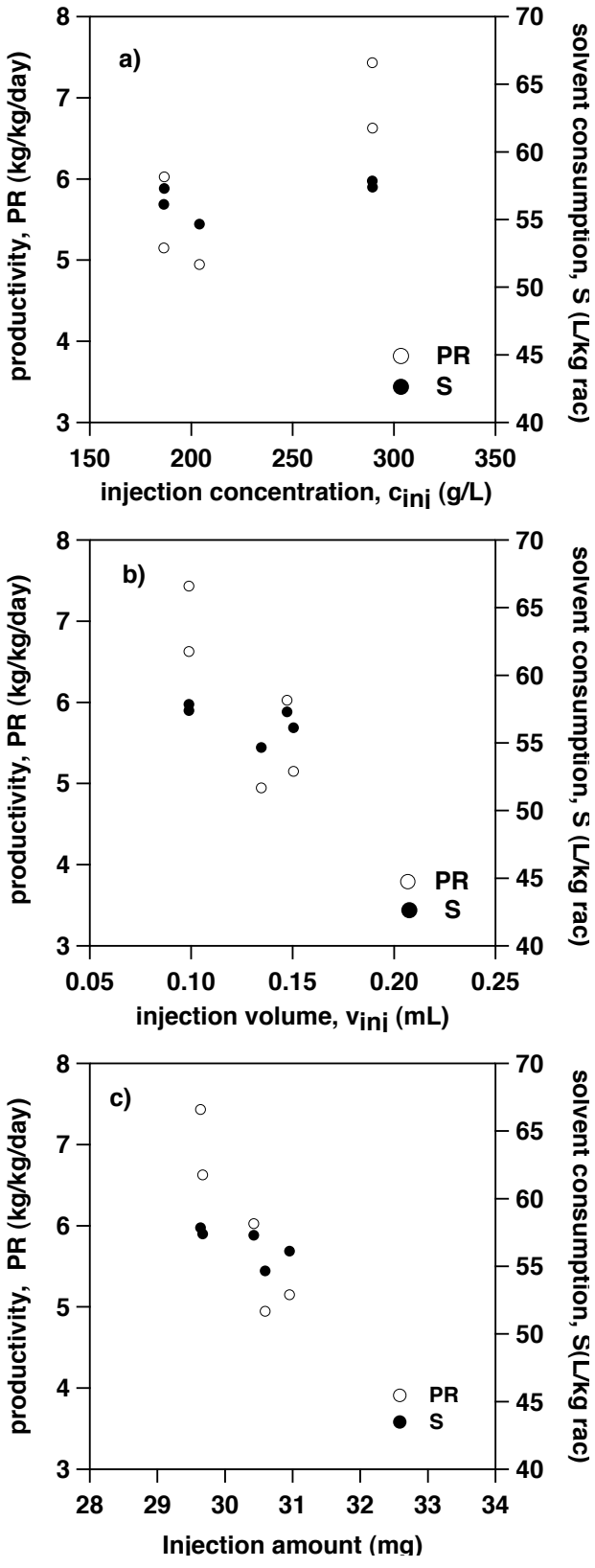

Figure 4.11: The effect of a) injection concentration, b) injection volume and c) injected amount on productivity and solvent consumption for Case II by step gradient. Purity: 97%, Recovery: 95%.

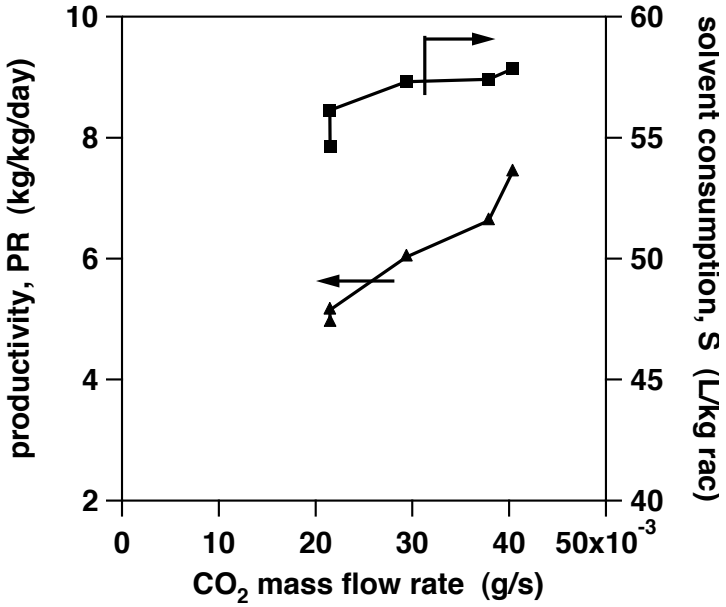

Figure 4.12: The effect of CO_2 mass flow rate on productivity and solvent consumption for Case II. Purity: 97%, Recovery: 95%.

4.7 Conclusions

Systematic optimization studies of step and linear gradient using SFC for enantioseparation of racemic flurbiprofen were performed in this chapter. Flow rate, injection volume, sample concentration and modifier gradient profile were chosen as the decision variables to maximize the productivity and minimize the solvent consumption simultaneously under different purity constraints. NSGA, a modified version of simple GA, was used to solve the optimization problem. The resulting optimal Pareto curves were presented and compared with those obtained under isocratic conditions. The results indicate that high flow rates with low purity constraints lead to large productivity and low solvent consumption. When the CO_2 flow rate is fixed, linear gradient shows best performance (high productivity with low solvent

consumption). It was found that when the unit is operated at conditions far from pressure drop limitations, gradient operation offers significant advantage compared to isocratic elution. When the CO_2 flow rate is chosen as decision variable, the difference between the optimal Pareto curves of isocratic, step and linear gradient becomes minor. Finally, the effects of decision variables on objective functions were discussed. The study also shows that flow rate is an important decision variable to enhance productivity.

Chapter 5

Experimental implementation of optimal results

The optimum operating conditions under both isocratic, step gradient and linear gradient conditions obtained in Chapter 3, 4 were experimentally implemented on an analytical scale laboratory instrument. The resulting experimental elution profiles were compared with theoretical simulations and the results are discussed. Collections of desired enantiomers were also carried out for isocratic optimum operating conditions. The cut time was strictly set by the optimization results considering the dead volume in the collectors. Finally, the fractions collected were analyzed by a SFC method. The results of the implementation along with the limitations are discussed.

Keywords: Supercritical fluid chromatography, Fraction collection, Experimental implementation.

5.1 Introduction

As mentioned in previous chapters, few studies have focused on rigorous optimization of SFC process. As a result, experimental implementation of a theoretical optimization is rarely reported. However, such experiments are important due to the following reasons. Firstly, it is well known that the transition of a theoretical calculation to a practical application is not straightforward and requires certain efforts. Secondly, it is crucial to implement the real operation to prove the correctness of simulation and show the ability of the unit. Thus in this chapter, experiments were carried out to validate the optimization results given in Chapter 3 and 4.

One attractive feature of SFC is the instantaneous separation of the mobile phase from the solute. The solvent power of supercritical CO_2 can be controlled by altering the pressure. At constant temperature, decrease in pressure from a supercritical pressure to a subcritical pressure greatly reduces the solvent power of CO_2 which results in solute precipitation. Such a feature of CO_2 was employed to facilitate the collection and product recovery, for example in cyclones. At ideal conditions, formation of a biphasic system occurs when pressure decreases. If the mobile phase is pure supercritical CO_2, the final product can be directly collected through precipitation. If a modified mobile phase is used, a small amount of organic solvent (modifier) together with desired product is collected. In both cases, the time and energy consumption to recovery the product is much less than HPLC because the concentration of solute is much higher [100].

There are several factors which can affect the collection process and results in

an undesired outcome. Aerosol formation is an important factor that affects both purity and recovery. It usually occurs inside the cyclone separator when the mobile phase velocity is high, a situation commonly encountered in preparative separations. The solute particle can be drawn into the aerosol and taken out of the cycle through the vortex which decreases the recovery. Many methods and equipments were used to solve this problem. For example, another manual pressure regulator located downstream of cyclone can be used to decrease the flow velocity thus preventing aerosol formation. In some cases, a water bath or jacket that regulates the temperature at the cyclone is also employed to overcome the problem. In the unit available in our labs, a modifier stream is introduced right after the back pressure regulator to help maintain the recovery. The mixture is then sent to different collection vessels through switching valve and the gas is released from the outlet located on top. Such feature is expected to increase the separation efficiency and product recovery. Another factor which may worsen the collection is the solute residual inside the system especially on the tubing wall. Some solutes are viscous and tend to remain inside the tubing. This situation leads to cross contamination and thus reduces purity.

In this chapter, the main objective is to demonstrate the validity of optimizations by experimentally implementing the optimum operating conditions and collecting the desired enantiomers. The obtained elution profiles are compared with simulation results and the product was collected and analyzed by injecting back to the same SFC system to obtain the purity and recovery.

5.2 Experimental set-up and procedure

5.2.1 Experimental set-up and procedure

The experimental system used for separation and collection is shown in Fig. 5.1. The equipment up to the back pressure regulator is identical to the one described in chapter 2. In order to facilitate collection, a collection pump and a series of collection vessels were provided. When the unit is operated in a collection mode, the pressure of the mobile phase downstream of the back pressure regulator reduces to 1 atm. Under these conditions, CO_2 behaves as a rather poor solvent and the modifier and solute precipitate out of it. This leads to the formation of a biphasic system consisting of the gas phase (CO_2) and liquid phase (solute dissolved in modifier). A collection pump which continues pumping the solvent during the collection is used to improve the solvent power in order to prevent precipitation inside pipes. This function prevents the formation of aerosol and keeps the solute soluble in the modifier. Collections both with and without the solvent pump were implemented whose results are not presented here. It shows that the purity and recovery were significantly increased by using the solvent pump. A switching valve connecting the back pressure regulator and collection vessels was used to deliver desired enantiomers to designated vessels. The gas liquid mixture was sent to the collection vessels through a small tubing and a pipe located at the top of vessel was used to release the CO_2.

Usually a 30 min to 1 hour waiting period was provided for the system to reach equilibrium after which the injection was started. The injection loop

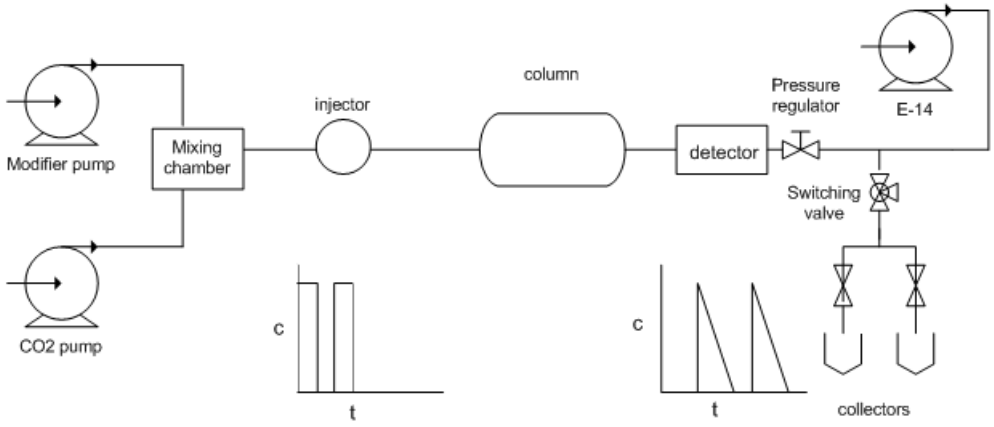

Figure 5.1: Schematic of a preparative SFC chromatographic and collection system

was firstly positioned at load mode and the sample was manually injected into the loop. Full loop injection was made to ensure the precision of injection amount. After injection, the loop was switched to the injection mode in which the mobile phase flowed through the loop to produce a pulse injection into the column. The switching between two modes was automatically controlled by the injector. Once the injection was made, the data collection was initiated. A collection time given by simulation results was used to decide the start and ending points of a fraction. The collection was done by manually switching the effluent to different vessels at designated time. At the downstream of the back pressure regulator, the biphasic mobile phase was sent to a switching valve where different fractions were delivered to the designated collection vessel. Inside the collection vessels, the solute and modifier drip through the wall and congregate at the vessel bottom and the gaseous CO_2 was sent to waste through the release piping. After the collection was completed, the vessels were sealed using parafilm to avoid contamination and sample loss. The collected fractions were injected back to the column for a composition

analysis. From the chromatogram, peak areas were used to calculate the purity by 5.1.

$$Pur_i = \frac{(Area)_i}{(Area)_R + (Area)_S}, i = R, S \tag{5.1}$$

The calculation of recovery is not as straightforward as purity. The collection vessels were weighted before and after the collection and mass difference was recorded. Once the solution density is known, the volume of collected fraction can be calculated. Due to the collection solvent pump, the solution is diluted, thus the density of pure methanol was used to calculate the fraction volume. Peak area was used to obtain sample concentration based on a UV calibration curve.The collected amount of product can thus be known by the product of the concentration and the volume. Recovery is calculated as the ratio of collected amount versus total injection amount of each enantiomer.

5.2.2 Measurement of dead volume

One of the primary objective of the study was to compare theoretical results with the experimental ones. Hence, it is important to characterize the dead volume in the system which refers to the volume of the tubing between column outlet and UV cell. The dead volume measured here is not the same as analytical injection since for collection system, there is a tubing connecting UV cell and back pressure regulator which results in a time delay between the back pressure regulator outlet and UV detector. Since the cut time is based on the chromatogram at column exit and the collection is done at the downstream of back pressure regulator, the dead volume of the tubing must

be determined to convert the cut time to an operational one.

A direct method for the dead volume measurement is to measure the length of the tubing connecting UV detector and back pressure regulator. However, it is difficult to precisely obtain the tubing length due to the bends, production inaccuracies and other factors. An alternative way to calculate the dead volume is to install two UV detectors in the system, one at the column outlet and the other located at downstream of back pressure regulator. Time difference between two UV profiles from two detectors is used to calculate the dead volume provided flow rate is known. The resulting chromatograms from two UV detectors are shown in Fig. 5.2. The time difference of two chromatogram is 0.9 min. Based on the corresponding volumetric flow rate, the dead volume was calculated to be 1.23 mL.

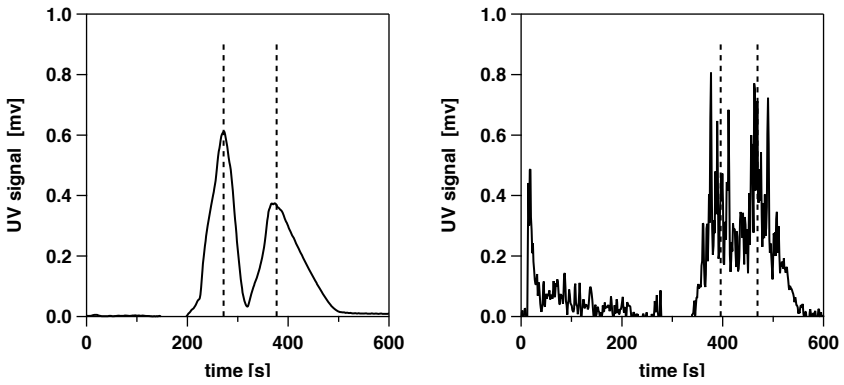

Figure 5.2: Experimental UV profiles upstream (left) and downstream (right) of the back pressure regulator. The dotted lines indicate the retention time. CO_2 flow rate: 1 mL/min, MeOH flow rate: 0.3466 mL/min, back pressure: 135 bar, injection volume: 100 μL, sample concentration: 53 g/L, UV wavelength: 305 nm

5.2.3 Validation of the collection efficiency

As mentioned before, the efficiency of separator can be affected by the temperature, pressure, and the separator design. Thus a validation of the separator efficiency is necessary to eliminate interferences from extra column effects. Before each collection, the vessels were washed using methanol and the pure methanol inside the vessels was injected into the column to ensure that no residual flurbiprofen was presented. To implement the validation, a small amount of racemic flurbiprofen is injected into the column to obtain a baseline separation. The CO_2 flow rate was fixed to 1 mL/min and the modifier concentration, c_m: 16 %. Only one peak was collected per injection to prevent the mixing between peaks. After the collection, the collected fractions were directly injected back to the same column to analyze the composition. The procedure was repeated to collect and analyze both the enantiomers. The chromatogram with collection windows and the fraction analysis results are shown in Fig. 5.3 and 5.4 respectively. Theoretically, the purity for a baseline separation peak should be 100% because there is no overlap of the two peaks. As shown from the figures, for both fractions, the composition of the impurity is around 7 %. We conjecture that this can be caused due to the high viscosity and sticky nature of flurbiprofen. Before entering the switching valve, all the fractions flow through the same line that connects the valve and pressure regulator outlet. It is highly possible that the undesired flurbiprofen enantiomer sticks to the tubing wall and was washed later causing cross contamination. The only way to solve this problem is to decrease the tubing length connecting back pressure regulator and switching valve which

was not possible due to the equipment limitations. This error should also be taken into account for a fair justification of optimization results since in the optimizer, the loss and contamination caused by collector is not taken into account.

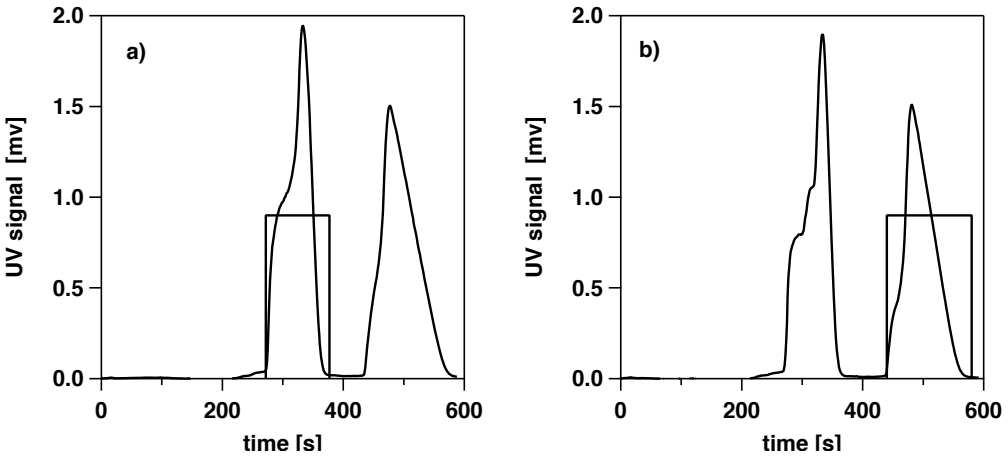

Figure 5.3: Experimental UV profile of injections for collection of a) R enantiomer and b) S enantiomer. The collection windows have been adjusted for dead volume. CO_2 flow rate: 1 mL/min, MeOH flow rate: 0.238 mL/min, back pressure: 135 bar, injection volume: 100 μL, racemic sample concentration: 16.7 g/L (left) and 12.1 g/L (right), UV wavelength: 295 nm

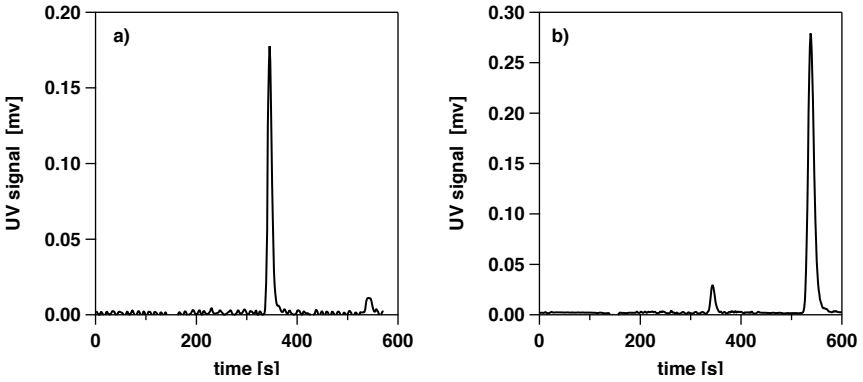

Figure 5.4: Chromatograms showing the fraction analysis of experiment reported in Fig. 5.3. a) Analysis of the fraction with a R flurbiprofen being the main component. b) Analysis of the fraction with S flurbiprofen being the main component. Injection conditons: CO_2 flow rate = 1 mL/min, MeOH flow rate = 0.3533 ml/min, back pressure = 135 bar, injection volume = 10 μL, UV wavelength = 295 nm.

5.3 Experimental implementation of optimum conditions under isocratic elution

5.3.1 Collection for fixed flow system with isocratic elution

The optimization for a system where the CO_2 flow rate is fixed to 1 mL/min was reported in Chapter 3. In this section, the experimental implementation and the collection under the optimal condition for isocratic elution with fixed flow was discussed. The optimal point was chosen from the Pareto curve with 99% purity and 95 % recovery constraints. The comparison of resulting experimental chromatogram and the simulation elution profiles are shown in Fig. 5.5. The experimental conditions are given in the caption. As observed from the figure, in experiment, the solutes eluted later than what is predicted by simulation. In order to analyze the results, a few injections were performed by varying the concentration of injections while keeping all other parameters identical. These results are shown in Fig. 5.6. A few trends are clearly observed. At an injection concentration of 100 g/L, the simulation predicts the experimental elution profile satisfactorily, although the experimental results show a larger spread compared to the simulation. While the injection concentration increases to 200 g/L, there is a deviation between the peak front of simulation and experimental results. However, the tail has been well described by simulation. This can possibly be a result of deviation of the adsorption equilibrium parameters at high concentrations compared to those measured at low concentrations. At the largest injection concentration, it appears that experimental profile shifts to a higher retention time, i.e., both

the peak front and the tails shift to higher retention times. This trend is not expected for systems exhibiting a Langmuir or bi-Langmuir isotherms. In these cases, the tail of the heavier component is always expected to match for mass overload injections. We conjecture that the cause for these profiles is the low solubility of flurbiprofen in CO_2. The injections used a concentration of 300 g/L is made. It is possible that under these conditions, the solubility of the solute in the supercritical mobile phase is rather low. This can lead to the precipitation of solute at the column inlet which gradually gets eluted as the mobile phase continues to flush through the column. This can result in trend observed in Fig. 5.6. Other reasons such as damage of stationary phase issues, validity of isotherm parameters, competitive effect of CO_2 and modifier seem less likely as these cannot explain the observed trends. Generally damage of stationary phase results in change of retention parameters which is not the case as the injections at linear conditions are comparable with experiments that were performed at least a year before showing that the stationary phase is indeed intact. Further, experiments at lower concentrations do not show significant shift in profiles compared to experiments. The other reason, which is common when moving from analytical to overloaded conditions is the validity of isotherm parameters measured at very low concentrations when used to predict injections at much higher concentrations. Although this may cause deviation between predicted and experimental elution profiles, they cannot explain why the tails of the heavier component can shift. Finally the competitive effect of modifier and CO_2 also seems less likely as these components are expected to adsorb weakly on the chiral selectors compared to the solute. The competition with a lighter components cannot

account for a shift in the elution profiles of the heavier component. From the above arguments, the only plausible reason seems to the effect of solubility. This aspect deserves attention in the future as it seems to affect experimental implementation significantly.

Fig. 5.5 also reveals that the width of the chromatogram is comparable to the predicted values. Hence, collection windows calculated from the simulation were implemented by using their relative times starting from the elution time of the first peak.

The collection was processed manually by opening the switching valve to different vessels at an appointed time. Totally two fractions were obtained and each of them mainly contains one enantiomer. Before injecting back for fraction analysis, the collected samples were sealed in vessels to prevent sample degradation or loss. Since flurbiprofen can be remained on the tubing wall, pure methanol was injected before each fraction analysis injection to eliminate the effect of residual. The results for fraction analysis are shown in Fig. 5.7. The purity for R enantiomer in first fraction is 94% and for S enantiomer in second fraction is 92%. Compared with the purity constraint of 99% in optimization, there is some deviation. However, it is worth pointing out that even for a baseline separation whose fraction purity is expected to be 100% the purity for collected fraction was only 93%. This fact indicates that the reduction in purity is perhaps caused by extra column effects. Nevertheless, the purity obtained here is close to a purity from baseline separation.

Next the satisfaction of the recovery constraint needs to be examined. The

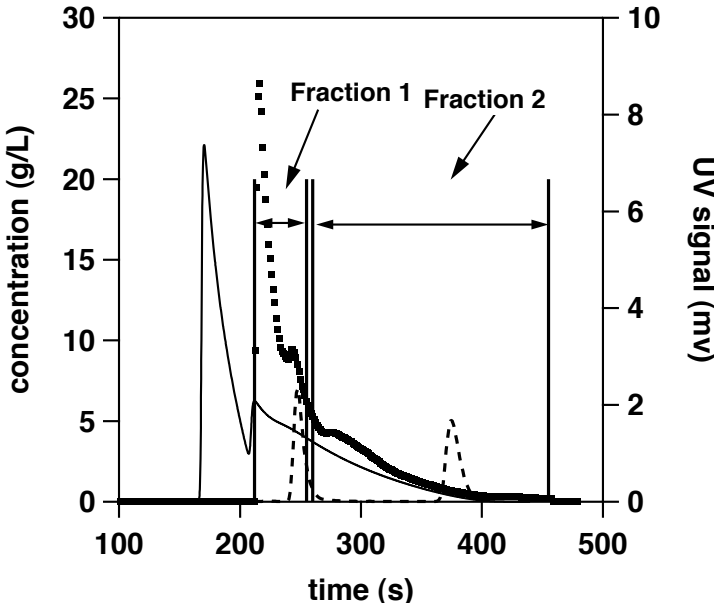

Figure 5.5: Comparison of experimental (dotted line: implementation of optimum condition, dash line: analytical injection represented by UV signal) and simulation (solid line) results for optimal solution with operational cut time. Purity constraint: 99%, Recovery constraint: 95%. CO_2 flow rate:1 mL/min, MeOH flow rate: 0.3533 mL/min (c_m: 22.2%), back pressure: 135 bar, injection volume: 70 μL, injection concentration: 290 g/L. UV wavelength: 220 nm

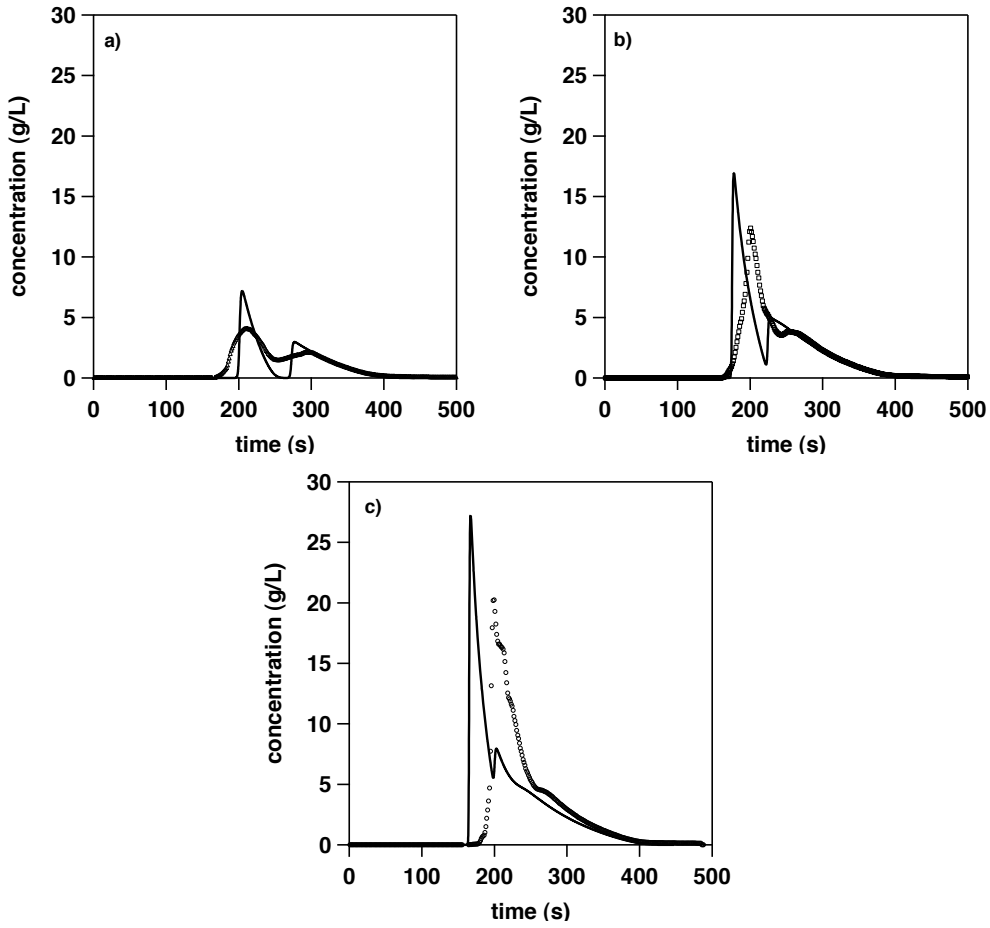

Figure 5.6: Comparison of experimental (lines) and simulation (symbols) results for three different injection concentration, namely, a) 100 g/L, b) 220 g/L, c) 300 g/L. CO_2 flow rate: 1 mL/min, modifier composition (c_m): 22.0%, back pressure: 135 bar, injection volume: 80 μL

procedure described before was used to calculate the recovery. The calculated recovery of R enantiomer for 1st fraction is 67% and for S enantiomer in 2nd fraction this value is 91%. For the S enantiomer, the recovery constraint of 95% is generally satisfied but a significant deviation with the constraint for R enantiomer in 1st fraction was observed. This can be explained in several aspects. Firstly, the peak appeared under pure methanol injection shows that even after wash, some flurbiprofen can still remain in the system. This would lead to a loss in recovery. Secondly, the collection results for baseline separation show that there exists cross contamination between two collection vessels and along the joint tubing which also cause the decrease in the desired product amount. Finally, although the solvent pumped downstream of the back pressure regulator prevents the formation of aerosol and kept solute soluble in the solvent, it is still possible that a portion of solute particles suspend in the gas phase and leaves the system with CO_2. Since the purities obtained are comparable to these from the baseline separation, it can be argued that the optimum injection can indeed be experimentally implemented. However, the collection efficiency has to be markedly improved in order to fully reach the optimum results. It indicates that to improve the product quality, more effort should be put on the design of collection system which mainly caused the deteriorating in recovery.

5.3.1.1 Collection for variable flow system with isocratic elution

The collection for optimum operating condition with constraints of both 95% recovery and purity when CO_2 flow rate was selected as decision variable was also implemented. The procedure and fraction analysis method were same as

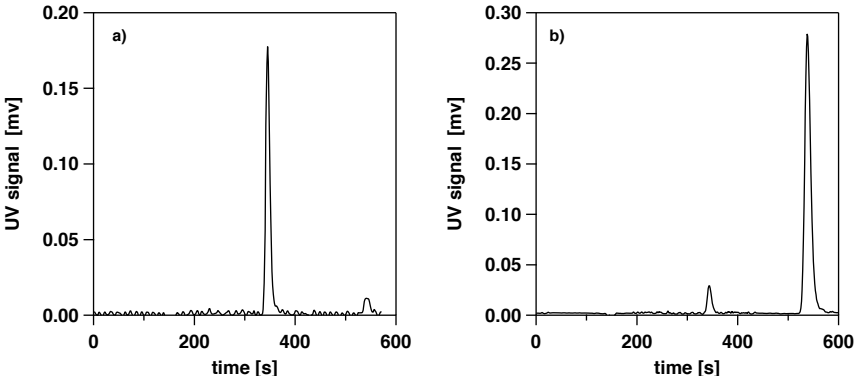

Figure 5.7: Chromatograms showing the fraction analysis for experiments reported in Fig. 5.5. a) Analysis of first peak collected. b) Analysis of second peak collected. CO_2 flow rate: 1 mL/min, MeOH flow rate: 0.238 mL/min, back pressure: 135 bar, injection volume: 10 μL,UV wavelength: 220 nm

the collection for fixed flow system. The corresponding chromatogram with cut time is shown in Fig. 5.8. Delay in the retention time of experimental elution profile compared with simulation was also observed in this case. The collected fractions were analyzed and the results are shown in Fig. 5.9. The purity of R enantiomer for 1st fraction is 86% and for S enantiomer of 2nd fraction the purity is 73%. Compared with the purity constraint of 95%, the deviation for R enantiomer is 10 % and for S enantiomer is 23 %. As mentioned before, cross contamination happens at the downstream of the back pressure regulator which caused a decrease in purity. The high flow rate which is about 2 times of that in fixed flow system might increase such effect since it increases the potential dispersion and mixing. Moreover the high throughput of sample raises the possibility that the solute remain on the tubing wall which could also cause lower purity than expected. The recovery of R enantiomer in 1st fraction is 77% and that of the S enantiomer is 90%. In general, the obtained recoveries are indeed low compared to expected values.

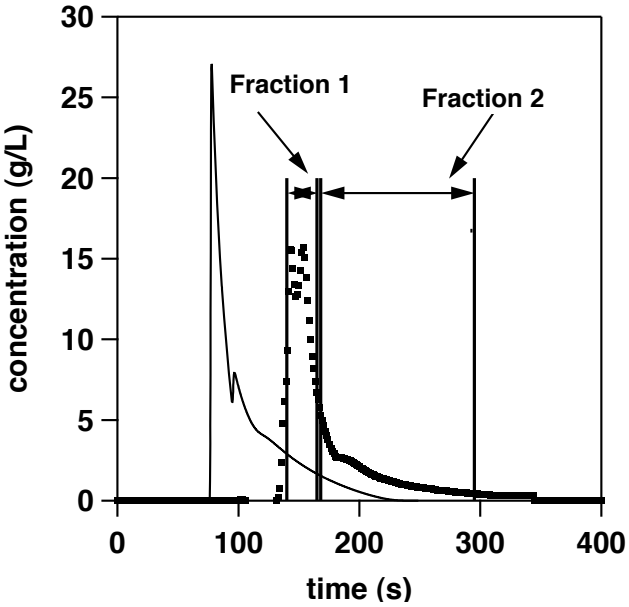

Figure 5.8: Comparison of experimental (dotted line) and simulation (solid line) results for optimal solution with operational cut time. Purity constraint: 95%, Recovery constraint: 95%. CO_2 flow rate: 2.3 mL/min, MeOH flow rate: 0.59 mL/min, back pressure: 135 bar, injection volume: 130 μL, injection concentration: 220 g/L.

5.4 Conclusion

In this chapter the results of the attempts to experimentally realize the optimization results were discussed. Attempts were also made to collect fractions. The experimental implementations proved challenging. Firstly, the experimental elution profiles showed deviation from the calculated values. These deviations are possibly caused due to effect of solubility of the solute in the supercritical mobile phase. Secondly, the results of fraction collection showed that cross contamination and possible formation of solvent mist reduced purities and recovery values. In any case for experiments with low CO_2 flow

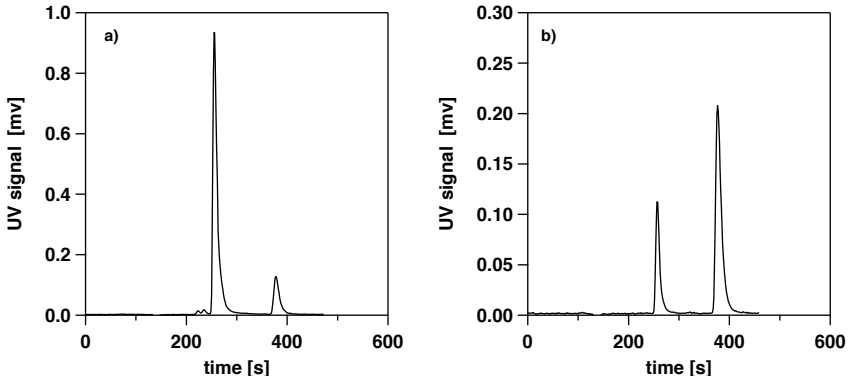

Figure 5.9: Chromatograms showing the fraction analysis for experiments reported in Fig. 5.8. a) Analysis of first peak collected. b) Analysis of second peak collected. CO_2 flow rate:1 mL/min, MeOH flow rate: 0.238 mL/min, back pressure: 135 bar, injection volume: 10 μL,UV wavelength: 220 nm

rate showed that purities greater than 90% were possible.

It is worth noting that in this work, we have pushed requirement to the limit of what is possible theoretically. However, practical implementations have revealed limitations that can be only solved by better design of collection systems and by better injection methods [84]. They also highlight the importance of taking into account the solute solubility when performing optimization. These results provide clear indications about area that deserve further investigation.

Chapter 6

Concluding remarks

6.1 Conclusion

The thesis addresses key issues concerning SFC, namely, fundamentals of retention, process optimization and the experimental realization of optimal results. Both experimental and theoretical tools have been used to study enantioseparation process by SFC. The isotherm parameters under linear and non-linear range has been investigated by a series of experiments. The effect of various operating factors on the separation performance have been studied and integrated into a proper mathematical model which was developed to simulate the separation process. Based on the experimental data and the modeling, optimizations problems for the SFC enantioseparation process were constructed as multi-objective optimization problems which aim to maximize the productivity and minimize the solvent consumption for different elution modes. These problems were solved by a non-dominated sorting generic algorithm (NSGA) algorithm. Unlike other optimization algorithm, NSGA tends to search for the optimal solution within a large domain through different directions thus avoiding local optimal solutions. Finally, enantioseparation and product collection were experimentally implemented on an analytical scale set-up. The experimental results were compared with simulation and qualitatively support the optimal solutions.

Several important observations have been made. Firstly, the high efficiency offered by SFC and the use of 5 μm particles have been clearly demonstrated. It was seen in Chapter 2 that all elution profiles at high loading are describable by the equilibrium theory of chromatography and the mass transfer parameters obtained by the inverse method indicate the same. Secondly, it was shown that standard models to describe solute adsorption in HPLC and GC conditions also seem to adequately describe adsorption equilibrium under SFC conditions as well. The usefulness of isotherm parameters and the potential of SFC in preparative scale have been demonstrated by the optimization. The optimization results in Chapter 3 show that owing to favorable physical properties, it is possible to achieve a productivity of up to 8 kg/kg stationary phase per day at a recovery and purity of 95%. These values of productivities are considered very favorable for chromatographic enantioseparation.

The goal of the thesis was to develop scale-up methods based on mathematical models. The procedures developed in this work namely description of adsorption equilibrium and mass transfer properties at supercritical conditions, development of optimization tools that use realistic constraints will help practitioners to obtain desired product specifications. Based on a few experiments at an analytical scale, users can obtain realistic estimation of productivity and solvent consumption, the key economic indicators of process performance. This quality by design approach also allows to decide and compare alternatives, e.g. HPLC vs SFC, SMB vs SFC at a much earlier stage implementing the separation. The rule of thumb in industrial chro-

matography is to consider an SMB process for productivities greater than 1 kg/kg/day which typically has a solvent consumption of 200 L/kg racemate [94]. The organic solvent consumption in SFC is found to be about 52 L/kg racemate. This is a very important result that clearly highlights the "green" aspect of SFC compared even with complex multi-column process. These results show that the investment costs which tend to be high for SFC, owing to high pressure operation, can be easily offset by low operating costs.

Not only the simple isocratic operation has been studied, but also the gradient elution has been investigated. Unlike HPLC, the gradient of modifier or pressure in SFC has a much more profound effect on the separation. In Chapter 4, the rational design of modifier gradients was presented. Simple profiles were considered and modeled. This is one of the first studies to consider modifier gradients in SFC. It was shown that at moderate flow rates, modifier gradient offers significant improvement in process performance. However, when the unit is to be operated at higher flow rates, the advantages of gradient operation is rather modest and users might prefer to consider the isocratic mode that is easier to implement.

In the final chapter, an attempt was made to experimentally implement the results of the optimization. Before the collection of product under optimal conditions, the efficiency of collection system has been tested by baseline separation. For baseline separations, collection efficiency was observed to be satisfactory. Samples with optimal values of concentration and volume were then injected. Deviations between simulation and experimental results were observed at high overloading conditions. It was conjectured that the poor

solubility could cause these differences and it should be taken into account in the future work. For the collection of high sample loading, the results are less satisfactory when the flow rate increases. Formation of aerosol inside collection vessels could most likely lead to such deviation since it is enhanced under high flow rate. All of these results indicate that the effort should also be spent on the collection system improvement to assure the product quality.

6.2 Outlook

This work has demonstrated the potential of SFC for preparative separations. However there are several open issues that need to be addressed in order to better understand and design SFC processes. The effect of solubility on the preparative separation needs to be addressed not only in solvent but also in the supercritical mobile phase. First steps in this direction has been started [101]. In order to obtain high productivity, concentrated solution is usually preferred . The issue of solubility in solvent has been noticed before but such concern in the aspect of supercritical fluid is not yet discussed in literature. In some cases, the injection concentration of solute in pure solvent is higher than the solubility limit in the supercritical fluid. The injection profile might be changed due to the solubility issue thus affects the elution profile. Models and optimization methods that take into account this aspect has to be developed. Another issue which needs to be investigated in the future is the adsorption of mobile phase in SFC. The models used in this study have not explicitly account for the competitive adsorption of CO_2 and modifier. These have to be performed to understand the effect of this

phenomena on preparative separations.

Although not explored here, various modifier shapes should be studied particularly in light of multi component separations. These may be important to extend the capacity of SFC also to bio-separations. Although only modifier gradient has been discussed in this thesis, the use of pressure gradient can be attractive to separate non-polar solutes where the mobile phase can be pure CO_2. Different injection methods need to be developed to avoid the precipitation of the solids at the column inlet. These might lead to the results with unexpected peak shapes allowing the realization of optimal conditions. Finally collection systems have to be designed to take into account low solubility of solutes and the high viscosity they exhibit when they precipitate from the mobile phase. The system also needs to minimize the formation of aerosol which might greatly decrease the purity and recovery of final product. These studies will improve the understanding of SFC and will allow improved process performance.

Roman symbols

a	parameter in Henry constant correlation,Eq. 2.3 [-]
$Area$	peak area based UV signal [mV s]
b_1	UV calibration parameter [g L^{-1}]
b_2	UV calibration parameter [μV]
b_3	UV calibration parameter [μV^{-1}]
c	fluid phase concentration of solute [g L^{-1}]
c^{loop}	injected concentration [g L^{-1}]
c_{m}	modifier concentration [w/w]
D_{ax}	axial dispersion coefficient [cm^2 s^{-1}]
d	parameter in Henry constant correlation, Eq. 2.3 [-]
H	Henry constant
J	objective function in UV calibration [-]
K	equilibrium constant in Langmuir isotherm [L g^{-1}]
k_f	mass transfer coefficient [s^{-1}]
L	length of the column [cm]
m	mass flow rate [g s^{-1}]
N	number of theoretical plates [-]
n	solid phase concentration of solute [g L^{-1}]
n^*	equilibrium solid-phase concentration of solute [g L^{-1}]
P	purity [%]
PR	productivity [kg/kg/day]
p	parameter in Henry constant correlation, Eq. 2.3 [-]
ΔP	pressure drop [bar]
P	pressure [bar]
Q	volumetric flow rate [cm^3 min^{-1}]
q	parameter in Henry constant correlation, Equation 2.3 [-]
r	parameter in Henry constant correlation, Eq. 2.3 [-]
S	solvent consumption [L kg^{-1}]
Sig	UV signal [μV]
t	time [s]
t_c	cycle time [s]
t_g	gradient time [s]
t_0	column hold-up time [s]
t_i^R	retention time [s]
T	temperature [K]
v	interstitial velocity [cm s^{-1}]
V^{loop}	volume of injection loop [cm^3]
w_{csp}	weight of stationary phase [g]
Y	recovery [%]
z	axial coordinate [cm]

Greek symbols

α	selectivity
ϵ	total porosity
ρ	density [kg·cm^3]
Γ	saturation capacity [g L^{-1}]
Ψ	objective function [s]

Subscripts & superscripts

c	critical
exp	experiment
i	component i
$init$	initial state
k	injection number
m	modifier
ns	non-selective
R	enantiomer R
S	enantiomer S
sel	selective
0	reference state

References

[1] R. L. Smith, S. B. Lee, S. Suzuki, C. Saito, H. Inomata, and K. Arai. Densities of carbon dioxide + methanol mixtures at temperatures from 313.2 to 323.2 K and at pressures from 10 to 20 MPa. *J. Chem. Eng. Data*, 47:608–612, 2002.

[2] Walle Thomas and Walle. U. Kristina. Pharmacokinetic parameters obtained with racemates. *Trends Pharmacol. Sci.*, 7:155–158, 1986.

[3] U.S. Food Administration and Drugs. FDA's policy statement for the development of new stereoisomeric drugs. *Chirality*, 4:338–340, 1992.

[4] S. Erb. Single-enantiomer drugs poised for further market growth. *Pharmaceutical Technology (SUPPL)*, 30:s14–s18, 2006.

[5] H. Lorenz, D. Polenske, and A. Seidel-Morgenstern. Application of preferential crystallization to resolve racemic compounds in a hybrid process. *Chirality*, 18:828–840, 2006.

[6] L. He and T. E. Beesley. Applications of enantiomeric gas chromatography: A review. *J. Liq. Chromatogr. Relat. Technol.*, 28:1075–1114, 2005.

[7] R. I. Stefan-Van Staden and R. M. Nejem. Determination of L-vesamicol in serum samples using enantioselective, potentiometric membrane electrodes based on antibiotics. *Anal. Lett.*, 39:675–682, 2006.

[8] P. Hadik, L. P. Szabo, E. Nagy, and Z. Farkas. Enantioseparation of D,L-lactic acid by membrane techniques. *J. Membr. Sci.*, 251:223–232, 2005.

[9] E. Miyako, T. Maruyama, N. Kamiya, and M. Goto. A supported liquid membrane encapsulating a surfactant-lipase complex for the selective separation of organic acids. *Chem - Eur J.*, 11:1163–1170, 2005.

[10] B. Simandi, S. Keszei, E. Fogassy, S. Kemeny, and J. Sawinsky. Separation of enantiomers by supercritical fluid extraction. *J. Supcrit. Fluids, The*, 13:331–336, 1998.

[11] T. J. Ward. Chiral separations. *Anal. Chem.*, 72:4521–4528, 2000.

[12] Richard Thompson. A practical guide to hplc enantioseparations for pharmaceutical compounds. *J. Liq. Chromatogr. Relat. Technol.*, 28:1215 – 1231, 2005.

[13] T. A. Berger and Royal Society of Chemistry (Great Britain). *Packed column SFC*. The Royal Society of Chemistry, Cambridge, 1995.

[14] J. F. Deye, T. A. Berger, and A. G. Anderson. Nile red as a solvatochromic dye for measuring solvent strength in normal liquids and mixtures of normal liquids with supercritical and near critical fluids. *Anal. Chem.*, 62:615–622, 1990.

[15] D. R. Gere. Supercritical fluid chromatography. *Science*, 222:253–259, 1983.

[16] W. Majewski, E. Valery, and O. Ludemann-Hombourger. Principle and applications of supercritical fluid chromatography. *J. Liq. Chromatography R.T.*, 28:1233–1252, 2005.

[17] M. Perrut. Advances in supercritical fluid chromatographic processes. *J. Chromatogr. A*, 658:293–313, 1994.

[18] T. A. Berger and W. H. Wilson. Packed-column supercritical-fluid chromatography with 220000 plates. *Anal. Chem.*, 65:1451–1455, 1993.

[19] Lynam G. Kenneth and Edgar C. Nicolas. Chiral HPLC versus chiral SFC: Evaluation of long-term stability and selectivity of chiralcel OD using various eluents. *J. Pharm. Biomed. Anal.*, 11:1197–1206, 1993.

[20] D. A. Turner E.Klesper, A.H.Corwin. *J. Org. Chem.*, 27:700–701, 1962.

[21] Ganapathy Subramanian. *Chiral Separation Techniques (Second Edition)*. 2001.

[22] F. Denet, W. Hauck, R. M. Nicoud, O. Di Giovanni, M. Mazzotti, J. N. Jaubert, and M. Morbidelli. Enantioseparation through supercritical fluid simulated moving bed (sf-smb) chromatography. *Ind. Engg. Chem. Res.*, 40:4603–4609, 2001.

[23] C. Desmortreux, M. Rothaupt, C. West, and E. Lesellier. Improved separation of furocoumarins of essential oils by supercritical fluid chromatography. *J. Chromatogr. A*, 1216:7088–7095, 2009.

[24] E. Lesellier and A. Tchapla. Retention behavior of triglycerides in octadecyl packed subcritical fluid chromatography with co2/modifier mobile phases. *Anal. Chem.*, 71:5372–5378, 1999.

[25] X Lou, H.-G. Janssen, and C. A. Cramers. Temperature and pressure effects on solubility in supercritical carbon dioxide and retention in supercritical fluid chromatography. *J. Chromatogr. A*, 785:57–64, 1997.

[26] D. Upnmoor and G. Brunner. Retention of acidic and basic compounds in packed column supercritical fluid chromatography. *Chromatographia*, V28:449–454, 1989.

[27] M. Ashraf-Khorassani, S. Shah, and L. T. Taylor. Column efficiency comparison with supercritical fluid carbon dioxide versus methanol-modified carbon dioxide as the mobile phase. *Anal. Chem.*, 62:1173–1176, 2002.

[28] T. A. Berger and J. F. Deye. Separation of phenols by packed column supercritical fluid chromatography. *J. Chromatogr. Sci.*, 29:54–59, 1991.

[29] J. W. Coym and J. G. Dorsey. Chromatographic shape selectivity with carbon dioxide-acetonitrile mobile phases: Effect of mobile phase composition and density. *J. Chromatogr. A*, 971:61–72, 2002.

[30] J. A. Blackwell and R. W. Stringham. Characterization of temperature dependent modifier effects in sfc using linear solvation energy relationships. *Chromatographia*, 46:301–308, 1997.

[31] T. A. Berger. Separation of polar solutes by packed column supercritical fluid chromatography. *J. Chromatogr. A*, 785:3–33, 1997.

[32] T. A. Berger and W. H. Wilson. Separation of anilines, benzamides, benzylamines, and phenylethylamines by packed-column supercritical fluid chromatography. *J. Chromatogr. Sci.*, 31:127–132, 1993.

[33] T. A. Berger and J. F. Deye. Effect of basic additives on peak shapes of strong bases separated by packed-column supercritical fluid chromatography. *J. Chromatogr. Sci.*, 29:310–317, 1991.

[34] P. S. Mukherjee. Validation of direct assay of an aqueous formulation of a drug compound azy by chiral supercritical fluid chromatography (sfc). *J. Pharm. Biomed. Anal.*, 43:464–470, 2007.

[35] Y. Zhao. Chiral separation of selected proline derivatives using a polysaccharide-type stationary phase by supercritical fluid chromatography and comparison with high-performance liquid chromatography. *J. Chromatogr. A*, 1189:245–253, 2008.

[36] F. M. Chou, W. T. Wang, and G. T. Wei. Using subcritical/supercritical fluid chromatography to separate acidic, basic, and neutral compounds over an ionic liquid-functionalized stationary phase. *J. Chromatogr. A*, 1216:3594–3599, 2009.

[37] R. Duval, Lévěque., Y. Prigent, and H. Y. Aboul-Enein. Enantioseparation of aminoglutethimide and thalidomide by high performance liquid chromatography or supercritical fluid chromatography on mono-2

and mono-6-O-pentenyl-β-cyclodextrin-based chiral stationary phases. *Biomed. Chromatogr.*, 15:202–206, 2001.

[38] M. J. Del Nozal, L. Toribio, J. L. Bernal, E. M. Nieto, and J. J. Jiménez. Separation of albendazole sulfoxide enantiomers by chiral supercritical-fluid chromatography. *J. Biochem. Biophys. Methods*, 54:339–345, 2002.

[39] L. Toribio, M. J. Nozal, J. L. Bernal, and E. M. Nieto. Use of semipreparative supercritical fluid chromatography to obtain small quantities of the albendazole sulfoxide enantiomers. *J. Chromatogr. A*, 1011:155–161, 2003.

[40] J. Dönnecke, L. A. Svensson, O. Gyllenhaal, K. E. Karlsson, A. Karlsson, and J. Vessman. Evaluation of a vancomycin chiral stationary phase in packed capillary supercritical fluid chromatography. *Journal of Microcolumn Separations*, 11:521–533, 1999.

[41] P. Oswald, K. Desmet, P. Sandra, J. Krupčík, P. Májek, and D. W. Armstrong. Determination of the enantiomerization energy barrier of some 3-hydroxy-1,4-benzodiazepine drugs by supercritical fluid chromatography. *Journal of Chromatography B: Analytical Technologies in the Biomedical and Life Sciences*, 779:283–295, 2002.

[42] Y. Liu, A. Berthod, C. R. Mitchell, T. L. Xiao, B. Zhang, and D. W. Armstrong. Super/subcritical fluid chromatography chiral separations with macrocyclic glycopeptide stationary phases. *J. Chromatogr. A*, 978:185–204, 2002.

[43] L. A. Svensson and P. K. Owens. Enantioselective supercritical fluid chromatography using ristocetin a chiral stationary phases. *Analyst*, 125:1037–1039, 2000.

[44] N. Wu, Z. Chen, J. C. Medina, J. S. Bradshaw, and M. L. Lee. Fast chiral separations using packed capillary columns and near-critical fluid carbon dioxide mobile phase. *Journal of Microcolumn Separations*, 12:454–461, 2000.

[45] Y. Liu, R. V. Rozhkov, R. C. Larock, T. L. Xiao, and D. W. Armstrong. Fast super/subcritical fluid chromatography enantiomeric separations of dihydrofurocoumarin derivatives with macrocyclic glycopeptide stationary phases. *Chromatographia*, 58:775–779, 2003.

[46] K. Yaku, K. Aoe, N. Nishimura, and F. Morishita. Thermodynamic study and separation mechanism of diltiazem optical isomers in packed-column supercritical fluid chromatography. *J. Chromatogr. A*, 848:337–345, 1999.

[47] R. J. Strife, M. L. Mangels, and J. A. Skare. Separation and analysis of dimethylaniline isomers by supercritical fluid chromatography-electrospray ionization tandem mass spectrometry. *J. Chromatogr. A*, 1216:6970–6973, 2009.

[48] G. Lavison and D. Thiébaut. Evaluation of a ristocetin bonded stationary phase for subcritical fluid chromatography of enantiomers. *Chirality*, 15:630–636, 2003.

[49] F. Geiser and R. Shah. Enantioseparation of hydrochloride salts using carbon dioxide-based mobile phases with on-line polarimetric detection. *Chirality*, 16:263–266, 2004.

[50] L. Toribio, M. J. Del Nozal, J. L. Bernal, J. J. Jiménez, and C. Alonso. Chiral separation of some triazole pesticides by supercritical fluid chromatography. *J. Chromatogr. A*, 1046:249–253, 2004.

[51] M. Johannsen. Separation of enantiomers of ibuprofen on chiral stationary phases by packed column supercritical fluid chromatography. *J. Chromatogr. A*, 937:135–138, 2001.

[52] Y. K. Ye, K. G. Lynam, and R. W. Stringham. Effect of amine mobile phase additives on chiral subcritical fluid chromatography using polysaccharide stationary phases. *J. Chromatogr. A*, 1041:211–217, 2004.

[53] K. W. Phinney and L. C. Sander. Additive concentration effects on enantioselective separations in supercritical fluid chromatography. *Chirality*, 15:287–294, 2003.

[54] M. J. del Nozal, L. Toribio, J. L. Bernal, C. Alonso, and J. J. Jiménez. Chiral separation of omeprazole and several related benzimidazoles using supercritical fluid chromatography. *J. Sep. Sci.*, 27:1023–1029, 2004.

[55] Baogen Su, Zongbi Bao, Huabin Xing, Yiwen Yang, and Qilong Ren. Enantioseparation of paroxetine intermediate on an amylose-derived

chiral stationary phase by supercritical fluid chromatography. *J. Chromatogr. A*, 1216:5140–5146, 2009.

[56] C. White. Integration of supercritical fluid chromatography into drug discovery as a routine support tool: Part I. fast chiral screening and purification. *J. Chromatogr. A*, 1074:163–173, 2005.

[57] F. Geiser, M. Schultz, L. Betz, M. Shaimi, J. Lee, and W. Champion Jr. Direct, preparative enantioselective chromatography of propranolol hydrochloride and thioridazine hydrochloride using carbon dioxide-based mobile phases. *J. Chromatogr. A*, 865:227–233, 1999.

[58] M. J. Del Nozal, L. Toribio, J. L. Bernal, and N. Castaño. Separation of triadimefon and triadimenol enantiomers and diastereoisomers by supercritical fluid chromatography. *J. Chromatogr. A*, 986:135–141, 2003.

[59] G. Guiochon. Preparative liquid chromatography. *J. Chromatogr. A*, 965:129–161, 2002.

[60] Douglas M. Ruthven and C. B. Ching. Counter-current and simulated counter-current adsorption separation processes. *Chem. Eng. Sci.*, 44:1011–1038, 1989.

[61] L. Miller, C. Grill, T. Yan, O. Dapremont, E. Huthmann, and M. Juza. Batch and simulated moving bed chromatographic resolution of a pharmaceutical racemate. *J. Chromatogr. A*, 1006:267–280, 2003.

[62] M. Juza, M. Mazzotti, and M. Morbidelli. Simulated moving-bed chromatography and its application to chirotechnology. *Trends Biotechnol.*, 18:108–118, 2000.

[63] M. Mazzotti, G. Storti, and M. Morbidelli. Supercritical fluid simulated moving bed chromatography. *J. Chromatogr. A*, 786:309–320, 1997.

[64] A. Depta, T. Giese, M. Johannsen, and G. Brunner. Separation of stereoisomers in a simulated moving bed-supercritical fluid chromatography plant. *J. Chromatogr. A*, 865:175–186, 1999.

[65] A. Rajendran, S. Peper, M. Johannsen, M. Mazzotti, M. Morbidelli, and G. Brunner. Enantioseparation of 1-phenyl-1-propanol by supercritical fluid-simulated moving bed chromatography. *J. Chromatogr. A*, 1092:55–64, 2005.

[66] S. Peper, M. Lübbert, M. Johannsen, and G. Brunner. Separation of ibuprofen enantiomers by supercritical fluid simulated moving bed chromatography. *Sep. Sci. Technol.*, 37:2545–2566, 2002.

[67] A. Seidel-Morgenstern. Experimental determination of single solute and competitive adsorption isotherms. *J. Chromatogr. A*, 1037:255–272, 2004.

[68] J. R. Strubinger, H. Song, and J. F. Parcher. High-pressure phase distribution isotherms for supercritical fluid chromatographic systems. 1. pure carbon dioxide. *Anal. Chem.*, 63:98–103, 1991.

[69] A. Rajendran, M. Mazzotti, and M. Morbidelli. Enantioseparation of 1-phenyl-1-propanol on chiralcel od by supercritical fluid chromatography: I. linear isotherm. *J. Chromatogr. A*, 1076:183–188, 2005.

[70] A. Rajendran, T. S. Gilkison, and M. Mazzotti. Effect of pressure drop on solute retention and column efficiency in supercritical fluid chromatography - part 2: Modified carbon dioxide as mobile phase. *J. Sep. Sci.*, 31:1279–1289, 2008.

[71] J. L. Eriksen, S. A. Sagi, T. E. Smith, S. Weggen, P. Das, D. C. McLendon, V. V. Ozols, K. W. Jessing, K. H. Zavitz, E. H. Koo, and T. E. Golde. Nsaids and enantiomers of flurbiprofen target Y-secretase and lower aβ42 in vivo. *J. Clin. Invest.*, 112:440–449, 2003.

[72] L. Gasparini, E. Ongini, D. Wilcock, and D. Morgan. Activity of flurbiprofen and chemically related anti-inflammatory drugs in models of alzheimer's disease. *Brain Research Reviews*, 48:400–408, 2005.

[73] http://www.clinicaltrials.gov/ct/gui/show/nct00045123.

[74] Ding-Yu Peng and Donald B. Robinson. New two-constant equation of state. *Ind Eng Chem Fundam*, 15:59–64, 1976.

[75] W. H. Pirkle and C. J. Welch. A convenient void volume marker for several chiral hplc columns. *J. Liq. Chromatogr.*, 14:1–8, 1991.

[76] W. H. Wilson. Direct enantiomeric resolution of ibuprofen and flurbiprofen by packed column sfc. *Chirality*, 6:216–219, 1994.

[77] M.S. Villeneuve and L. A. Miller. in: G. cox (ed.),preparative enantioselective chromatography, blackwell , blackwell, oxford/ames, ia, 2005. *in: G. Cox (Ed.),Preparative Enantioselective Chromatography, Blackwell , Blackwell, Oxford/Ames, IA, 2005.*

[78] G. Cox, R. Stringham, and A. Matabe. Resolution of flurbiprofen enantiomers by preparative chiral supercritical fluid chromatography. *LC-GC North America*, 20:24, 2002.

[79] S. Ottiger, J. Kluge, A. Rajendran, and M. Mazzotti. Enantioseparation of 1-phenyl-1-propanol on cellulose-derived chiral stationary phase by supercritical fluid chromatography. ii. non-linear isotherm. *J. Chromatogr. A*, 1162:74–82, 2007.

[80] L. Asnin and G. Guiochon. Calibration of a detector for nonlinear responses. *J. Chromatogr. A*, 1089:105–110, 2005.

[81] A. Felinger, A. Cavazzini, and G. Guiochon. Numerical determination of the competitive isotherm of enantiomers. *J. Chromatogr. A*, 986:207–225, 2003.

[82] G. Guiochon, S. Golshan-Shirazi, and A. M. Katti. *Fundamentals of Preparative and Nonlinear Chromatography, Academic Press, 1994*, 1994.

[83] S. Golshan-Shirazi and G. Guiochon. Analytical solution for the ideal model of chromatography in the case of a langmuir isotherm. *Anal. Chem.*, 60:2364–2374, 1988.

[84] Larry T. Taylor. Supercritical fluid chromatography for the 21st century. *J. Supcrit. Fluids*, 47:566–573, 2009.

[85] C. H. Tseng and T. W. Lu. Minimax multiobjective optimization in structural design. *Int. J. Numer. Meth. Eng.*, 30:1213–1228, 1990.

[86] A. Messac. Physical programming: Effective optimization for computational design. *AIAA Journal*, 34:149–158, 1996.

[87] M. Amanullah and M. Mazzotti. Optimization of a hybrid chromatography-crystallization process for the separation of träger's base enantiomers. *J. Chromatogr. A*, 1107:36–45, 2006.

[88] A. Rajendran, O. Kräuchi, M. Mazzotti, and M. Morbidelli. Effect of pressure drop on solute retention and column efficiency in supercritical fluid chromatography. *J. Chromatogr. A*, 1092:149–160, 2005.

[89] K. Liu and E. Kiran. Viscosity, density and excess volume of acetone + carbon dioxide mixtures at high pressures. *Ind. Engg. Chem. Res.*, 46:5453–5462, 2007.

[90] Chen Wenda and Arvind Rajendran. Enantioseparation of flurbiprofen on amylose-derived chiral stationary phase by supercritical fluid chromatography. *J. Chromatogr. A*, 1216:8750–8758, 2009.

[91] M. Amanullah, C. Grossmann, M. Mazzotti, M. Morari, and M. Morbidelli. Experimental implementation of automatic 'cycle to cycle' control of a chiral simulated moving bed separation. *J. Chromatogr. A*, 1165:100–108, 2007.

[92] G. Paredes and M. Mazzotti. Optimization of simulated moving bed and column chromatography for a plasmid dna purification step and for a chiral separation. *J. Chromatogr. A*, 1142:56–68, 2007.

[93] Ziyang Zhang, Marco Mazzotti, and Massimo Morbidelli. Multiobjective optimization of simulated moving bed and varicol processes using a genetic algorithm. *J. Chromatogr. A*, 989:95–108, 2003.

[94] J.R. Bruno. The economics of smb. *Chimica Oggi*, 22:32–34, 2004.

[95] D. P. Poe. Efficiency for unretained solutes in packed column supercritical fluid chromatography: I. theory for isothermal conditions and correction factors for carbon dioxide. *J. Chromatogr. A*, 1078:152–161, 2005.

[96] L. Miller, C. Orihuela, R. Fronek, D. Honda, and O. Dapremont. Chromatographic resolution of the enantiomers of a pharmaceutical intermediate from the milligram to the kilogram scale. *J. Chromatogr. A*, 849:309–317, 1999.

[97] C. M. Grill, L. Miller, and T. Q. Yan. Resolution of a racemic pharmaceutical intermediate: A comparison of preparative hplc, steady state recycling, and simulated moving bed. *J. Chromatogr. A*, 1026:101–108, 2004.

[98] A. Seidel-Morgenstern. Preparative gradient chromatography. *Chem. Eng. and Technol.*, 28:1265–1273, 2005.

[99] L. R. Baker, M. A. Stark, A. W. Orton, B. A. Horn, and S. R. Goates. Density gradients in packed columns. i. effects of density gradients on retention and separation speed. *J. Chromatogr. A*, 1216:5588–5593, 2009.

[100] T. Q. Yan and C. Orihuela. Rapid and high throughput separation technologies-steady state recycling and supercritical fluid chromatography for chiral resolution of pharmaceutical intermediates. *J. Chromatogr. A*, 1156:220–227, 2007.

[101] G. J. Chin, Z.H. Chee, W. Chen, and A. Rajendran. Solubility of flurbiprofen in co_2 and co_2 + methanol. *J. Chem. Eng. Data*, In Press, 2009.

[102] M. A. Trebble and P. R. Bishnoi. Accuracy and consistency comparisons of ten cubic equations of state for polar and non-polar compounds. *Fluid Phase Equilib.*, 29:465–474, 1986.

[103] Y. Houndonougbo, H. Jin, B. Rajagopalan, K. Wong, K. Kuczera, B. Subramaniam, and B. Laird. Phase equilibria in carbon dioxide expanded solvents: Experiments and molecular simulations. *J. Phys. Chem. B*, 110:13195–13202, 2006.

Appendix A

Calculation of mobile phase physical properties

A.1 Calculation of mobile phase density

To calculate phase equilibria, activity coefficient models are used to describe liquid-phase non-idealities and an equation of state to describe vapor phase non-idealities. This method has proven to be accurate from low to moderate pressures and can be utilized to represent non-ideal systems. However, difficulties and inaccuracies arise when using this kind of models to calculate high pressure equilibria and equilibria for mixtures containing supercritical compounds.

Cubic equation of state does not have such kind of limitation inherently. For hydrocarbons and slightly polar systems, cubic equations of state provide a simple robust and computationally economical method to calculate phase equilibria. For moderately polar and highly polar mixtures, the predictions are not accurate. However, since the supercritical CO_2 is non-polar and modifiers are slightly polar substances, this kind of equations of state could be used to calculate the density of the supercritical mixture with acceptable accuracies. Among several equations of state, the Peng-Ronbinson equation [74] is one of the most used equations for supercritical fluids. It exhibits performance similar to the Soave equation, but it is generally superior in

predicting the liquid densities of many materials, especially non-polar ones [102].

The equation of state provide by Peng and Robinson is shown as following:

$$P = \frac{RT}{v-b} - \frac{a\alpha}{v(v+b)+b(v-b)} \tag{A.1}$$

where

$$a = \frac{0.45724R^2T_c^2}{P_c}$$

$$b = \frac{0.07780RT_c}{P_c}$$

$$\alpha = \left[1 + m\left(1 - \sqrt{\frac{T}{T_c}}\right)\right]^2$$

$$m = 0.37464 + 1.54226\omega - 0.26992\omega^2$$

where R is the universal gas constant, T is the temperature, P is the pressure, V is the molar volume, P_c and T_c are the critical pressure and temperature respectively, ω is the acentric factor for the species.

To calculate the density of the supercritical mixture, a mixing rule is needed. Most of the mixing rules for cubic equations of state calculate the mixture parameters a and b for the equations of state, in the following fashion:

$$a = \sum_{i=1}^{N}\sum_{j=1}^{N} x_i x_j a_{ij} \tag{A.2}$$

$$b = \sum_{i=1}^{N}\sum_{j=1}^{N} x_i x_j b_{ij} \tag{A.3}$$

The only difference between them is the combining rule that determines how the cross coefficients a_{ij} and b_{ij} are calculated. In this case, a quadratic

mixing rule which only offers two adjustable parameters for binary system was used. One binary interaction parameter is used to adjust the mixture parameter a and the other is used to adjust the mixture parameter b.

$$a_{ij} = \sqrt{a_i a_j}(1 - k_{ij}) \tag{A.4}$$

$$b_{ij} = \frac{b_i + b_j}{2}(1 - l_{ij}) \tag{A.5}$$

with $k_{ij} = k_{ji}$ and $l_{ij} = l_{ji}$. The value of mixing binary parameter k_{ij}, l_{ij} are obtained from literature [103]. The calculated results are compared to the experimental results from literature whose conditions are close to those of this study [1] as shown in Fig. 3.1. The maximum deviation is less than 5%.

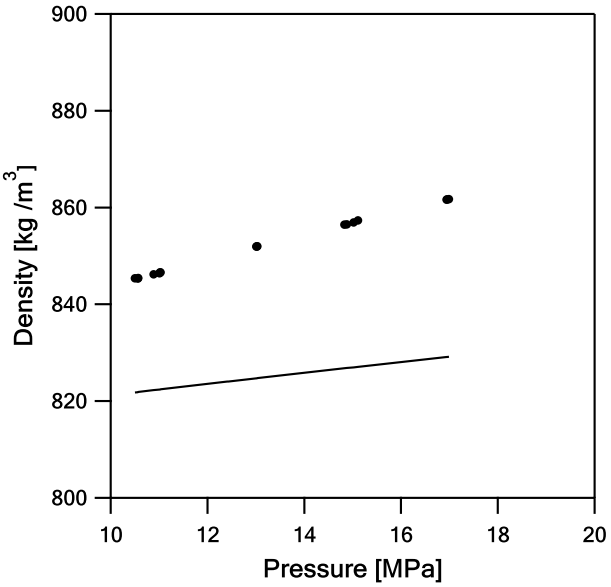

Figure A.1: Comparison of estimated fluid density and experimental results [1]. Points represent experimental results from literature, while lines are calculated using the Peng-Robinson equation of state with a quadratic mixing rule. Temperature: 313 K modifier concentration (mole ratio): 0.58

The final density of supercritical mixture of CO_2 and MeOH is shown in Table A.1

Table A.1: Density of supercritical mixture of CO_2 and MeOH.

c_m (% w/w)	Pressure (bar)	ρ (g L^{-1})
13	100	894.7
	135	914.9
	170	932.3
	205	947.7
18	100	907.0
	135	921.3
	170	934.1
	205	945.6
20	100	908.4
	135	921.1
	170	932.4
	205	942.8
23	100	907.7
	135	918.3
	170	928.1
	205	937.0

A.2 Calculation of mobile phase viscosity

It is necessary to obtain the viscosity of supercritical mixture for the calculation of pressure drop. The viscosity of pure CO_2 is obtained from NIST Chemistry Webbook. The dependence of viscosity on pressure is shown in Figure A.2. A clear linear trend was observed. Thus by regressing the data, the following equations were used to calculate the individual viscosity. The pressure has minor effect on the viscosity of pure MeOH. Thus the viscosity of MeOH at 30°C was used for all the calculation.

$$\mu_{CO_2} = 0.1974P + 49.957 \tag{A.6}$$

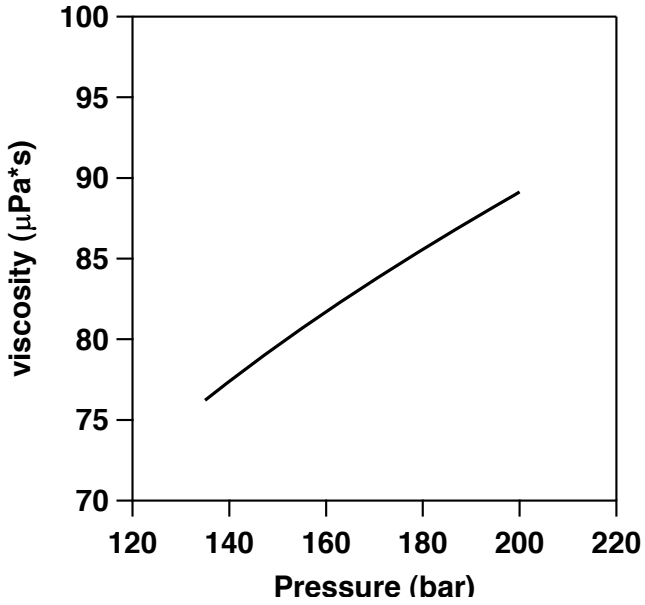

Figure A.2: Dependence of CO_2 viscosity on pressure at constant temperature: 30°C.

There are several methods to calculate the mixture viscosity provided the values of pure components are known. One simple method is to calculate it by the mole ratio of individual substances as shown in Equation A.7.

$$\mu_{mix} = \sum_{i=1}^{n} x_i \mu_i \tag{A.7}$$

Here μ_{mix} and μ_i are the viscosities of the mixture and the component i, respectively and x_i is the mole fraction. The validity of such relationship has been examined for similar pressure and temperature conditions for acetone and CO_2 [89], thus it was used for all the simulations in this thesis.

Appendix B

Results of overloaded racemic injections

The comparison of simulation and experimental elution profiles for all 4 different modifier and pressure conditions are shown in the following figures. Since the difference between bi-Langmuir and Langmuir isotherm is minor, only the simulation results based on Langmuir isotherm are presented here.

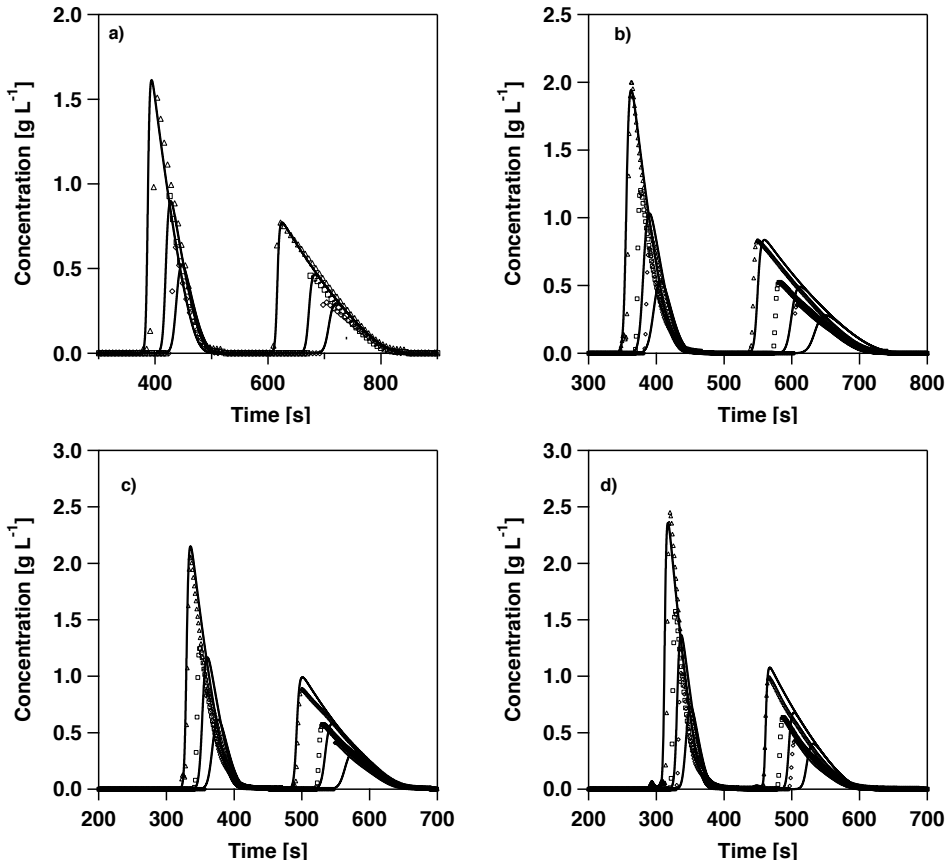

Figure B.1: Experimental (symbols) and simulated (lines) pulse response of the racemate of flurbiprofen on Chiralpak AD-H. Pressure: a) 100 bar, b) 135 bar, c) 170 bar, d) 205 bar, modifier concentration: 13% (w/w). Triangle symbol: 300 g/L, square symbol: 150 g/L, cycle symbol: 75 g/L

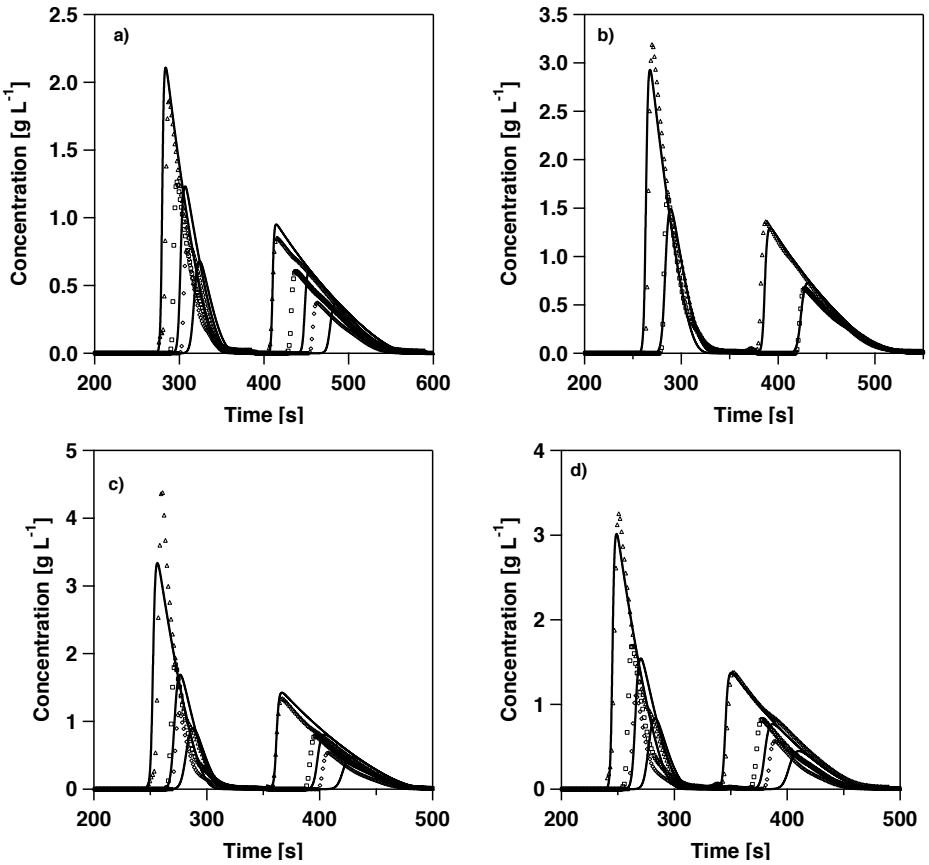

Figure B.2: Experimental (symbols) and simulated (lines) pulse response of the racemate of flurbiprofen on Chiralpak AD-H. Pressure: a) 100 bar, b) 135 bar, c) 170 bar, d) 205 bar, modifier concentration: 18% (w/w). Triangle symbol: 300 g/L, square symbol: 150 g/L, cycle symbol: 75 g/L

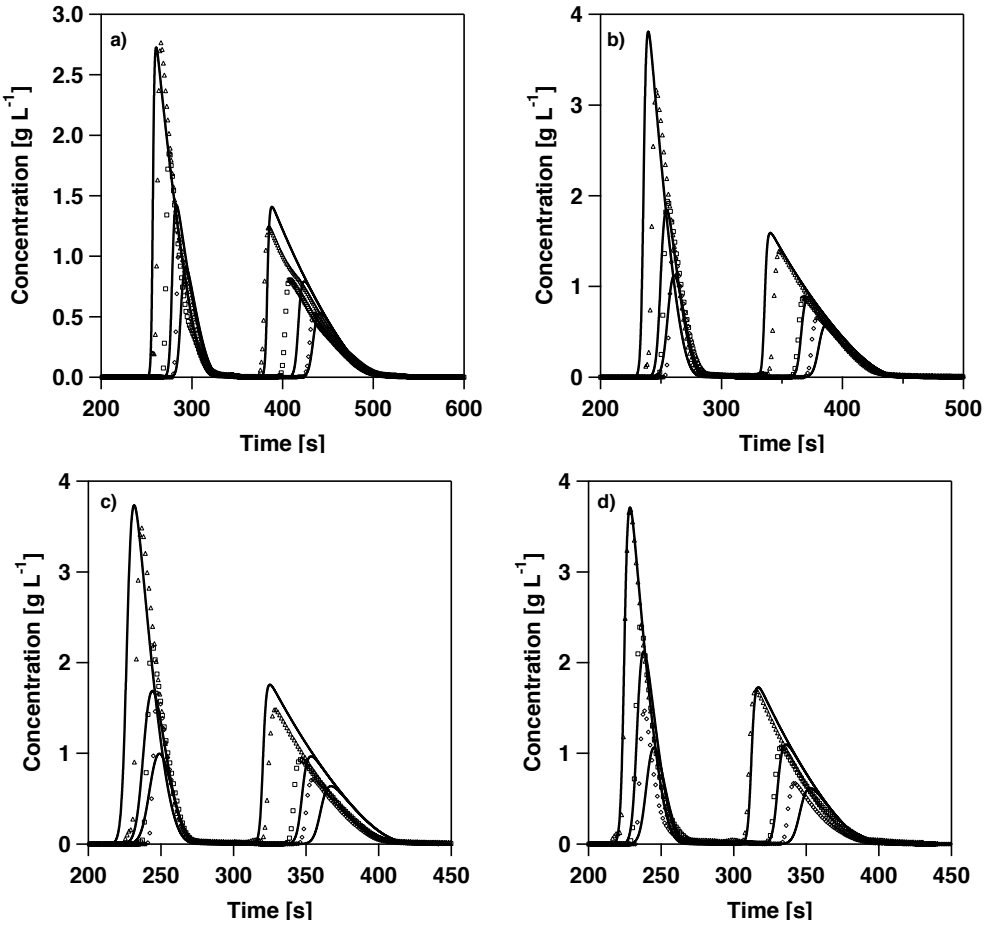

Figure B.3: Experimental (symbols) and simulated (lines) pulse response of the racemate of flurbiprofen on Chiralpak AD-H. Pressure: a) 100 bar, b) 135 bar, c) 170 bar, d) 205 bar, modifier concentration: 20% (w/w). Triangle symbol: 300 g/L, square symbol: 150 g/L, cycle symbol: 75 g/L

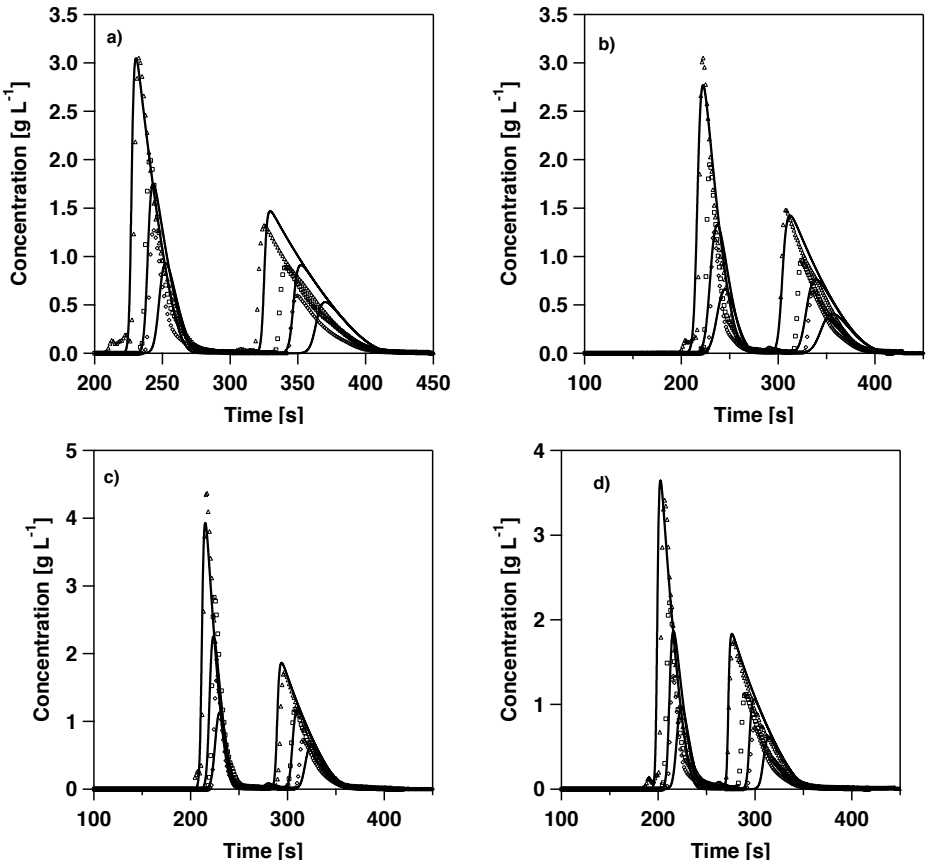

Figure B.4: Experimental (symbols) and simulated (lines) pulse response of the racemate of flurbiprofen on Chiralpak AD-H. Pressure: a) 100 bar, b) 135 bar, c) 170 bar, d) 205 bar, modifier concentration: 23% (w/w). Triangle symbol: 300 g/L, square symbol: 150 g/L, cycle symbol: 75 g/L